



저작자표시-비영리-변경금지 2.0 대한민국

이용자는 아래의 조건을 따르는 경우에 한하여 자유롭게

- 이 저작물을 복제, 배포, 전송, 전시, 공연 및 방송할 수 있습니다.

다음과 같은 조건을 따라야 합니다:



저작자표시. 귀하는 원저작자를 표시하여야 합니다.



비영리. 귀하는 이 저작물을 영리 목적으로 이용할 수 없습니다.



변경금지. 귀하는 이 저작물을 개작, 변형 또는 가공할 수 없습니다.

- 귀하는, 이 저작물의 재이용이나 배포의 경우, 이 저작물에 적용된 이용허락조건을 명확하게 나타내어야 합니다.
- 저작권자로부터 별도의 허가를 받으면 이러한 조건들은 적용되지 않습니다.

저작권법에 따른 이용자의 권리는 위의 내용에 의하여 영향을 받지 않습니다.

이것은 [이용허락규약\(Legal Code\)](#)을 이해하기 쉽게 요약한 것입니다.

[Disclaimer](#)

**A THESIS
FOR THE DEGREE OF DOCTOR OF PHILOSOPHY**

**Backstepping Based Control Algorithm of Roll-to-
Roll Web System for Printed Electronics**

Tran Trung Thanh

Department of Mechanical and System Engineering
GRADUATE SCHOOL
JEJU NATIONAL UNIVERSITY

2012. 06

Backstepping Based Control Algorithm of Roll-to-Roll Web System for Printed Electronics

Tran Trung Thanh

(Supervised by Professor Kyung-Hyun Choi)

A thesis submitted in partial fulfillment of the requirement for the
degree of Doctor of Philosophy

2012. 06

The thesis has been examined and approved.

Ki-Rin Kwon

Ki-Rin Kwon, Professor, Department of Mechanical and System Engineering

Jung b. W.

Dong-Won Jung, Professor, Department of Mechanical and System Engineering

Yang Hoi Doh

Yang-Hoi Doh, Professor, Department of Electronic Engineering

Jeongdai Jo

Jeong-Dai Jo, Ph. D., Korea Institute of Machinery and Materials

OHZ. Kyup Hyun

Kyung-Hyun Choi, Professor, Department of Mechatronics Engineering

June, 2012

Date

Department of Mechanical and System Engineering
GRADUATE SCHOOL
JEJU NATIONAL UNIVERSITY
REPUBLIC OF KOREA

*To
My wife, Nguyen Hong Vi, my daughter, Tran Nguyen Vy Linh
and
my brothers, sisters and parents,*

Acknowledgements

This dissertation is the conclusions of five years of research at the Department of Mechanical and System Engineering of Jeju National University. Many people have helped me over the past five years and it is my great pleasure to take this opportunity to express my gratitude to them all.

The first person I would like to thank is my supervisor professor Kyung Hyun Choi, PhD. I have been with him since very earlier days of 2008 when I started my Ph.D. program. During these years I have known Prof. Kyung Hyun Choi as a sympathetic and principle-centered person. His overly enthusiasm and integral view on research and his mission for providing only high quality work and not less, has made a deep impression on me. I owe him lot of gratitude for having me shown this way of research. He could not even realize how much I have learned from him. Besides of being an excellent supervisor, Prof. Choi was as close as a father and a good friend to me. I am really glad that I have come to get know Prof. Kyung Hyun Choi in my life.

I would like to thank Dr. Dong Soo Kim for his support and mental guide and encouragement had helped me in all the time of research. His deep physical insight and wide knowledge in the field of roll-to-roll web (R2R) was always of great assistance. I would also like to thank the other members of my Ph.D. committee who monitored my work and took effort in reading and providing me with valuable comments on earlier versions of this dissertation: Prof. Kirin Kwon, Prof. Dongwon Jung, Prof. Yang-Hoi Doh and Dr. Jeongdai Jo, I thank you all.

I wish to offer my humble gratitude to professors Prof. Yang Hoi Doh, Prof. Gui Shik Kim, Prof. Youn Cheol Park, Prof. Dong Won Jung and Prof. Kim Sang-Jae for their inspiring and encouraging way to lead me to a deeper understanding of knowledge, and their invaluable comments during the course works.

I am fortunate enough to have chance to work with many people directly or indirectly. Mr. Ko Jeong-Beom has helped me initially when I joined the lab. He has been a real mentor and provided motivation to achieve something big in life. Mr. Bong Su Yang has been so kind and helped me whenever I faced some difficulty in the work. He always motivated me to work and I never felt alone or stressed with work. Mr. Kyung Hyun Lee helped me study and perform the experiments. The

experiments performed in this thesis are performed with his help. Ko Jeong-beom, Gameshthangaraj P., Yang Bong Soo, and Lee Kyung-Huyn have been good friends and they provided good support and were helpful in assisting me in numerous ways.

Staying away from home is always challenging and tough. However, I am glad to have friends in Jeju National University who always made me believe they are there when it matters and has been part of my happiness and hard ships. Nguyen Ngoc Han, Nguyen Minh Nam, Nong Minh Ngoc, Pham Minh Anh, Pham Ngoc Sao, Vo Thi Thanh The, Nguyen Quyen, Le Thanh Cuong, Abhijit saha, Shrikant, Gunasekaran, Muhammad Asif Ali Rehmani, Khalid Rahman, Malik Nauman, Adnan Ali, Saleem Khan, Arshad Khan, Naeem Awais, Kim Chang Jong, Ko Jeong-beom, Yang Bong Soo, Dang Hyun Hoo, Lee Kyung Hyun, Kim Hyung Chan, Ganesh Thangaraj, Shridharan, Muhammad Zubair and all Vietnamese students. I thank them all for giving me so many memories to cherish during my stay in Jeju. I also thank all the members of JISO who has been very cooperative and supportive.

I am also grateful for the Department of Mechanical and System Engineering at Jeju National University for providing me an excellent work environment during my study and I also thank all for their cheerful assistance in the office work.

Many thanks to Korean Ministry of Knowledge Economy funded by Korean government for supporting me during my stay in Korea, and also Graduate school of Jeju National University has been grateful to wave the tuition fee for my doctoral studies.

Finally, I will never find words enough to express the gratitude that I owe to my wife, Nguyen Hong Vi, my daughter, Tran Nguyen Vy Linh, brothers, sisters and parents. Their tender love and affection has always been the cementing force for building the blocks of my academic career. They all round support rendered by them provided the much needed stimulant to sail through the phases of stress and strain.

I would like to thank all those whom I have not mentioned above but helped me in numerous ways to my success.

Abbreviations and Notations

AMM	Advanced Micro Mechatronics
BSC	Backstepping Controller
CLF	Control Lyapunov Function
FPGA	Field-Programmable Gate Array
GA	Genetic Algorithm
GAS	Globally Asymptotical Stability
MBS	Modified Backstepping
MGA	Modified Genetic Algorithm
MIMO	Multi Input and Multi Output
PC	Personal Computer
PI	Proportional- Integral
PID	Proportional –Integral-Derivative
ODE	Ordinary Differential Equation
RFID	Radio Frequency Identification
R2R	Roll to Roll
SBX	Simulated Binary Crossover
SISO	Single Input and Single Output
ZN	Ziegler-Nichols

J	Objective function
A, B, C	Matrix representing the linear control system
f, g, h	N-dimensional vector valued function
f_i, g_i, h_i	Real valued functions
u, v	Control inputs
x, ξ, η, z	State space variables
x^0	Initial state space vector
y	Output variables
U, V, W	Subspaces

T, Φ	Transformation matrix and coordinate transformation
T^{-1}, Φ^{-1}	Inversion coordinate transformation
t	Time variable
R	Real numbers
R^n, R^m	Real column vector space with n and m entries
$R^{m \times n}$	Real matrices of dimension $m \times n$
$[,]$	Lie bracket
$L_f(\cdot)$	Lie derivative
α, β	Real numbers
Φ_t^f, Φ_s^g	Flows of vector fields
ω	Co-vector field
Ω	Co-vector space
Δ	Distribution
x_e	Equilibrium points
r	Relative degree of the system
$\det(A)$	Determinant of the matrix A
i, j, k	Variable number
T_i	Web Tension in i^{th} span
R_r, R_u	Radii of the Rewinder and Unwinder
$\omega_r, \omega_u, \omega_i$	Angular velocity of rollers
τ_u, τ_r, τ_i	Moments on rollers
ρ	Density of the web
ε	Longitudinal deformation
l_i	The length of i^{th} span
V_i	Web velocity at i^{th} span
J_i	Inertial moment of rollers
E	Young's module of elasticity

Contents

List of Figures	i
List of Tables	iv
Abstract	v
1. Introduction	1
1.1 Overview	1
1.2 Background and Motivation	3
1.3 Objectives of Research	6
1.4 Dissertation Outline	7
2. Theoretical Background	9
2.1 Geometric View of Linear Control Systems	9
2.2 Notations and Concepts for Nonlinear Control Systems	12
2.3 Local Decomposition of Control Systems	18
2.4 SISO Nonlinear Feedback Theory	20
2.4.1 Normal Form of Equations of SISO	20
2.4.2 Exact Linearization via Nonlinear Feedback	21
2.5 MIMO Nonlinear Feedback Theory	23
2.5.1 Normal Form of Equations of MIMO	23
2.5.2 Exact Linearization via Nonlinear feedback	26
2.6 Theory of Lyapunov Stability	28
2.6.1 Some Definitions	28
2.6.2 Second Method of Lyapunov	30
2.7 Backstepping Based Design Theory	31
2.7.1 Concepts of Basic Backstepping Design	32
2.7.2 Backstepping Design of Modified Strict-feedback Form	34
2.8 Some Comments	38
3. Modified Genetic Algorithm	39
3.1 Introduction	39
3.2 Classical Approach of Genetic Algorithm	40
3.3 Modified Genetic Algorithm and Application	42
3.4 Control System Design of Automatically Tuning Controller	45
4. R2R Web Control System for Printed Electronics	48
4.1 Literature Survey	48
4.1.1 Concepts of R2R Web Control System	48
4.1.2 Perspective of Web Tension and Velocity Control	50
4.2 Mathematical Model Development	52
4.2.1 Assumptions	52
4.2.2 Development of Dynamic Equations	52
4.3 R2R Web Control System Design	55
4.3.1 Hardware Design	56
4.3.2 Software Design	58
5. Single-span R2R Web Velocity and Tension Control	60
5.1 Mathematical Model Single-span R2R Web System	60

5.2 Feedback Linearization Based Approach	62
5.2.1 State Space Feedback Controller Design.....	62
5.2.2 Numerical Simulation	64
5.3 Backstepping Approach of Single-span R2R Web Control System.....	65
5.3.1 Backstepping Controller Design.....	65
5.3.2 Backstepping Based Control Algorithm.....	68
5.4 Numerical Simulation	69
5.4.1 Simulation Conditions and Parameters.....	69
5.4.2 Simulation Results	70
5.5 Experimental Implementation.....	74
5.6 Analysis and Discussions	78
6. Two-span R2R Web Velocity and Tension Control	79
6.1 Mathematical Model Two-span R2R Web System	79
6.2 Backstepping Controller Design.....	81
6.3 Backstepping Based Control Algorithm.....	88
6.4 Numerical Simulation	89
6.4.1 Simulation Conditions and Parameters.....	89
6.4.2 Simulation Results	90
6.5 Experimental Implementation.....	92
6.5.1 Experimental Setup.....	92
6.5.2 Experimental Results	93
6.6 Analysis and Discussions	95
7. Three-span R2R Web Velocity and Tension Control.....	96
7.1 Mathematical Model Three-span R2R Web System	96
7.2 Backstepping Controller Design.....	99
7.3 Backstepping Based Control Algorithm.....	109
7.4 Numerical Simulation	109
7.4.1 Simulation Conditions and Parameters.....	109
7.4.2 Simulation Results	110
7.5 Experimental Implementation.....	111
7.6 Analysis and Discussions	115
8. Conclusions and Future Works	117
8.1 Conclusions.....	117
8.2 Future Works	118
References.....	120
Curriculum Vitae.....	127

List of Figures

Figure 1.1: Concepts of roll-to-roll web system.....	1
Figure 1.2: Flexible glass substrate.....	1
Figure 1.3: Offset-gravure R2R printing technology.....	2
Figure 1.4: AMM Lab approach.....	6
Figure 2.1: Geometric interpretation of invariant subspace.....	10
Figure 2.2: Geometric interpretation of reachable point.....	11
Figure 2.3: Triangular decomposition of affine control system.....	18
Figure 2.4: Triangular decomposition of affine control system.....	19
Figure 2.5: Block diagram of normal form of equations.....	21
Figure 2.6: The input/output feedback linearization.....	21
Figure 2.7: Backstepping based system design.....	32
Figure 2.8: Introduction of control.....	32
Figure 2.9: Backstepping control via Integrator.....	33
Figure 3.1: Block diagram of the GA.....	41
Figure 3.2: Block diagram of the MGA.....	43
Figure 3.3: The change of PID gains in time.....	45
Figure 3.4: Step response of the third order system.....	45
Figure 3.5: Control system design of automatically tuning controller scheme.....	46
Figure 3.6: The algorithm diagram of automatically tuning controller scheme.....	47
Figure 4.1: R2R Web system based Inkjet Printing System at AMM Lab.....	49
Figure 4.2: The control volume.....	52
Figure 4.3: Deformation of web materials.....	53
Figure 4.4: The relation between Rollers and web in a zone.....	53
Figure 4.5: Isolated small element of web.....	54
Figure 4.6: Relation between nip roller and web movement.....	55
Figure 4.7: Drawing of R2R web ESD system.....	56
Figure 4.8: Drawing of gravure/offset printing units.....	57
Figure 4.9: Block diagram for control program.....	58
Figure 4.10: Interface of control program of R2R ESD system.....	59
Figure 5.1: The R2R web control system at AMM laboratory.....	60
Figure 5.2: Model of single-span web control system.....	61

Figure 5.3: Comparison of web tension response in two cases: state space based design and PI based design methods.....	64
Figure 5.4: FPGA module of input/outputs	69
Figure 5.5: Block diagram of web tension and velocity control system.....	69
Figure 5.6: Prescribed web tension of sudden change in time.....	70
Figure 5.7: The tension change in time in case 1.....	71
Figure 5.8: The angular velocity change in time of rewinder in case 1.....	72
Figure 5.9: The angular velocity change in time of unwinder in case 1.....	72
Figure 5.10: The tension change in time in case 2.....	73
Figure 5.11: The angular velocity change in time of rewinder in case 2.....	73
Figure 5.12: The angular velocity change in time of unwinder in case 2.....	73
Figure 5.13: Block diagram of experimental study	74
Figure 5.14: Tension control program of R2R web system.....	75
Figure 5.15: The change of web tension in time of experimental study	76
Figure 5.16: The change of angular velocity of the rewinder and unwinder of experimental study	76
Figure 5.17: The change of web tension in time of experimental stud.....	77
Figure 5.18: The change of angular velocity of rewinder and unwinder of experimental study.....	77
Figure 6.1: Two-span R2R web control system	80
Figure 6.2: Model of two-span R2R web control system.....	80
Figure 6.3: Block diagram of the two-span R2R web tension and velocity control system	89
Figure 6.4: The angular velocity change in time of infeeder.....	90
Figure 6.5: The tension change in time of span 1 and 2.....	91
Figure 6.6: Block diagram of experimental study of two-span R2R web system.....	92
Figure 6.7: Tension control program of R2R web system.....	93
Figure 6.8: Angular velocity change of infeeder roller	93
Figure 6.9: Web tension change in time of span 1 and 2.....	94
Figure 7.1: Three-span R2R web control system for printed electronics	97
Figure 7.2: Model of three-span R2R web control system.....	97
Figure 7.3: The algorithm diagram for three-span R2R web system.....	109

Figure 7.4: Web tension change in span 1, 2 and 3 (N)	110
Figure 7.5: The angular velocity change in time of infeeders	111
Figure 7.6: Diagram of three-span R2R web control system setup	112
Figure 7.7: The PXI 7813R reconfigurable I/O	112
Figure 7.8: User interface of three-span R2R web control system	113
Figure 7.9: Web tension change of span 1, 2 and 3 in time	114
Figure 7.10: Web tension response with nonzero initial condition	114
Figure 7.11: Angular velocity change in time of infeeders	115

List of Tables

Table 3.1: Parameters of the MGA.....	44
Table 3.2: Simulation Results of the Third Order System	44
Table 4.1: Devices of R2R Web ESD at AMM Lab	57
Table 5.1: Parameters for the MGA for R2R web control system	67
Table 5.2: Simulation Parameters of Single-span R2R Web control system	69
Table 6.1: Simulation Parameter of Two-span R2R Web control system.....	89
Table 7.1: Simulation Parameters of Three-span R2R Web Control System	109

Abstract

There have been many applications which employed roll-to-roll (R2R) web technology for mass production such as web printing, papers machine, film processing, and textiles fabrics. Especially, radio frequency identification (RFID) and printed electronics are using the principles of R2R manufacturing to create devices at high speeds and lower cost. Due to the increasing demand of high accuracy in printed electronics industry at a micrometer-level in which linear control system based algorithms are not able to meet the requirement of performance specifications. Also, it is proven due to linearization, some nonlinearity is neglected and the actual system performance is different from the simulated results. Thus, it is necessary to have a precise control scheme for the nonlinear R2R web system in the presence of varying parameters and disturbances.

In the first section of this dissertation, some concepts and applications of R2R web manufacturing technology are introduced and a theoretical background is provided for analyzing and designing nonlinear control systems. And then state space exact linearization method for SISO and MIMO nonlinear control system which utilizes the sequence of coordinate transformation and state feedback in order to transform the original system into a linear and controllable system is presented. Using the classical design methods for linear control system and return the original coordinates, a state feedback law is proven to meet the demands of the performance specifications and stability. However, such an approach often leads us to the complex expressions and sometimes fails to obtain the final state feedback law. The question arises if the resultant nonlinear feedback law is able to be obtained by dividing the whole system into several subsystems and coordinate transformations and state feedbacks are able to implement alternately for each subsystem. The idea of backstepping based design approach comes up to get over this obstacle. In this proposal, the whole system is divided into several subsystems in a principle such that the n^{th} subsystem consists of the $(n-1)^{\text{th}}$ subsystem and the n^{th} subsystem is the original system via coordinate transformations and state feedbacks. By applying consecutively the coordinate transformation and choosing feedback law via Control Lyapunov Function (CLF) to each subsystem from the lowest to highest order and rewrite the feedback law in the original coordinates, the resulted controllers called

backstepping controller make original system a well-tracking command and asymptotically global stable. After that a generalized mathematical model of a class of nonlinear control system encountered in practical problems is proposed and a systematic procedure is presented for formulating the backstepping controller (BSC) for this MIMO nonlinear control system using the above proposed approach.

In the next section, some recent works of R2R web system control technology are reviewed and analyzed. By using several assumptions on R2R web system, a mathematical model of R2R web control system is derived from the Newton's Second law and the principle of mass conservation and then a design scheme for formulating the BSC and precise control algorithm are implemented for a nonlinear single-span, two-span and three-span R2R web control system based on the backstepping based design approach. By the numerical simulation and experimental implementation, it is also proven that the performances of R2R Web system are able to be improved by optimal gains. Thus, an introduction of genetic algorithm (GA) is briefly mentioned and a modified genetic algorithm (MGA) is proposed to determine optimally the design parameters of the BSC and an algorithm using the MGA is for updating online the gains is presented in the presence of changing radii and viscous friction.

Finally, simulation and experimental results that confirm the reliability and robust stability of the proposed algorithm are presented and discussed and then some conclusions are made by summarizing the main contributions in the dissertation and some discussions such as applicability and limitations of the proposed control algorithm in reality. Also, future works also are addressed further to improve the precision and applicability of control algorithms.

1. Introduction

The chapter briefly describes concepts, developments, and applications and challenges of R2R manufacturing technology in printed electronics. Background and motivations are discussed and then the main targets of the dissertation are mentioned and the outline of dissertation is given in the last section of the chapter.

1.1. Overview

R2R processing is when a web or continuous sheet of material on a roll is fed out from an unwind unit through one or more mid-process steps such as deposition, patterning and packaging and rewind again into a roll of material shown in Figure 1.1.

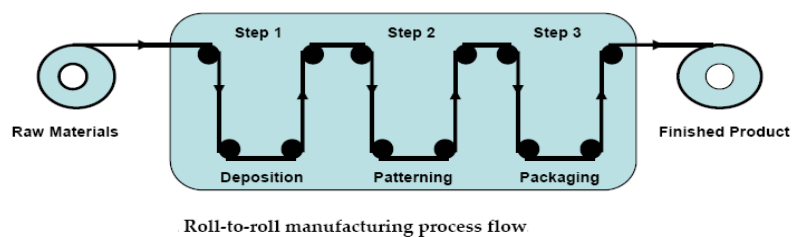


Figure 1.1: Concepts of roll-to-roll web system

Roll materials can be anywhere from less than one inch wide to over 72 inches depending on manufacturing techniques. Roll material falls into four categories: Plastic based products, paper based products, metal based products, and composites of above substrates. Figure 1.2 shows an example of roll materials for printed electronics technology.



Figure 1.2: Flexible glass substrate

R2R processing has been identified by the display industry as a technology that could significantly reduce the costs associated with manufacturing displays. R2R manufacturing can be most easily conceptualized as the process by which low cost products such as labels and newspapers are currently produced, where thousands of square feet of printed material can be printed for just a few cents. Although electronic display materials are much more expensive than newspaper materials, the R2R printing process itself is inherently low cost and extremely scalable. Industry efforts to achieve R2R manufacturing aspire to implement more arcane materials and controls into this fundamentally mundane process in order to realize order of magnitude reductions in the display manufacturing cost structure. If each layer of a display could be patterned onto a roll of substrate in a continuous deposition process, then it could be possible to realize a profound decrease in the cost of manufacturing an electronic display relative to the conventional approaches used in the industry (Michael A. Randolph, MIT, 2006). The basic concepts of R2R can be illustrated by Figure 1.3, where a functional layer is transferred onto a substrate by contacting the surface to a patterned roll that contains the layer material in an ink form. Although this direct contact printing is one approach to achieve a R2R compatible deposition, there are other additive approaches that are compatible with R2R processing such as ink jet printing or laser patterning.



Figure 1.3: Offset-gravure R2R printing technology

The fundamental difference between R2R manufacturing and the manufacturing approaches currently used in the display industry is that R2R is a web process whereas the conventional display manufacturing techniques utilize batch processes. This allows the layers and processing operations to be applied to the display continuously as it is moved through the manufacturing facility. The cost reductions are expected to be derived primarily from a reduction in the material handling cost of moving the work-in-progress inventory from process to process within a plant. Additionally, if additive patterning techniques can be used in the R2R process then it is conceivable that a reduction in the cost of materials could also be achieved.

1.2. Background and Motivation

From the advantages of R2R manufacturing technology and applications, in the last decades, there have been many applications which employed the R2R web technology for mass production such as web printing, papers machine, film processing, and textiles fabrics and so on to make cheaper production in shorter time. Especially, RFID (radio frequency identification) and printed electronics use the principle of R2R manufacturing to create devices at high speed and lower cost, and they have a big impact on the printed electronics and publishing industries. Several developments have pushed the burgeoning printed electronics industry and up to now the R2R web system based technologies are seen as the key to producing flexible electronic components, such as organic thin film transistors and other applications. With the rapid development of mathematical tools and digital computers, nonlinear control systems are getting more attention (D. Knittel, E. Laroche, H. Koc, 2001, Alan F. Lynch, Scott A. Bortoff, and Klaus Robenack, 2004, Bong-Ju Lee, Sung-Hwan Kim, Chul-Goo Kang, 2006). Depending on the mathematical model and experimental researches, some algorithms for a web tension and velocity control for an R2R web system have been proposed. (K. H. Shin, 2003) and (K. C. Lin, 2001 and Prabhakar R. Pagilla, Nilesh B. Siraska, 2004) have achieved low cost and high quality through the implementation of observer techniques, the synthesis of an observer-based controller in place of tension transducer, and the estimation of friction, and rotational inertias of the rewinder and the unwinder.

An important aspect in R2R web control system design is to fully understand the physical and mathematical models (Brian Thomas Boulter, 2001, Seung rohk Oh, 2006, Kee-Hyun Shin, Soon-Oh Kwon, Sang-Hoon Kim, and Seung-Ho Song, 2003) and to come up with disturbance rejection algorithms (Seung-Ho Song, Seung-Ki Sul, 1998, Alan F. Lynch, Scott A. Bortoff, and Klaus Robenack, 2004 and Brian Thomas Boulter, 2001). In reality, one usually uses linearized models to design the control systems but due to the linearization, some crucial nonlinearity is ignored and as a result there is a discrepancy between the actual system performance and the simulated results (Kee-Hyun Shin, Jeung-In Jang, Hyun-Kyoo Kang, Seung-Ho Song, 2003). In the recent years, many researchers addressed in designing nonlinear controllers by using the backstepping techniques (Petar V. Kokotović, 1992) that have the advantages of avoiding the cancellation of benign dynamic nonlinearity, and not forcing the designed system to appear linear. Nowadays, the rapid development of digital computer, sensor technology, and PC integrated devices leads many researchers and scientists to address design methods for nonlinear control systems. There are many methods to analyze and design for the nonlinear control systems. However, the exact feedback linearization and backstepping approaches are considered much in the literature. The state space exact linearization method for MIMO nonlinear control systems which utilizes the sequence of coordinate transformation and state feedback in order to transform the original system into a linear and controllable system is presented. However, such an approach often leads us to the complex expressions with MIMO nonlinear control systems and sometimes fails to obtain the final state feedback law. The question arises if coordinate transformations and state feedbacks are able to implement alternately for each subsystem. The idea of backstepping based design approach comes up to get over this obstacle. In this proposal, the whole system is divided into several subsystems. By applying consecutively the coordinate transformation and choosing feedback law via Control Lyapunov Function (CLF) to each subsystem from the lowest to highest order and rewrite the feedback law in the original coordinates, the resulted controllers called backstepping controller make original system a well-tracking command and asymptotically global stable

In reality, there are many plants with the changing parameters in time in operating progress such as roll-to-roll web system and under the effect of disturbances in operating process. Therefore, detecting the system errors and automatically recovering the errors are necessary and have been given attention by researchers in recent years. Some modifications of the GA are proposed and applied to automation systems (Aytekin Bagis, 2007; H. Madadi Kojabadi and Q. Cao, 2005; Jin-Sung Kim, Jin-Hwan Kim, Ji-Mo Park, Sung-Man Park, Won-Yong Choe and Hoon Heo, 2008 ;Y.P. Wang, H.H. Chung, N.R. Watson, and S.S. Matar, 2000). To achieve more effective search, the optimization algorithm (Aytekin Bagis, 2007) is based on the integration of classical genetic algorithm structure and systematic neighborhood structure. The simulation results show that the proposed algorithm is applied only on the limit range such SISO linear system. The analytical procedures (M. Zhunang and D. P. Atherton, 1993) for obtaining optimum PID controller settings for minimization of time weighted integral performance criteria is employed for the dead time plant model. A method to design an optimal disturbance rejection PID controller is proposed by (Renato A. Kronhling and Joost P. Rey, 2001) based on optimization of the disturbance rejection constraints. The simulation outcomes prove the slow response in time. An optimization algorithm is proposed for designing PID controllers (H. Madadi Kojabadi and Q. Cao, 2005; Chen-Huei Hsieh and Jyh-Hong Chou (2007)), which minimizes the asymptotic open-loop gain of a system with uncertainty using the quantitative feedback theory

In the present dissertation, a general mathematical model is developed and applied to formulating the BSC for R2R web control system and a backstepping based control algorithm is applied using the backstepping controllers. The design parameters in the BSC are chosen optimally using the modified the MGA (K. H. Choi, Thanh T. Tran and D. S. Kim, 2009). Also, the MGA can be applied to design the intelligent control systems which can detect the system errors and automatically recover the errors at every time interval due to the changing of the radii and viscous friction in the different operating conditions. The reliability and robust stability of the closed-loop control system is demonstrated throughout simulation results in Matlab/Simulink and experimental results implemented on a real R2R web system

The research group at Advanced Micro Mechatronics (AMM) Laboratory is established and developed. The approach of AMM Lab is divided into two main groups. The first one addresses the issues related to the development of inkjet and offset/gravure printing technology and device improvement and the second one is working on developing the web transport system control algorithms:

- Web tension and velocity control technology
- Web printing pressure control technology
- Web lateral and register control technology
- Web system integrated control technology

Figure 1.4 shows the approach of AMM Lab research group.



Figure 1.4: AMM laboratory approach

In this dissertation, the author centers on developing the backstepping based algorithm of web tension and velocity control of nonlinear R2R web control system for printed electronic technology.

1.3. Objectives of research

- A generalized mathematical model of a class of nonlinear control system is proposed and a systematic procedure is presented for formulating the BSC using the modified backstepping approach.
- Some concepts, developments, applications, and challenges of R2R web manufacturing technology are studied. Also, some recent works of R2R web control algorithm are reviewed and analyzed.

- Some assumptions on R2R web system are given and a mathematical model of R2R web control system is derived from the second Newton law and principle of mass conservation. And then a precise control algorithm is developed for nonlinear single-span, two-span and three-span R2R web control systems based on the proposed theory.
- An introduction of the GA is briefly mentioned and a modified genetic algorithm is proposed to determine optimally the design parameters of the BSC and then the MGA based plan used to update online the gains in the presence of the change of radii and viscous friction is investigated.
- Numerical simulations are implemented for web tension and velocity control of the single-span R2R web system, two-span R2R web system and three-span R2R web system via Matlab/Simulink.
- A hardware and software schedule is developed using the FPGA technology and Labview FPGA module and a field-programmable gate array (FPGA) technology for experiment.
- Experimental study is employed and compared to the numerical simulation for validation of the proposed algorithm.

1.4. Dissertation Outline

In this dissertation, eight chapters are considered as follows:

In the first chapter, an overview of concepts, applications and potentials of R2R manufacturing technology, background and motivation, objectives of study and research contents of dissertation are made.

In the second chapter, a theoretical background about Lie derivative, normal form of equations for SISO and MIMO, input-output decoupling problem, stabilizing control, Control Lyapunov Function (CLF) and Lyapunov Stability Theorem is given and then a generalized mathematical model of a class of nonlinear control system is proposed and a systematic procedure is presented to formulating the BSC using the modified backstepping approach.

In the third chapter, an introduction of the GA is briefly mentioned and a modified genetic algorithm is proposed to determine optimally the design parameters of the BSC. Also, the MGA is used to update online the gains in the presence of the

changing parameters and disturbances. The reliability of the proposed algorithm is validated through numerical simulations and experiments.

In the fourth chapter, a brief summary and concepts and definitions of R2R web control system is derived and some recent researches of R2R web system technology are reviewed firstly. Secondly, depending on several assumptions on R2R web control system, a mathematical model of R2R web control system is derived from the second Newton law and principle of mass conservation. Also, some design concepts and introductions about the hardware of R2R web system and application of FPGA technology are given and then software schedule is developed using the Labview FPGA module

In the fifth, sixth and seventh chapters, mathematical model and precise control algorithm are developed for a nonlinear single-span, two-span and three-span R2R web control system based on the proposed theory in chapter 2, chapter 3, and chapter 4. After that, a hardware and software schedule is developed and finally, simulation and experimental results are analyzed and discussed.

In the last chapter, some conclusions are made by summarizing and analyzing the proposed approach, results and overall achievement of the work listed in this manuscript and some discussions such as applicability and limitations in reality and then future works also are addressed to improve the precision and applicability of control algorithms.

2. Theoretical Background

The purpose of this chapter is to develop a basic tool for input-affine nonlinear control systems. Firstly, an overview of linear control theory is introduced in geometric approach. Secondly, the concepts of an invariant subspace of \mathbb{R}^n , vector field, and flow of vector field, Lie Bracket, Lie derivative, distribution, involutive, and invariant distribution are given and then Frobenius theorem is generated and proven. By using the mentioned concepts, there exists a coordinate transformation in which an input-affine nonlinear system is able to be written in triangular decomposition. Also, a necessary condition for local reachability and sufficient condition for being locally indistinguishable are introduced. In the next section, we will provide a means of finding the condition for nonlinear control systems which are reachable from the initial condition using the minimal, smooth, and nonsingular distribution. Also, a normal form of equations and zero dynamics of the control system are presented. After that, show how to transform the normal form of equations exactly to linear control systems via feedback law. The necessary and sufficient conditions are shown to verify that a nonlinear control system is solvable or state space exact linearizable via coordinate transformations and feedback law. These results will be applied for SISO and MIMO systems. In the next section, the Lyapunov stability theory is presented and some definitions and theorems are given. Finally, the design concepts of backstepping approach are introduced and a systematic design for a class of nonlinear control system is proposed for formulating the backstepping controller. Some comments also discussed in the end of the chapter.

2.1 Geometric View of Linear Control Systems

Consider a linear control system as follows:

$$\dot{x} = Ax + Bu \quad (2.1)$$

$$y = Cx \quad (2.2)$$

where $x \in \mathbb{R}^n$, $u \in \mathbb{R}^m$, $y \in \mathbb{R}^p$, A : $n \times n$ – dimensional matrix, B : $n \times m$ – dimensional matrix, C : $m \times n$ – dimensional matrix

Definition 2.1: Subspace $V \in \mathbb{R}^n$ is invariant under $A \in \mathbb{R}^{n \times n}$ if $Ax \in V$ for all $x \in \mathbb{R}^n$

$N=3, d=2$

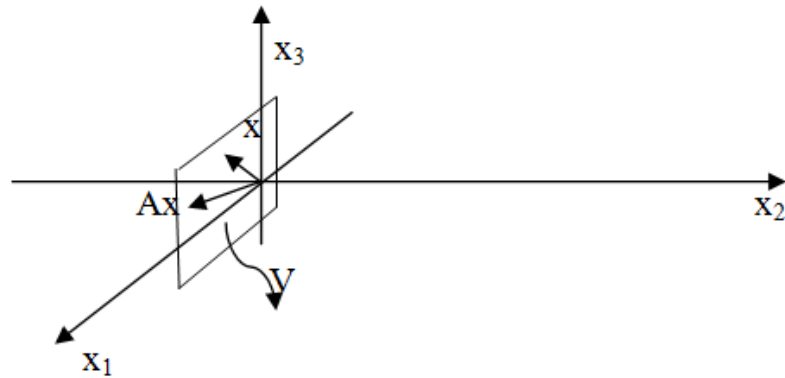


Figure 2.1: Geometric interpretation of invariant subspace

$d = \dim(V) = 2$

Theorem 2.1: Suppose that V is any d -dimensional subspace of R^n then there exists a coordinate transformation T such that $x \in V$ if and only if

$$z = Tx = \begin{bmatrix} z_1 \\ z_2 \\ \vdots \\ z_d \\ 0 \\ 0 \\ \vdots \\ 0 \end{bmatrix}_n \quad (2.3)$$

Observing that T can be applied as a state-space transformation of the linear control system as follows

$$(A, B, C) \xrightarrow{T} (\bar{A}, \bar{B}, \bar{C}) \quad (2.4)$$

where $\bar{A} = TAT^{-1}, \bar{B} = TB, \bar{C} = CT^{-1}$

Proposition 2.1: if $x \in R^n$ can be reached at time $t=T$ from $x(0)$ then x can be decomposed as

$$x = x(0) + v \quad (2.5)$$

where $v \in V$ is an invariant subspace under A which contains the $\text{Im}(B)$.

Theorem 2.2: (Wonhan)

Suppose V is a subspace of R^n such that

- i) V is invariant under A
- ii) $\text{Im}(B) \subset V$
- iii) V is the smallest subspace which satisfies i) and ii) then V is the subspace of reachable state for (A, b) i.e. $V = \text{Im}(R(A, b))$

Remarks:

Let V be a subspace that satisfies the conditions in Theorem 2.2. Let $p \in R^n$. By defining the subset:

$$S_p \triangleq \{x \in R^n: x = p + v, v \in V\} \tag{2.6}$$

Then set of reachable point at time $t = T$ when $p = e^{AT} x(0)$

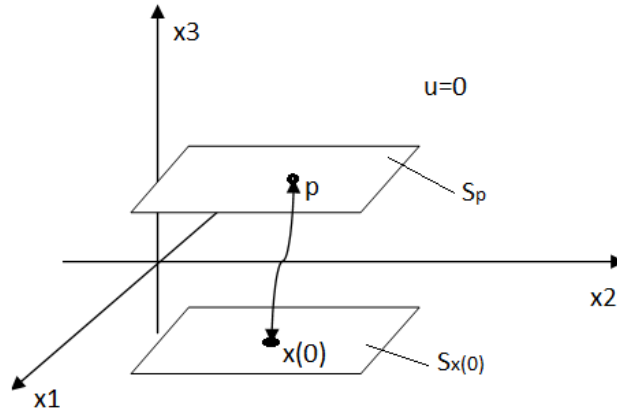


Figure 2.2: Geometric interpretation of reachable point

Theorem 2.3: (Triangular decomposition)

Let W is a subspace of R^n such that

- i) W is invariant under A
- ii) $W \subset \ker(C)$
- iii) W is the largest subspace which satisfies i) and ii)

then the system (2.1) and (2.2) can be decomposed as

$$\left. \begin{aligned} \dot{x}_1 &= A_{11}x_1 + A_{12}x_2 + B_1u \\ \dot{x}_2 &= A_{22}x_2 + B_2u \end{aligned} \right\} \tag{2.7}$$

$$y = C_2x_2 \tag{2.8}$$

Thus, the state x_1 has no affect on y .

Remarks:

- i) Two different initial conditions with the same x_2^0 component are indistinguishable at the output. Thus, this deference is an element of W
- ii) Condition iii) infers that two different initial conditions are indistinguishable at the output only if their difference is in W or

$$W = \ker \left(\begin{bmatrix} C \\ CA \\ \vdots \\ CA^{n-1} \end{bmatrix} \right) \tag{2.9}$$

If the pair (A, C) is observable then (A, C) has full rank or $W = \{0\}$, thus no states are distinguishable

iii) $S_p \triangleq \{x \in R^n: x = p + w, w \in W\}$ is the set of initial states that are indistinguishable

iv) So, using either W (observability) or V (controllability) can foliate R^n into “shuts” of “leave”

2.2 Notations and Concepts for Nonlinear Control System

Consider an input- affine nonlinear control system

$$\dot{x} = f(x) + g(x)u \quad (2.10)$$

$$y = h(x) \quad (2.11)$$

where $x \in U \subset R^n$, $f(x)$ and $g(x)$ are valued functions, $u \in R$, $y \in R$, $h(x) \in R$

It is assumed that f , g and h are smooth vector fields. Thus, the derivatives of f , g , and h exist also and continuous on U .

Definition 2.2: A mapping $\Phi: R^n \rightarrow R^n$

$$x \mapsto z = \Phi(x) \in R^n$$

is a global diffeomorphism if

i) For each $z \in R$ the inverse mapping $\Phi^{-1}(z)$ is well-defined or

$$\begin{cases} \Phi(\Phi^{-1}(z)) = z \\ \Phi^{-1}(\Phi(z)) = z \end{cases} \quad (2.12)$$

ii) Φ and Φ^{-1} to be smooth in R^n

Remarks:

1. If R^n is replaced by $U \in R^n$, then Φ is local diffeomorphism
2. What is the effect of $z \in \Phi(x)$ in a reachable (f, g, h)

Definition 2.3: (Lie Brackets)

Let f and g be a smooth vector field, $U \in R^n$ likewise for, then the Lie bracket of f and g is

$$[f, g](x) = \left. \frac{\partial g}{\partial x} \right|_x f(x) - \left. \frac{\partial f}{\partial x} \right|_x g(x) \quad (2.13)$$

where

$$\frac{\partial \underline{g}}{\partial \underline{x}} \Big|_x = \begin{bmatrix} \frac{\partial g_1}{\partial x_1} & \frac{\partial g_1}{\partial x_2} & \dots & \frac{\partial g_1}{\partial x_n} \\ \frac{\partial g_2}{\partial x_1} & \frac{\partial g_2}{\partial x_2} & \dots & \frac{\partial g_2}{\partial x_n} \\ \dots & \dots & \dots & \dots \\ \frac{\partial g_n}{\partial x_1} & \frac{\partial g_n}{\partial x_2} & \dots & \frac{\partial g_n}{\partial x_n} \end{bmatrix}, \quad \frac{\partial \underline{f}}{\partial \underline{x}} \Big|_x = \begin{bmatrix} \frac{\partial f_1}{\partial x_1} & \frac{\partial f_1}{\partial x_2} & \dots & \frac{\partial f_1}{\partial x_n} \\ \frac{\partial f_2}{\partial x_1} & \frac{\partial f_2}{\partial x_2} & \dots & \frac{\partial f_2}{\partial x_n} \\ \dots & \dots & \dots & \dots \\ \frac{\partial f_n}{\partial x_1} & \frac{\partial f_n}{\partial x_2} & \dots & \frac{\partial f_n}{\partial x_n} \end{bmatrix}$$

is called Jacobian

Remarks:

- i) $[f, g]$ is smooth vector field
- ii) Likewise for $f_n [f, [f, g]], \dots, [f, [\dots [f, g]] \dots] = \text{ad}_f^k g$
- iii) More properties of the Lie Brackets
- iv) $[\alpha f_1 + \beta f_2, g] = \alpha [f_1, g] + \beta [f_2, g]$
- v) $[f, \alpha g_1 + \beta g_2] = \alpha [f, g_1] + \beta [f, g_2]$, where $\alpha, \beta \in R$
- vi) Skew symmetry: $[f, g] = -[g, f]$
- vii) Jacobi identity: $[f_1, [f_2, f_3]] + [f_2, [f_1, f_3]] + [f_3, [f_1, f_2]] = 0$

Theorem 2.4:

Let f and g be a vector field with flow Φ_t^f and Φ_s^g , that is

$$\frac{d}{dt} \Phi_t^f = f(\Phi_t^f) \quad \text{And} \quad \frac{d}{ds} \Phi_s^g = g(\Phi_s^g) \tag{2.14}$$

Then

$$\Phi_t^f \circ \Phi_s^g = \Phi_s^g \circ \Phi_t^f \Leftrightarrow [f, g] = 0 \tag{2.15}$$

Definition 2.4

Let f be a smooth vector field on $U \in R^n$ on L , $\lambda: U \mapsto R$ the Lie derivative of λ with respect to f is

$$L_f \lambda(\cdot) = \langle d\lambda(\cdot), f \rangle \tag{2.16}$$

Remarks:

- i) $L_f \lambda$ is the ‘directional derivative’ when $\langle f, f \rangle = 1$
- ii) Note $L_f \lambda: U \mapsto R$ so Lie derivative can be computed iteratively, or

$$L_f(L_f \lambda) = L_f^2 \lambda = \langle d(L_f \lambda), f \rangle$$

$$L_g(L_f \lambda) = L_g L_f \lambda = \langle d(L_f \lambda), g \rangle$$

- iii) Let $\alpha: U \mapsto R$ then $L_{\alpha f} \lambda(x) = \alpha(x) L_f \lambda(x)$
- iv) $L_{[f, g]} \lambda(x) = L_f L_g \lambda(x) - L_g L_f \lambda(x)$
- v) Let $\alpha, \beta: U \mapsto R$ then

$$[\alpha f, \beta g](x) = \alpha(x)\beta(x)[f, g](x) + (L_f \beta(x))\alpha(x)g(x) - (L_g \alpha(x))\beta(x)f(x)$$

- vi) The Lie derivative of a co-vector field ω with respect to vector field f is defined as

$$L_f \omega(\cdot) \triangleq \omega(\cdot) \frac{\partial f}{\partial x} + \left(\frac{\partial \omega^T}{\partial x} f(x) \right)^T$$

Suppose that we are given d smooth vector field f_1, f_2, \dots, f_n on $U \in R^n$. At each $x \in U \in R^n$, we can associate a vector space

$$\Delta(x) \triangleq \text{span}(f_1(x), f_2(x), \dots, f_n(x)) \quad (2.17)$$

The dim of $\Delta(x)$ is

$$\text{Dim}(\Delta(x)) = \text{rank}([f_1(x), f_2(x), \dots, f_n(x)]) \leq d \quad (2.18)$$

Definition 2.5:

A smooth vector distribution on $U \in R^n$ is a smooth mapping from U to the vector space $\{\Delta(x): x \in U\}$

Remarks

- i) A smooth distribution can be described by a set of smooth vector field

$$\Delta(x) = \text{span}(f_1(x), f_2(x), \dots, f_d(x))$$

- ii) Δ is said to be nonsingular with dimension d if $\text{dim}(\Delta(x)) = d, \forall x \in U$.

Otherwise, Δ is said to be singular

Proposition 2.3

Let X_0 be a regular point and smooth distribution Δ with $\text{dim}(\Delta(x)) = d, \forall x \in U$.

There exists a neighborhood of U_0 and smooth vector fields $\{f_1(x), f_2(x), \dots, f_d(x)\}$ such that

- i) $\Delta(x) = \text{span}(f_1(x), f_2(x), \dots, f_d(x))$ on U
 ii) Given Δ , there exists smooth scalar-valued functions

$c_1(x), c_2(x), \dots, c_d(x)$ such that

$$g(x) = \sum_{i=1}^d c_i(x) f_i(x) \forall x \in U_0 \quad (2.19)$$

Definition 2.6:

A distribution Δ is involutive if $g_1, g_2 \in \Delta \Rightarrow [g_1, g_2] \in \Delta$

Lemma 2.1:

Let Δ be a nonsingular distribution defined by smooth vector field $\Delta(x) = \text{span}\{f_1(x), f_2(x), \dots, f_d(x)\}$ then Δ is involutive if and only if $[f_i, f_j] \in \Delta \forall i, j$

Remark: This gives a finite test for involution

Proof: suppose that Δ is involutive then trivially $[f_i, f_j] \in \Delta \forall i, j$. Conversely, let suppose that $[f_i, f_j] \in \Delta \forall i, j$. If $g_1, g_2 \in \Delta$ then

$$g_1(x) = \sum_{i=1}^d c_i(x)f_i(x)$$

$$g_2(x) = \sum_{i=1}^d d_i(x)f_i(x)$$

$$\begin{aligned} \text{So, } [g_1, g_2] &= [\sum_{i=1}^d c_i(x)f_i(x), \sum_{i=1}^d d_i(x)f_i(x)] \\ &= \sum_{i,j=1}^d [c_i f_i, d_j f_j] = \sum_{i,j=1}^d c_i d_i [f_i, f_j] = L_{f_i} d_j c_i f_i - L_{f_j} c_i d_j f_j \end{aligned}$$

$\Rightarrow [g_1, g_2] \in \Delta \forall x \blacksquare$

Definition 2.7: A smooth co-distribution on $U \in R^n$ is a smooth assignment of a ‘co-vector space’ $\Omega(x)$ for each $x \in U$

Remarks:

i) 1-d co-distribution $\lambda: U \mapsto R, \Omega(x) = \text{span}\{d\lambda(x)\}$

ii) Suppose $\omega_1, \omega_2, \dots, \omega_d$ are smooth co-vector fields

$$\Omega(x) = \text{span}\{\omega_1(x), \omega_2(x), \dots, \omega_d(x)\}$$

iii) Suppose Δ is a distribution on $U \in R^n$

$$\Omega(x) = \Delta^\perp(x) \triangleq \{\omega \in (R^n)^*: \langle \omega^*, v \rangle = 0, \forall v \in \Delta\}$$

called annihilator of Δ

Let Δ be a smooth, nonsingular distribution on U . Suppose $x_0 \in U$

$$\Delta(x) = \text{span}\{f_1(x), f_2(x), \dots, f_d(x)\}$$

then there exists a set of (n-d) smooth function:

$\lambda: U \mapsto R$ such that $\text{span}\{d\lambda_1, d\lambda_2, \dots, d\lambda_{n-d}\} = \Delta^\perp$ at some neighborhood of x^0 ,

such that $U^0 \in U$

Definition 2.8: if such definition exists for each $x_0 \in U$ then we say that Δ is completely integrable

Theorem 2.5 (Frobenius Theorem)

A smooth, nonsingular distribution is completely integrable if and only if it is involutive

Proof: Pick any $x^0 \in U$ then on neighborhood U_0 of x_0 there exists a smooth vector field $\{f_1, f_2, \dots, f_d\}$ such that $\Delta = \text{span}(\{f_1, f_2, \dots, f_d\})$ on U

Now, suppose Δ is completely integrable. Then there exists $\lambda_1, \lambda_2, \dots, \lambda_{n-d}$ such that

$$\begin{aligned} \langle d\lambda_i, f_j \rangle &= 0 \text{ for } i = 1, 2, \dots, n-d; j = 1, 2, \dots, d \\ \Leftrightarrow L_{f_i} d\lambda_i &= 0 \Rightarrow \text{span}\{d\lambda_1, d\lambda_2, \dots, d\lambda_{n-d}\} = \Delta^\perp \end{aligned}$$

Thus, need to show $[f_i, f_j] \in \Delta \forall i, j$, indeed,

$$\langle d\lambda_i, [f_i, f_j] \rangle = L_{[f_i, f_j]} \lambda_i = L_{f_j} L_{f_i} \lambda_i - L_{f_i} L_{f_j} \lambda_i = 0, \forall i, j \text{ (Identity) or}$$

$$\begin{bmatrix} d\lambda_1(x) \\ d\lambda_2(x) \\ \dots \\ d\lambda_{n-d}(x) \end{bmatrix} [f_i, f_j] = 0, \forall x \in U^0$$

Thus, $[f_i, f_j] \in (\Delta^\perp)^\perp = \Delta \forall i, j \Rightarrow \Delta$ is involutive ■

Theorem 2.6

Suppose that Δ is involutive, there exists $\lambda_1, \lambda_2, \dots, \lambda_{n-d}$ such that

$$\text{span}\{d\lambda_1, d\lambda_2, \dots, d\lambda_{n-d}\} \in \Delta^\perp$$

Proof: For any $f \in \Delta$, define the flow of f , $\Phi_t^f(x)$ such that

$$\begin{aligned} x(t) &= \Phi_t^f(x^0) \\ \dot{x} &= F(x), x(0) = x^0 \end{aligned}$$

Since $\Delta = \text{span}(\{f_1, f_2, \dots, f_d\})$, Φ is smooth and nonsingular, then there always

$$\text{exists } f_{d+1}, f_{d+2}, \dots, f_n \text{ such that } \text{span} \left(\underbrace{\{f_1, f_2, \dots, f_d\}}_{\text{given}}, \underbrace{\{f_{d+1}, f_{d+2}, \dots, f_n\}}_{\text{find}} \right) = \mathbb{R}^n$$

Now define $F(t_1, t_2, \dots, t_n) \rightarrow \Phi_{t_1}^{f_1} \circ \Phi_{t_2}^{f_2} \circ \dots \circ \Phi_{t_n}^{f_n}(x^0)$, where $|t_i| < \varepsilon, \forall i = 1, 2, \dots, n$

Definition 2.9: Distribution Δ is said to be invariant under a vector field if $[f, \tau] \in \Delta, \forall \tau \in \Delta$

Remarks: Δ is nonsingular distribution of d -dimensional. Let

$$\Delta(x) = \text{span}\{\tau_1(x), \tau_2(x), \dots, \tau_d(x)\}$$

then $[f, \tau] \in \Delta, \forall \tau \in \Delta \Leftrightarrow [f, \tau_i] \in \Delta \forall i = 1, 2, \dots, d$

Lemma 2.2 (Triangular decomposition)

Suppose that Δ is a d-dimensional involutive that is invariant under a vector field then if $x_0 \in U$ then there is a local coordinate transformation $z = \Phi(x)$ such that f can be represented as:

$$\bar{f}(z) = \begin{bmatrix} \bar{f}_1(\zeta_1, \zeta_2) \\ \bar{f}_2(\zeta_2) \end{bmatrix}, \forall z \in \Phi(U^0) \quad (2.20)$$

Proof:

From the theorem 2.4 (Frobenius Theorem), there exists a local transformation Φ on some neighborhood of U^0 of x^0 such that

$$\tau \in \Delta \Leftrightarrow \tau(z) = \begin{bmatrix} \bar{\tau}_1(z) \\ \dots \\ \bar{\tau}_d(z) \\ 0 \\ \dots \\ 0 \end{bmatrix}, \forall z \in \Phi(U^0)$$

Consider the following constant vector field belonging to Δ or

$$\tau \in \Delta \Leftrightarrow \tau(z) = e_i = \begin{bmatrix} 0 \\ \dots \\ 0 \\ 1, j^{th} \\ 0 \\ \dots \\ 0 \end{bmatrix}, \forall z \in \Phi(U^0), i = 1, 2, \dots, d$$

Since Δ is invariant under f , we have;

$$[\bar{f}, \tau] = 0 - \frac{\partial \bar{f}}{\partial z} \tau = - \begin{bmatrix} \frac{\partial \bar{f}_1}{\partial z_1} \\ \frac{\partial \bar{f}_2}{\partial z_2} \\ \dots \\ \frac{\partial \bar{f}_n}{\partial z_n} \end{bmatrix}_{n \times n} \begin{bmatrix} 0 \\ \dots \\ 0 \\ 1 \\ 0 \\ \dots \\ 0 \end{bmatrix}_{n \times 1} = - \begin{bmatrix} \frac{\partial \bar{f}_1}{\partial z_i} \\ \frac{\partial \bar{f}_2}{\partial z_i} \\ \dots \\ \frac{\partial \bar{f}_n}{\partial z_i} \end{bmatrix} \in \Delta$$

Thus, (n-d) term must be zero or $\frac{\partial \bar{f}_k}{\partial z_i} = 0, i = 1, 2, \dots, d; k = d + 1, d + 2, \dots, n$.

Hence, $\bar{f}_k (d + 1 \leq k \leq n)$ cannot depend on z_1, z_2, \dots, z_d .

Equivalently, $\bar{f}_2(z) = \bar{f}_2 \left(\underbrace{z_1, z_2, \dots, z_d}_{\zeta_1}, \underbrace{z_{d+1}, \dots, z_n}_{\zeta_2} \right) = \bar{f}_2(\zeta_2) \blacksquare$

2.3 Local Decomposition of Control System

Consider the input-affine control system (2.11) and (2.12), the objective of this section is to find the necessary condition for some point x_7^0 reachable from x^0 and also to find the sufficient condition for initial state x^a and x^b to be indistinguishable at the output

Lemma 2.3 (Triangular decomposition)

Let Δ is nonsingular distribution of d-dimensional. Assume that

- i) Δ is involutive
- ii) Δ is invariant under f
- iii) $\text{Span}\{g_1, g_2, \dots, g_m\} \in \Delta$

Then for each $x^0 \in U$, there exists a local co-ordinate transformation Φ defined on a neighborhood of U^0 of x^0 such that

$$\left. \begin{aligned} \dot{\zeta}_1 &= \bar{f}_1(\zeta_1, \zeta_2) + \sum_{i=1}^m \bar{g}_{1i}(\zeta_1, \zeta_2) u_i \\ \dot{\zeta}_2 &= \bar{f}_2(\zeta_2) \end{aligned} \right\} \quad (2.21)$$

where $Z = [\underbrace{z_1 \ z_2 \ \dots \ z_d}_{\zeta_1} \ \underbrace{z_{d+1} \ z_{d+2} \ \dots \ z_n}_{\zeta_2}]^T$ then ζ_2 is unaffected by u

or

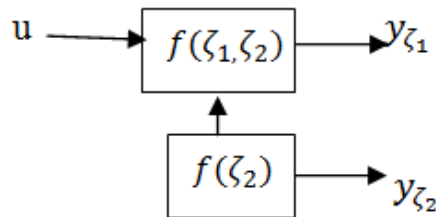


Figure 2.3: Triangular decomposition of affine control system

Proof: From i) and ii) that exists a Φ defined on a neighborhood of U^0 of x^0 such that

$$\bar{f}_i(z) = \begin{bmatrix} \bar{f}_1(\zeta_1, \zeta_2) \\ \bar{f}_2(\zeta_2) \end{bmatrix}, \forall z \in \Phi(U^0)$$

From iii) $g_i \in \Delta, i = 1, 2, \dots, m$

So, necessary

$$\bar{g}_i(z) = \begin{bmatrix} \bar{g}_{ij}(z) \\ 0 \end{bmatrix} \blacksquare$$

Lemma 2.4: Let Δ is nonsingular distribution of d-dimensional. Assume that

- i) Δ is involutive
- ii) Δ is invariant under g_1, g_2, \dots, g_m
- iii) $\Delta \in \text{Span}\{dh_1, dh_2, \dots, dh_p\}^\perp$

Then for each $x^0 \in U$, there exists a local transformation Φ defined on a neighborhood of U^0 of x^0 such that

$$\begin{cases} \dot{\zeta}_1 = \bar{f}_1(\zeta_1, \zeta_2) + \sum_{i=1}^m \bar{g}_{1i}(\zeta_1, \zeta_2) u_i \\ \dot{\zeta}_2 = \bar{f}_2(\zeta_2) + \sum_{i=1}^m \bar{g}_{2i}(\zeta_2) u_i \end{cases} \quad (2.22)$$

and

$$y_i = h_i(\zeta_2), i = 1, 2, \dots, p; \forall z \in \Phi(U^0) \quad (2.23)$$

or

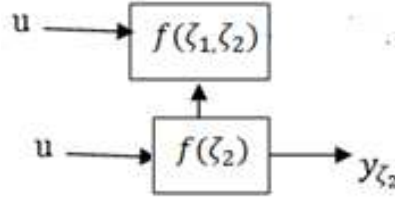


Figure 2.4: Triangular decomposition of affine control system

Proof From i) and ii), we have:

$$\bar{f}(z) = \begin{bmatrix} \bar{f}_1(\zeta_1, \zeta_2) \\ \bar{f}_2(\zeta_2) \end{bmatrix}, \forall z \in \Phi(U^0), \bar{g}_i(z) = \begin{bmatrix} \bar{g}_{1i}(\zeta_1, \zeta_2) \\ \bar{g}_{2i}(\zeta_2) \end{bmatrix}, \forall z \in \Phi(U^0)$$

We have, $\bar{h}_i(z) = h_i \circ \Phi^{-1}(z)$

If $\tau \in \Delta$ then by ii) $\tau \in \text{span}\{\bar{d}h_1, \bar{d}h_2, \dots, \bar{d}h_p\}^\perp$

So, in particular, $\langle \bar{d}h_i, \tau \rangle = 0, i = 1, 2, \dots, p$. By considering the element, Δ of the form, $\tau(z) \in e_i, i=1, 2, \dots, d$ then

$$\langle dh_i, e_j \rangle = \begin{bmatrix} \frac{\partial \bar{h}_i}{\partial z_1} & \frac{\partial \bar{h}_i}{\partial z_2} & \dots & \frac{\partial \bar{h}_i}{\partial z_n} \end{bmatrix} \begin{bmatrix} 0 \\ 0 \\ \vdots \\ 0 \\ 1 \\ 0 \\ \vdots \\ 0 \end{bmatrix}$$

We have, $\frac{\partial \bar{h}_i}{\partial z_j} = 0, i = 1, 2, \dots, p, j = 1, 2, \dots, d \Leftrightarrow \bar{h}_i(z) = \bar{h}_i(\underbrace{z_{d+1}, z_{d+2}, \dots, z_n}_{\zeta_2}) \blacksquare$

2.4 SISO Nonlinear Feedback Theory

Further, this section will provide a means of finding the condition for systems (2.10) and (2.11) which are reachable from the initial condition using the minimal, smooth, and nonsingular distribution. Also, a normal form of equation and zero dynamics of the control system are presented. After that, show how to transform the system (2.10) and (2.11) exactly to linear control system using the two steps: Applying a special coordinate transformation and then applying the nonlinear state feedback.

2.4.1 Normal Form of Equations

Consider an affine nonlinear system as form:

$$\dot{x} = f(x) + g(x)u \quad (2.24)$$

$$y = h(x) \quad (2.25)$$

Definition 2.10 A SISO affine nonlinear system (f, g, h) is said to have relative degree r at x^0 if

- i) $L_g L_f^k h(x) = 0, \forall x \in U^0 \subset U, k = 0, 1, 2, \dots, r - 2$
- ii) $L_g L_f^{r-1} h(x) \neq 0$

Two key facts:

- i) The functions $L_f^k h(x), k = 1, 2, \dots, r - 1$ such that $dh(x^0), dL_f h(x^0), \dots, dL_f^{r-1} h(x^0)$ are linearly independent ($r \leq n$)
- ii) Define the $\Phi_i(x) = L_f^{i-1} h(x), i = 1, 2, \dots, r$. There exists a set of complimentary $\Phi_{r+1}(x), \Phi_{r+2}(x), \dots, \Phi_n(x)$ defined on U^0 such that $L_g \Phi_i(x) = 0, i = 1, 2, \dots, n$ on U^0 and $\Phi(x) = [\Phi_1 \ \Phi_2, \dots, \Phi_n]$ has a nonsingular Jacobian. Hence, Φ is a local diffeomorphism.

Lemma 2.5: (Normal Form Equation)

Given a system (2.24) and (2.25), with relative degree r at x^0 , then there exist a local coordinate transformation $z = \Phi(x)$ on a neighborhood U^0 of x^0 such that

$$\begin{cases} \dot{z}_1 = z_2 \\ \dot{z}_2 = z_3 \\ \dots \\ \dot{z}_{r-1} = z_r \\ \dot{z}_r = b(z) + a(z)u \\ \dot{z}_{r+1} = q_{r+1}(z) \\ \dots \\ \dot{z}_n = q_n(z) \end{cases} \quad (2.26)$$

and

$$y = z_1 \quad (2.27)$$

And the zero dynamics

$$\begin{cases} \dot{z}_{r+1} = q_{r+1}(z) \\ \dot{z}_{r+2} = q_{r+2}(z) \\ \dots \\ \dot{z}_n = q_n(z) \end{cases} \quad (2.28)$$

Here the block diagram of normal form equation

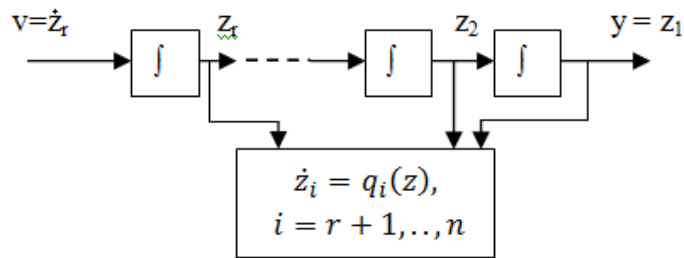


Figure 2.5: Block diagram of normal form of equations

2.4.2 Exact Linearization via Nonlinear Feedback

The problem is to determine $\alpha(x)$ and $\beta(x)$ to make the input/output map $v \mapsto y$ exactly linear as shown in the Figure 2.6.

The Input/output linearization

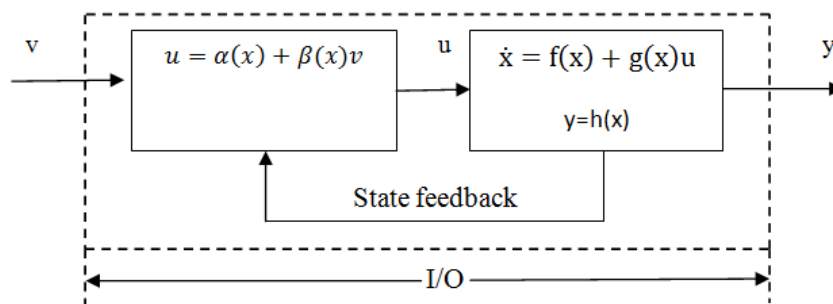


Figure 2.6: The input/output feedback linearization

Four steps:

- i) (f, g, h) must have the full relative degree $r = n$ at x^0

ii) A coordinate transformation $\Phi(x)$ as

$$\Phi(x) = \begin{bmatrix} \Phi_1(x) \\ \Phi_2(x) \\ \dots \\ \Phi_{n-1}(x) \end{bmatrix} = \begin{bmatrix} h(x) \\ L_f h(x) \\ \dots \\ L_f^{n-1} h(x) \end{bmatrix} \quad (2.29)$$

iii) Find $(\tilde{f}, \tilde{g}, \tilde{h})$ in z-coordinate or normal form equations or

$$\begin{cases} \dot{z}_1 = z_2 \\ \dot{z}_2 = z_3 \\ \dots \\ \dot{z}_{n-1} = z_n \\ \dot{z}_n = b(z) + a(z)u \end{cases} \quad (2.30)$$

iv) Applying a nonlinear linearizing feedback law

$$u = \frac{v - b(z)}{a(z)}$$

Some comments:

- i) If the feedback linearization is not exact then closed-loop system is unstable. Even if the pole/zero cancellation (linear system) is perfect this is still a problem that the output still have unstable internal (but not observable) dynamics
- ii) If the nonlinear system has zero dynamics which is locally asymptotically stable near the equilibrium point then the system is called locally minimum phase at the equilibrium point.
- iii) The problem “Zeros in the output” can be generalized to the problem of replacing the same output $y_R(t)$.
- iv) If (f, g, h) has relative degree $r = n$, then state dynamics or I/O mapping and completely and exactly linearizable by feedback and state space transformation.
- v) If (f, g, h) has relative degree $r < n$, then there may exist a \square which (f, g, h) have $r = n$. then the state dynamics are fully linearizable as mapping $v \mapsto y$, but in general, $v \mapsto y$ will not be linear. Should \square not exist or not be of practical use then at most only the I/O mapping $v \mapsto y$ can be linearized. The system has zero dynamics
- vi) If (f, g, h) has no well-defined relative degree at x^0 , then basic theory gives no guidance and advanced theory exist, i.e. dynamic extension.

2.5 MIMO Feedback Control System

In this section, we shall see how the theory developed for SISO systems can be extended to multi-inputs and multi-output nonlinear system. First, some concepts and definition such as relative degree for MIMO are presented and after that the normal form equations, zero dynamics and exact linearization via feedback is given. The application of this approach will be discussed in chapter 5 and 6.

2.5.1 Normal form of equations

Consider an input- affine nonlinear control system

$$\dot{x} = f(x) + \sum_{i=1}^m g_i(x)u_i \quad (2.31)$$

$$y_i = h_i(x), i = 1, 2, \dots, m \quad (2.32)$$

where

$x \in U \subset \mathbb{R}^n$, $f(x)$ and $g(x)$ are n – dimensional vector – valued functions

$u \in \mathbb{R}^m$, $y \in \mathbb{R}^p$, $h(x)$ is m – dimensional vector-valued function

It is assumed that f , g_i and h_i are smooth vector fields. Thus, the derivatives of f , g_i and h_i exist also and continuous on U .

Definition 2.11: (Relative degree for MIMO)

The system (2.1) and (2.2) is said to have a vector relative degree $\{r_1, \dots, r_m\}$ at a point x_0 if

- For each i , $1 \leq i \leq m$,

$$(L_{g_1} L_f^k h_i(x), \dots, L_{g_m} L_f^k h_i(x)) = (0, \dots, 0) \quad (2.32)$$

For all $k < r_i - 1$, and for all x in a neighborhood of x_0

- The $m \times m$ matrix

$$A(x) = \begin{pmatrix} L_{g_1} L_f^{r_1-1} h_1(x) & \dots & \dots & L_{g_m} L_f^{r_1-1} h_1(x) \\ L_{g_1} L_f^{r_2-1} h_2(x) & \dots & \dots & L_{g_m} L_f^{r_2-1} h_2(x) \\ \dots & \dots & \dots & \dots \\ L_{g_1} L_f^{r_m-1} h_m(x) & \dots & \dots & L_{g_m} L_f^{r_m-1} h_m(x) \end{pmatrix} \quad (2.34)$$

is non-singular at $x = x_0$

If the vector relative degree is well defined for the multivariable non-linear system (2.31) and (2.32), then there exists a feedback law which achieves decoupling of the input and output dynamics.

Lemma 2.6 Suppose the system has a (vector) relative degree $\{r_1, \dots, r_m\}$ at x_0 .

Then, the row vectors

$$\begin{cases} dh_1(x^0) dL_f h_1(x^0) \dots dL_f^{r_1-1} h_1(x^0) \\ dh_2(x^0) dL_f h_2(x^0) \dots dL_f^{r_2-1} h_2(x^0) \\ \dots \\ dh_m(x^0) dL_f h_m(x^0) \dots dL_f^{r_m-1} h_m(x^0) \end{cases} \quad (2.35)$$

are linearly independent.

Theorem 2.7

Consider the multivariable nonlinear system (2.31) and (2.32), with m inputs and m outputs. Suppose for each i , $1 \leq i \leq m$

$$(L_{g_1} L_f^k h_i(x), \dots, L_{g_m} L_f^k h_i(x)) = (0, \dots, 0) \quad (2.36)$$

for all $k < r_i - 1$, and for all x in a neighborhood of x_0

$$(L_{g_1} L_f^{r_i-1} h_i(x_0), \dots, L_{g_m} L_f^{r_i-1} h_i(x)) \neq (0, \dots, 0) \quad (2.37)$$

Then the decoupling control problem is solvable by the state feedback law if and only if the matrix $A(x_0)$ is non-singular, i.e. if the system has a vector relative degree $\{r_1, \dots, r_m\}$ at x_0 .

Proposition 2.4 Suppose a system of (2.31) and (2.32) has a (vector) relative degree $\{r_1, \dots, r_m\}$. Then

$$r_1 + r_2 + \dots + r_m \leq n$$

Set, for $1 \leq i \leq m$,

$$\begin{cases} \Phi_1^i(x) = h_i(x) \\ \Phi_2^i(x) = L_f h_i(x) \\ \dots \\ \Phi_{r_i}^i(x) = L_f^{r_i-1} h_i(x) \end{cases} \quad (2.38)$$

If $r = r_1 + r_2 + \dots + r_m$ is strict less than n . it always possible to find $n-r$ more functions $\Phi_{r+1}, \dots, \Phi_n$ such that the mapping

$$\Phi(x) = \text{col}(\Phi_1^1(x), \dots, \Phi_{r_1}^1(x), \Phi_1^m(x), \dots, \Phi_{r_m}^m(x), \Phi_{r+1}(x), \dots, \Phi_n(x))$$

has a jacobian matrix which is nonsingular at x^0 and therefore qualifies as a local coordinate transformation in a neighborhood of x^0 . The value at x^0 of these additional functions can be chosen arbitrarily. Moreover, if the distribution

$$G = \text{span}\{g_1, \dots, g_m\}$$

is involutive near x^0 . It is always possible to choose $\Phi_{r+1}, \dots, \Phi_n$ in such a way that

$$L_{g_j} \Phi_i(x) = 0$$

For all $r + 1 \leq i \leq n$, for all $1 \leq j \leq m$, and all x around x^0

The same steps are used as for SISO for calculating the description of the system

MIMO in the new coordinates:

$$\left\{ \begin{array}{l} \frac{d\Phi_1^1}{dt} = \Phi_2^1 \\ \frac{d\Phi_2^1}{dt} = \Phi_3^1 \\ \dots \\ \frac{d\Phi_{r_1-1}^1}{dt} = \Phi_{r_1}^1 \\ \frac{d\Phi_{r_1}^1}{dt} = L_f^{r_1} h_1(x) + \sum_{j=1}^m L_{g_j} L_f^{r_1-1} h_1(x) u_j \end{array} \right. \quad (2.39)$$

By introducing the new variable, that is,

$$\xi^i = \begin{pmatrix} \xi_1^i \\ \xi_2^i \\ \dots \\ \xi_{r_i}^i \end{pmatrix} = \begin{pmatrix} \Phi_1^i(x) \\ \Phi_2^i(x) \\ \dots \\ \Phi_{r_i}^i(x) \end{pmatrix} \text{ for } 1 \leq i \leq m \quad (2.40)$$

$$\xi = (\xi^1, \dots, \xi^m) \quad (2.41)$$

$$\eta = \begin{pmatrix} \eta_1 \\ \eta_2 \\ \dots \\ \eta_{n-r} \end{pmatrix} = \begin{pmatrix} \Phi_{r+1}(x) \\ \Phi_{r+2}(x) \\ \dots \\ \Phi_n(x) \end{pmatrix} \quad (2.42)$$

And

$$\left\{ \begin{array}{l} a_{ij}(\xi, \eta) = L_{g_j} L_f^{r_i-1} h_i(\Phi^{-1}(\xi, \eta)) \text{ for } 1 \leq i, j \leq m \\ b_i(\xi, \eta) = L_f^{r_i} h_i(\Phi^{-1}(\xi, \eta)) \text{ for } 1 \leq i, j \leq m \end{array} \right. \quad (2.43)$$

Then the equations can be rewritten as normal form of equations

$$\left\{ \begin{array}{l} \dot{\xi}_1^i = \xi_2^i \\ \dots \\ \dot{\xi}_{r_i-1}^i = \xi_{r_i}^i \\ \dot{\xi}_{r_i}^i = b_i(\xi, \eta) + \sum_{j=1}^m a_{ij}(\xi, \eta) u_j \end{array} \right. \quad (2.44)$$

And the output equation:

$$y_i = \xi_1^i \quad (2.45)$$

If the $G = \text{span}\{g_1, \dots, g_m\}$ is involutive distribution, the zero dynamics of the systems as

$$\left\{ \begin{array}{l} \dot{\eta}_1 = q_1(\xi, \eta) \\ \dot{\eta}_2 = q_2(\xi, \eta) \\ \dots \\ \dot{\eta}_{n-r-1} = q_{n-r-1}(\xi, \eta) \\ \dot{\eta}_{n-r} = q_{n-r}(\xi, \eta) \end{array} \right. \quad (2.46)$$

The equations (2.44) and (5.46) characterize the normal form of the equations describing the nonlinear system of equations (2.31) and (2.32), with m inputs and m outputs having a vector relative degree $\{r_1, \dots, r_m\}$ at x^0 .

2.5.2 Exact Linearization via Feedback

The purpose of this section is to illustrate how a system having m inputs and m outputs can be transformed into a linear and controllable system by means of feedback and change of coordinates in the state space.

Consider the system of (2.31) and (2.32); we want to find the static state feedback of form:

$$u_i = \alpha_i(x) + \sum_{j=1}^m \beta_{ij}(x) v_j \quad (2.47)$$

where $\alpha_i(x)$ and $\beta_{ij}(x)$, for $1 \leq i, j \leq m$: Smooth functions, v_j : Components of the new reference inputs

By combining the (2.47), (2.31), and (2.32), we have:

$$\dot{x} = f(x) + \sum_{i=1}^m g_i(x) \alpha_i(x) + \sum_{i=1}^m (\sum_{j=1}^m g_j(x) \beta_{ij}(x)) v_i \quad (2.48)$$

$$y_i = h_i(x), i = 1, 2, \dots, m \quad (2.49)$$

Using the (2.47) for more condensed expression

$$u = \alpha(x) + \beta(x)v \quad (2.50)$$

where

$$u = \begin{bmatrix} u_1 \\ \dots \\ u_m \end{bmatrix}, \alpha(x) = \begin{bmatrix} \alpha_1(x) \\ \dots \\ \alpha_m(x) \end{bmatrix}, \beta(x) = \begin{bmatrix} \beta_{11}(x) & \dots & \beta_{1m}(x) \\ \dots & \dots & \dots \\ \beta_{m1}(x) & \dots & \beta_{mm}(x) \end{bmatrix}, v = \begin{bmatrix} v_1 \\ \dots \\ v_m \end{bmatrix}$$

By combining the (2.31), (2.32) and (2.47), the closed loop system can be rewritten in more convenient ways as

$$\dot{x} = f(x) + g(x)\alpha(x) + g(x)\beta(x)v \quad (2.51)$$

$$y = h(x) \quad (2.52)$$

If $\beta(x)$ is nonsingular for all x , then the feedback (2.50) is called regular static state feedback.

Sate-space Exact Linearization Problem:

Given a set of vector fields $f(x)$ and $g_j(x), j = 1, 2, \dots, m$ and an initial state x^0 , find (if possible), a neighborhood of U of x^0 , a pair of feedback functions $\alpha(x), \beta(x)$ defined on U , a coordinates transformation $z = \Phi(x)$ also defined on U , a matrix $A \in R^{n \times n}$ and matrix $B \in R^{n \times m}$, such that

$$\left[\frac{\partial \Phi}{\partial x} (f(x) + g(x)\alpha(x)) \right]_{|x=\Phi^{-1}(z)} = Az \quad (2.53)$$

$$\left[\frac{\partial \Phi}{\partial x} (g(x)\beta(x)) \right]_{|x=\Phi^{-1}(z)} = B \quad (2.54)$$

and

$$\text{rank}(A \ AB \ \dots \ A^{n-1}B) = n$$

Lemma 2.7

Suppose the matrix $g(x^0)$ has rank m . Then, the State-space Exact Linearization Problem is solvable if and only if there exists a neighborhood U of x^0 and m real-valued functions $h_i(x), i = 1, 2, \dots, m$ defined on U such that the system (2.31) and (2.32) has some (vector) relative degree $\{r_1, \dots, r_m\}$ at x^0 and $r_1 + r_2 + \dots + r_m = n$

Remark: The condition that the matrix $g(x^0)$ has rank m is indeed necessary for the existence of any set of m outputs functions such that the system has some relative degree at x^0 in Proposition 2.1.

Lemma 2.8

Suppose the matrix $g(x^0)$ has rank m . Then, there exist a neighborhood of U of x^0 and m real-valued functions $\lambda_1(x), \lambda_2(x), \dots, \lambda_m(x)$ defined on U such that the system

$$\dot{x} = f(x) + g(x)u \text{ and } y = \lambda(x)$$

has some (vector) relative degree $\{r_1, \dots, r_m\}$ at x^0 with $r_1 + r_2 + \dots + r_m = n$

If and only if:

- i) For each $1 \leq i \leq n - 1$, the distribution G_i has constant dimension near x^0 :
- ii) The distribution G_{n-1} has dimension n :
- iii) For each $1 \leq i \leq n - 2$, the distribution G_i is involutive:

Theorem 2.8: (Exact Linearization Problem)

Suppose the matrix $g(x^0)$ has rank m . Then, the state space exact linearization feedback problem is solvable if and only if

- i) For each $1 \leq i \leq n - 1$, the distribution G_i has constant dimension near x^0 :
- ii) The distribution G_{n-1} has dimension n :
- iii) For each $1 \leq i \leq n - 2$, the distribution G_i is involutive:

By using above mentioned theorems, a feedback control law will be applied and synthesized in the next chapter for the single-span R2R web system. The numerical method is implemented and compared to the backstepping approach.

2.6 Theory of Lyapunov Stability

For the linear control systems, the Nyquist stability criterion, Routh's stability criterion, the first method of Lyapunov (indirect method of Lyapunov) is used for analyzing the stability of the system. For nonlinear systems, the second method of Lyapunov (direct method of Lyapunov) is used. Some definitions and theorems will be introduced in the following:

2.6.1 Some definitions

Consider the system:

$$\dot{x} = f(x, t) \quad (2.55)$$

Where $x, f \in R^n$, t-time, initial condition $x(t_0) = x_0$

Definition 2.12: (Equilibrium state)

A state x_e is called an equilibrium state of the system (2.55) if $f(x_e, t) = 0, \forall t$

Definition 2.13: (Stability in the sense of Lyapunov)

Let $S_\delta = \{x_0: \|x_0 - x_e\| \leq \delta(t_0), \forall t \geq t_0\}$, $\Phi(t; x_0, t_0)$ be solution of the equation (2.55), and $S_\varepsilon = \{\Phi(t; x_0, t_0): \|\Phi(t; x_0, t_0) - x_e\| \leq \varepsilon(t_0), \forall t \geq t_0\}$, then An equilibrium state x_e of the system (2.55) is said to be stable in the sense of Lyapunov if, each S_ε , there exists a S_δ such that trajectories starting in S_δ do not leave S_ε as t increases infinitely.

Definition 2.14 (Uniform stability)

If δ does not depend on t_0 then the equilibrium state is said to be uniform stable.

Definition 2.15 (Asymptotic stability)

An equilibrium state x_e of the system (2.55) is said to be asymptotically stable if it is stable in the sense of Lyapunov and if every solution starting within S_δ converges, without leaving S_ε , to x_e as t increases infinitely.

Definition 2.16 (Asymptotic stability in the large)

- If asymptotic stability holds for all states from which trajectories originate, the equilibrium state is said to be asymptotically stable in the large.

- A necessary for asymptotic stability in the large is that there is only one equilibrium state in the whole state space.

Definition 2.17 (Instability)

An equilibrium state x_e of the system (2.55) is said to be unstable if for some real number $\epsilon > 0$ and any real number $\delta > 0$, no matter how small, there is always a state x_0 in S_δ such that the trajectory starting at this state leaves S_ϵ .

Definition 2.18 (Positive definiteness of scalar function)

A scalar function $V(x)$ is said to be positive definite in a region Ω (which includes the origin of the state space) if $V(x) > 0$ for all nonzero states x in the region Ω and $V(0) = 0$.

Definition 2.19 (Negative definiteness of scalar function)

A scalar function $V(x)$ is said to be negative definite if $-V(x)$ is positive definite.

Definition 2.20 (Positive semi-definiteness of scalar function)

A scalar function $V(x)$ is said to be positive semi-definite if it is positive at all states in region Ω except at the origin and at certain other states, where it is zero.

Definition 2.21 (Negative semi-definiteness of scalar function)

A scalar function $V(x)$ is said to be negative semi-definite if $-V(x)$ is positive semi-definite.

Quadratic form:

$$V(x) = x^T P x = [x_1 \quad x_2 \quad \dots \quad x_n] \begin{bmatrix} p_{11} & p_{12} & \dots & p_{1n} \\ p_{21} & p_{22} & \dots & p_{2n} \\ \dots & \dots & \dots & \dots \\ p_{n1} & p_{n2} & \dots & p_{nn} \end{bmatrix} \begin{bmatrix} x_1 \\ x_2 \\ \dots \\ x_n \end{bmatrix} \quad (2.56)$$

Where x is a real vector and P is a real symmetric matrix

Hermititian form:

$$V(x) = x^T P x = [x_1 \quad x_2 \quad \dots \quad x_n] \begin{bmatrix} p_{11} & p_{12} & \dots & p_{1n} \\ \bar{p}_{12} & p_{22} & \dots & p_{2n} \\ \dots & \dots & \dots & \dots \\ \bar{p}_{1n} & \bar{p}_{2n} & \dots & p_{nn} \end{bmatrix} \begin{bmatrix} x_1 \\ x_2 \\ \dots \\ x_n \end{bmatrix} \quad (2.57)$$

Where x is a complex vector, P is a Hermititian matrix, and \bar{p}_{ij} is complex conjugate of p_{ij} , and for quadratic form $\bar{p}_{ij} = p_{ij}$.

Notes:

- The positive definiteness of the quadratic form or Hermititian form can be determined by Sylvester's criterion or the necessary and sufficient conditions

that quadratic form or Hermitian form $V(x)$ be positive are that all successive principal minors of P be positive.

- $V(x)$ is positive semi-definite if P is singular and all the principal minors are nonnegative.

2.6.2 Second Method of Lyapunov

The idea is from the fact that a vibratory system is stable if total energy (a positive definite function) is continuously decreasing (which means that the time derivative of the total energy must be negative definite) until an equilibrium state is reached.

Theorem 2.9: Consider the system (2.55) and an equilibrium state $x_e = 0$ ($f(0, t) = 0, \forall t$) if there exists a scalar function $V(x, t)$ having continuous, first partial derivative and satisfying the following condition:

- $V(x, t)$ is positive definite
- $\dot{V}(x, t)$ is negative definite

then the equilibrium state at origin is uniformly asymptotically stable.

Theorem 2.10: Consider the system (2.55) and an equilibrium state $x_e = 0$ ($f(0, t) = 0, \forall t$) if there exists a scalar function $V(x, t)$ having continuous, first partial derivative and satisfying the following condition:

- $V(x, t)$ is positive definite
- $\dot{V}(x, t)$ is negative semi-definitive
- $\dot{V}(\Phi(t; x_0, t_0), t)$ does not vanish identically in $t \geq t_0$ for any t_0 and any $x_0 \neq 0$, where $\Phi(t; x_0, t_0)$ denotes the trajectory or solution starting from x_0 and t_0

then the equilibrium state at origin is uniformly asymptotically stable in the large.

Theorem 2.11:

Let $V: R^n \rightarrow R$ be a C^1 radially unbounded function and $x = 0$ be an equilibrium point of $\dot{x} = f(x)$ such that

- $V(0) = 0$
- $V(x) > 0$ when $x \neq 0$
- $\dot{V}(x) < 0$ when $x \neq 0$

then the system is globally asymptotically stable (GAS) at $x = 0$

Theorem 2.12: Consider the system (2.55) and an equilibrium state $x_e = 0$ ($f(0, t) = 0, \forall t$) if there exists a scalar function $W(x, t)$ having continuous, first partial derivative and satisfying the following condition:

- $W(x, t)$ is positive definite in some region about the origin
- $\dot{W}(x, t)$ is positive definite in the same region

then the equilibrium state at origin is unstable.

2.7 Backstepping Based Design Theory

The backstepping design methodology was originally introduced in adaptive control theory to systematically construct a feedback control law. Various BS design techniques have been introduced such as integrator, strict-feedback systems, and adaptive, robust backstepping. In this research, a modified back-stepping approach is employed for the non-linear MIMO system. The modified backstepping approach for MIMO systems involves recursive processes which break a design problem on the full system down to a sequence of sub-problems on lower order systems. Considering each lower order system with a Control Lyapunov Function (CLF) and paying attention to the interaction between two subsystems makes it modular and easy to design the backstepping controller (BSC). The resultant final BSC for the full system meets the performance specifications and achieves globally asymptotical stability. First, the concepts and basic problem using the backstepping approach are presented and then in the second section, a systematic design for a class of nonlinear control system is proposed. The applicability and reliability of the proposed algorithm will be implemented and compared to the exact linearization approach in the next chapter.

2.7.1 Concepts of Basic Backstepping Design

Consider an affine form system as follows:

$$\dot{z} = f(z) + g(z)\xi \quad (2.58)$$

$$\dot{\xi} = u \quad (2.59)$$

A state feedback control law is designed to asymptotically globally stabilize system at the origin. This is addressed as a cascade connection of two components in which the first one is an integrator:

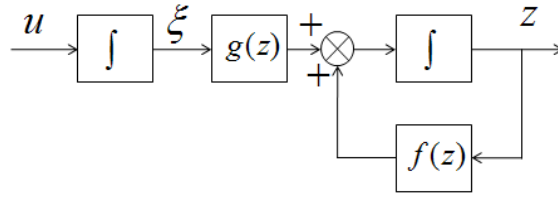


Figure 2.7: Backstepping based system design

Suppose we can asymptotically globally stabilize the first system of

$$\dot{z} = f(z) + g(z)\xi$$

We add a virtual control law $\xi = \phi(z)$ in which $\phi(0) = 0$, this implies that the origin of

$$\dot{z} = f(z) + g(z)\phi(z) \quad (2.60)$$

is asymptotically global stable as discussed in section 2.9 in chapter 2.

A Control Lyapunov Function (CLF) $V(z)$ is chosen and satisfies the inequality:

$$\frac{\partial V}{\partial z} [f + g\phi] \leq -W(z) \quad (2.61)$$

where $W(z)$ is a positive definite function. By adding and subtracting $g(z)\phi(z)$ to obtain the following equation:

$$\dot{z} = f(z) + g(z)\phi(z) + g(z)[\xi - \phi(z)] \quad (2.62)$$

$$\dot{\xi} = u$$

The resultant system is shown by block diagram as in Figure 2.8

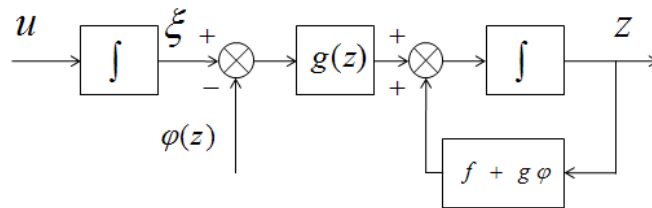


Figure 2.8: Introduction of control

The change of variables is added as follows:

$$y = \xi - \phi(z) \quad (2.63)$$

which generates the following system equations

$$\dot{z} = f(z) + g(z)\phi(z) + g(z)y \quad (2.64)$$

$$\dot{y} = u - \dot{\phi}(z) \quad (2.65)$$

which is shown in Figure 2.8. This change variable is often called backstepping since the “backstepping” of the control by $-\dot{\phi}(z)$ through the integrator

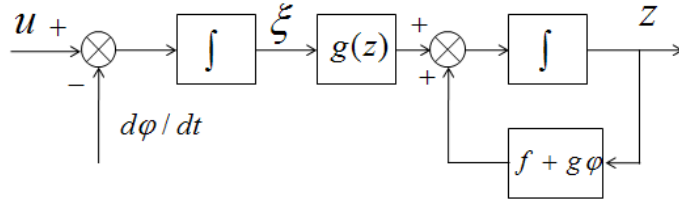


Figure 2.9: Backstepping control via integrator

Since f , g , and ϕ are gen functions, the time derivative can be written as:

$$\dot{\phi}(z) = \frac{\partial \phi}{\partial z} [f(z) + g(z)\xi] \quad (2.66)$$

A new variable $v = u - \dot{\phi}(z)$ is introduced to reduce the system to

$$\dot{z} = f(z) + g(z)\phi(z) + g(z)y \quad (2.67)$$

$$\dot{y} = v \quad (2.68)$$

Which has the same form as the system we started with the exception that we now know the first system is asymptotically stable at the origin. This modular property of backstepping will be exploited to stabilize the overall system.

This is done by considering a candidate Lyapunov function

$$V_c(z, \xi) = V(z) + \frac{1}{2}y^2 = V(z) + \frac{1}{2}(\xi - \phi(z))^2 \quad (2.69)$$

The time derivative of V_c is written as follows:

$$\dot{V}_c(z, \xi) = \frac{\partial V}{\partial z} [f + g\phi] + \frac{\partial V}{\partial z} g(z)y + yv \leq -W(z) + \frac{\partial V}{\partial z} g(z)y + yv \quad (2.70)$$

By choosing

$$v = -\frac{\partial V}{\partial z} g(z) - ky, k > 0$$

This implies that

$$\dot{V}_c(z, \xi) \leq -W(z) = ky^2 \quad (2.71)$$

which implies the origin is asymptotically stable at the origin. Since $\phi(0) = 0$, this implies that $z = 0$ and $\xi = 0$ is also asymptotically stable.

Lemma 2.9

Consider the system (2.58) and (2.59), let $\phi(z)$ be a stabilizing state feedback law for the system in Equations (2.58) and (2.59) where $\phi(0) = 0$. Let $V(z)$ be Lyapunov candidate function such that

$$\frac{\partial V}{\partial z} [f(z) + g(z)\phi(z)] \leq -W(z)$$

For some positive definite W , then the feedback law

$$u = \frac{\partial \phi}{\partial z} [f(z) + g(z)\xi] - \frac{\partial V}{\partial z} g(z) - k[\xi - \phi(z)], k > 0$$

asymptotically globally stabilizes the origin with the CLF:

$$V(z) = \frac{1}{2} [\xi - \phi(z)]^2$$

2.7. Backstepping Based Design of Modified Strict-feedback Form

The input-output decoupling problem for the nonlinear control system (2.72) - (2.77) can be obtained by a feedback control law with the conditions mentioned in the above theorems. The question arises on how to determine such a control law. In this dissertation, a systematic method is proposed to transform the nonlinear system into the equivalent linear system by a change of state coordinates and the state feedback using the backstepping approach.

Consider an MIMO affine nonlinear system in the following form

$$\dot{x}_1 = f_1(x_1, x_2, x_3) \quad (2.72)$$

$$\dot{x}_2 = f_2(x_1, x_2, x_3, x_4) + g_1(x_1, x_2, x_3, x_4)u_1 \quad (2.73)$$

$$\dot{x}_3 = f_3(x_1, x_2, x_3, x_4) \quad (2.74)$$

$$\dot{x}_4 = f_4(x_1, x_2, x_3, x_4) + g_2(x_1, x_2, x_3, x_4)u_2 \quad (2.75)$$

with the output equations:

$$y_1 = h_1(x) \quad (2.76)$$

$$y_2 = h_2(x) \quad (2.77)$$

Where $x \in \mathbb{R}^4$, $f(x)$ and $g(x)$ are 4 – dimensional vector – valued functions
 $u \in \mathbb{R}^2$, $y \in \mathbb{R}^2$, $h(x)$ is 2 – dimensional vector-valued function

It is assumed that the system has a well-defined relative degree at equilibrium points and the x_2, x_4 variables in Eqs. (2.72) and (2.74) are solvable explicitly in terms of the other variables. Thus, input-output decoupling problem is solvable by a state space feedback exact linearization law and the state feedback law is designed using the backstepping approach.

The objective is to design a control law for the nonlinear control system (2.72)-(2.77) such that $x_1 \rightarrow x_{1ref}$ and $x_3 \rightarrow x_{3ref}$ asymptotically where x_{1ref} and x_{3ref} are constant and globally asymptotical stability (GAS) in sense of the Theorem 2.11 is achieved with no overshoots in the system. The following are the steps for formulating the BSC for the system (2.72)-(2.77).

Step 1: x_2 is regarded as a control input in Eq. (2.72) that is considered as the first subsystem. Thus, x_2 is chosen to make the first subsystem GAS. The choice is called a virtual control law, i.e.

By putting

$$\zeta_1 = x_1 - x_{1ref} \quad (2.78)$$

By differentiating both sides of the Equation (2.78) in time and combining with the Equation (2.72), we have:

$$\dot{\zeta}_1 = \dot{x}_1 = f_1(\zeta_1 + x_{1ref}, x_2, x_3) \quad (2.79)$$

For the Equation (2.79), a CLF $V(\zeta_1)$ can be chosen such that when the virtual control law is applied, its time derivative becomes negative definite, i.e.

$$V_1 = \frac{1}{2}\zeta_1^2 \quad (2.80)$$

By taking derivative in time of the Equation (2.80) and combining with the Equation (2.79) results in;

$$\dot{V}_1 = \zeta_1 \dot{\zeta}_1 = \zeta_1 f_1(\zeta_1 + x_{1ref}, x_2, x_3) \quad (2.81)$$

By satisfying the GAS condition in a sense of Lyapunov in Theorem 2.11 for the Equation (2.81), a virtual control law α_1 can be chosen as follows;

$$\begin{aligned} -c_1 \zeta_1 &= f_1(\zeta_1 + x_{1ref}, x_2, x_3) \\ \rightarrow \alpha_1 &= \lambda_1(c_1, \zeta_1, x_3) \equiv x_2 \end{aligned} \quad (2.82)$$

where c_1 is the positive gain

By doing so, we have:

$$\dot{V}_1 = \zeta_1 \dot{\zeta}_1 = -c_1 \zeta_1^2 < 0 \quad \forall \zeta_1 \neq 0 \quad (2.83)$$

Step 2: By choosing the state feedback (2.82) and a change of coordinate (2.78) and (2.84), or

$$\zeta_2 = x_2 - \alpha_1 \quad (2.84)$$

The second subsystem can be rewritten as follows:

$$\left. \begin{aligned} \dot{\zeta}_1 &= -c_1 \zeta_1 \\ \dot{\zeta}_2 &= f_2(\zeta_1 + x_{1ref}, \zeta_2 + \alpha_1, x_3) + g_1(\zeta_1 + x_{1ref}, \zeta_2 + \alpha_1, x_3)u_1 - \dot{\alpha}_1 \end{aligned} \right\} \quad (2.85)$$

A CLF $V_2(\zeta_1, \zeta_2)$ can be chosen such that it makes the subsystem (2.85) GAS with the virtual control law, i.e.

$$V_2 = V_1 + \frac{1}{2}\zeta_2^2 \quad (2.86)$$

Taking the derivative of the Equation (2.86) in time and combining with the Equation (2.16) result in;

$$\begin{aligned} \dot{V}_2 = & -c_1\zeta_1^2 + \zeta_2(f_2(\zeta_1 + x_{1ref}, \zeta_2 + \alpha_1, x_3, x_4) \\ & + g_1(\zeta_1 + x_{1ref}, \zeta_2 + \alpha_1, x_3, x_4)u_1 - \dot{\alpha}_1) \end{aligned} \quad (2.87)$$

To meet the GAS condition in the sense of Lyapunov in Theorem 2.11 for the Equation (2.87), a control law u_1 can be chosen such that

$$\begin{aligned} -c_2\zeta_2 &= f_2(\zeta_1, \zeta_2, x_3, x_4) + g_1(\zeta_1, \zeta_2, x_3, x_4)u_1 - \dot{\alpha}_1 \\ \rightarrow u_1 &= \lambda_2(c_1, c_2, x_1, x_2, x_3, x_4) \end{aligned} \quad (2.88)$$

where c_2 is the positive gain

By doing so, we have:

$$\dot{V}_2 = -c_1\zeta_1^2 - c_2\zeta_2^2 < 0 \quad \forall \zeta_1, \zeta_2 \neq 0 \quad (2.89)$$

Step 3: by choosing the state feedbacks (2.82) and (2.88) and a change of state transformations (2.78) and (2.84), the third subsystem can be rewritten as follows:

$$\left. \begin{aligned} \dot{\zeta}_1 &= -c_1\zeta_1 \\ \dot{\zeta}_2 &= -c_2\zeta_2 \\ \dot{x}_3 &= f_3(\zeta_1 + x_{1ref}, \zeta_2 + \alpha_1, x_3, x_4) \end{aligned} \right\} \quad (2.90)$$

By putting

$$\zeta_3 = x_3 - x_{3ref} \quad (2.91)$$

The third subsystem can be rewritten as follows:

$$\left. \begin{aligned} \dot{\zeta}_1 &= -c_1\zeta_1 \\ \dot{\zeta}_2 &= -c_2\zeta_2 \\ \dot{\zeta}_3 &= f_3(\zeta_1 + x_{1ref}, \zeta_2 + \alpha_1, \zeta_3 + x_{3ref}, x_4) \end{aligned} \right\} \quad (2.92)$$

Now, x_4 is regarded as a control input in the subsystem (2.92). So, x_4 can be chosen to make the subsystem (2.92) GAS. A CLF $V_3(\zeta_1, \zeta_2, \zeta_3)$ can be chosen such that it makes the subsystem (2.92) GAS with the virtual control law, i.e.

$$V_3 = V_2 + \frac{1}{2}\zeta_3^2 \quad (2.93)$$

By taking the derivative of the Equation (2.93) in time and combining with the Equation (2.92) result in;

$$\dot{V}_3 = -c_1\zeta_1^2 - c_2\zeta_2^2 + \zeta_3 f_3(\zeta_1 + x_{1ref}, \zeta_2 + \alpha_1, \zeta_3 + x_{3ref}, x_4) \quad (2.94)$$

To satisfy the GAS condition in the sense of Lyapunov in Theorem 2.11 for the Equation (2.94), a virtual control law α_2 can be chosen such that

$$-c_3\zeta_3 = f_3(\zeta_1 + x_{1ref}, \zeta_2 + \alpha_1, \zeta_3 + x_{3ref}, x_4)$$

$$\rightarrow \alpha_2 = \lambda_3(c_1, c_2, c_3, \zeta_1, \zeta_2, \xi_3) \equiv x_4 \quad (2.95)$$

where c_3 is the positive gain

By doing so, we have:

$$\dot{V}_3 = -c_1\zeta_1^2 - c_2\zeta_2^2 - c_3\zeta_3^2 < 0 \quad \forall \zeta_1, \zeta_2, \zeta_3 \neq 0 \quad (2.96)$$

Step 4: by choosing the state feedbacks (2.82) (2.88) and (2.95) and a change of state transformations (2.78) (2.84) and (2.91), the complete system can be rewritten as follows:

$$\left. \begin{aligned} \dot{\zeta}_1 &= -c_1\zeta_1 \\ \dot{\zeta}_2 &= -c_2\zeta_2 \\ \dot{\zeta}_3 &= -c_3\zeta_3 \\ \dot{x}_4 &= f_4(\zeta_1 + x_{1ref}, \zeta_2 + \alpha_1, \zeta_3 + x_{3ref}, x_4) + \\ &g_2(\zeta_1 + x_{1ref}, \zeta_2 + \alpha_1, \zeta_3 + x_{3ref}, x_4)u_2 \end{aligned} \right\} \quad (2.97)$$

$$\text{By putting} \quad \zeta_4 = x_4 - \alpha_2 \quad (2.98)$$

The complete system is rewrite as follows:

$$\left. \begin{aligned} \dot{\zeta}_1 &= -c_1\zeta_1 \\ \dot{\zeta}_2 &= -c_2\zeta_2 \\ \dot{\zeta}_3 &= -c_3\zeta_3 \\ \dot{\zeta}_4 &= f_4(\zeta_1 + x_{1ref}, \zeta_2 + \alpha_1, \zeta_3 + x_{3ref}, \zeta_4 + \alpha_2) \\ &+ g_2(\zeta_1 + x_{1ref}, \zeta_2 + \alpha_1, \zeta_3 + x_{3ref}, \zeta_4 + \alpha_2)u_2 - \dot{\alpha}_2 \end{aligned} \right\} \quad (2.99)$$

A CLF $V_4(\zeta_1, \zeta_2, \zeta_3, \zeta_4)$ can be chosen such that it makes the subsystem (2.99) GAS with the real control law, i.e.

$$V_4 = V_3 + \frac{1}{2}\zeta_4^2 \quad (2.100)$$

By taking the derivative of the Equation (2.100) in time and combining with the Equation (2.99) Result in;

$$\dot{V}_4 = -c_1\zeta_1^2 - c_2\zeta_2^2 - c_3\zeta_3^2 + \zeta_4(f_4(\zeta_1, \zeta_2, \zeta_3, \zeta_4) + g_2(\zeta_1, \zeta_2, \zeta_3, \zeta_4)u_2 - \dot{\alpha}_2) \quad (2.101)$$

To satisfy the GAS condition in a sense of Lyapunov in Theorem 2.11 for the Equation (2.101), a control law u_2 can be chosen such that

$$\begin{aligned} -c_4\zeta_4 &= f_4(\zeta_1, \zeta_2, \zeta_3, \zeta_4) + g_1(\zeta_1, \zeta_2, \zeta_3, \zeta_4)u_2 - \dot{\alpha}_2 \\ u_2 &= \lambda_4(c_1, c_2, c_3, c_4, x_1, x_2, x_3, x_4) \end{aligned} \quad (2.102)$$

where c_4 is the positive gain

By doing so, we have:

$$\dot{V}_4 = -c_1\zeta_1^2 - c_2\zeta_2^2 - c_3\zeta_3^2 - c_4\zeta_4^2 < 0 \quad \forall \zeta_1, \zeta_2, \zeta_3, \zeta_4 \neq 0 \quad (2.103)$$

Thus, by choosing the state feedbacks (2.82) (2.88) (2.95) and (2.102) and a change of state transformations (2.78) (2.84), (2.91) and (2.98), the nonlinear control system (2.72) – (2.77) is transformed into the decoupled linear control system as follows

$$\left. \begin{aligned} \dot{\zeta}_1 &= -c_1 \zeta_1 \\ \dot{\zeta}_2 &= -c_2 \zeta_2 \\ \dot{\zeta}_3 &= -c_3 \zeta_3 \\ \dot{\zeta}_4 &= -c_4 \zeta_4 \end{aligned} \right\} \quad (2.104)$$

By examining the system (2.104), it is clear that the system is stable and converges to zero with positive gains and the response of the system has no overshoots. The desired settling time and rising time of system are obtained by tuning the gains. Thus, the stability and performance specifications on the system (2.71)-(2.77) are achieved with the BSC.

In summary, the BSC for the system (2.72) – (2.77) is given as follows

$$\left. \begin{aligned} u_1 &= \lambda_2(c_1, c_2, x_1, x_2, x_3, x_4) \\ u_2 &= \lambda_4(c_1, c_2, c_3, c_4, x_1, x_2, x_3, x_4) \end{aligned} \right\} \quad (2.105)$$

where c_1, c_2, c_3 and c_4 are positive gains that are determined optimally by using the modified genetic algorithm in chapter 3.

2.8 Some Comments

It is clear that the idea of backstepping based design approach is feasible by applying consecutively the coordinate transformation and choosing feedback law via Control Lyapunov Function (CLF) to each subsystem from the lowest to highest order and rewrite the feedback law in the original coordinates, By examining the system (2.104), it is clear that the system is stable and converges to zero with positive gains and the response of the system has no overshoots and the resulted controllers (2.105) called backstepping controller make original system a well-tracking command and asymptotically global stable.

3. Modification of Genetic algorithm

In this chapter, a brief summary of genetic algorithm (GA) and recent GA based control algorithm are outlined, a proposed modification of the GA for control system is addressed and then an example of application is given to prove the reliability of the MGA. Finally, an algorithm is proposed for the intelligent control systems which can detect the system errors and automatically recover the errors at every time interval due to the changing parameters and disturbances in the different operating conditions.

3.1. Introduction

With the rapid development of digital computer in recent years, the genetic algorithm (GA) is considered as a key role in developing the modern automation systems and the other fields that have the ability of detecting the system errors due to the external and internal disturbances and automatically recovering the errors in order to make system stable and improve the precision. Until now, some modifications of GA are proposed and applied to automation systems (Aytakin Bagis, 2007; H. Madadi Kojabadi and Q. Cao, 2005; Jin-Sung Kim, Jin-Hwan Kim, Ji-Mo Park, Sung-Man Park, Won-Yong Choe and Hoon Heo, 2008 ;Y.P. Wang, H.H. Chung, N.R. Watson, and S.S. Matair, 2000). To achieve more effective search, the optimization algorithm (Aytakin Bagis, 2007) is based on the integration of classical genetic algorithm structure and systematic neighborhood structure. The simulation results show that the proposed algorithm is applied only on the limit range such SISO linear system. The analytical procedures (M. Zhunang and D. P. Atherton, 1993) for obtaining optimum PID controller settings for minimization of time weighted integral performance criteria is employed for the dead time plant model. A method to design an optimal disturbance rejection PID controller is proposed by (Renato A. Kronhling and Joost P. Rey, 2001) based on optimization of the disturbance rejection constraints. The simulation outcomes prove the slow response in time. An optimization algorithm is proposed for designing PID controllers (H. Madadi Kojabadi and Q. Cao, 2005; Chen-Huei Hsieh and Jyh-Hong Chou (2007)), which minimizes the asymptotic open-loop gain of a system with uncertainty using the quantitative feedback theory. Hung-Cheng Chen and Sheng-Hsiung Chang (2006)

suggested a PID controller design for an active magnetic bearing using the genetic algorithm. The results show that the proposals are convenient for control system with fixed parameters and with no high accuracy requirement. In reality, there are many plants with the varying parameters in time in operating progress such as roll-to-roll web control system and under the effect of disturbances in operating process. Therefore, detecting the system errors and automatically recovering the errors are necessary and are has been given attention by researchers in recent years. In this paper, an algorithm is proposed for the non-linear control systems with the changing parameters in time and due to the impact of disturbances. The contributions of the proposed algorithm are the following:

- The proposed algorithm is able to design the optimal controller of non-linear system based on the state space approach and classic genetic algorithm
- With rapid development of calculation speed of digital computer and sensor technology, the algorithm can be applied to design the intelligent control systems which can detect the system errors and automatically recover the errors at every time interval due to the changing parameters and disturbances in the different operating conditions

3.2 A Classical Approach of Genetic algorithm

Genetic algorithm is stochastic search method that mimics the metaphor of natural biological evolution. Genetic algorithm starts with no knowledge of the correct solution and depends completely on responses from its environment and evolution operators (i.e. reproduction, crossover and mutation) to arrive at the best solution. By beginning with the initial populations and searching in parallel, the algorithm avoids local minima and converging to sub optimal solutions. Figure 1 shows the structure of a genetic algorithm. Genetic algorithms work on populations of individuals instead of single solutions. In this way the search is performed in a parallel manner. There are three main stages of a genetic algorithm; these are known as reproduction, crossover, and mutation

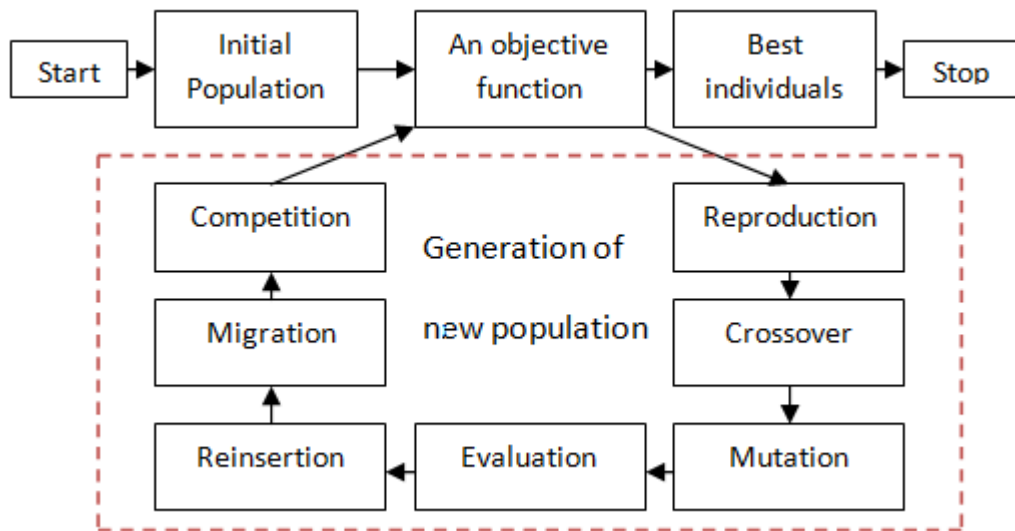


Figure 3.1: Block diagram of the GA

Reproduction: During the reproduction phase the fitness value of chromosome is assessed. This value is used in the selection process to provide bias towards fitter individuals. It is suitable with the evolution process that the best elements will be selected to reproduce in the next generations.

Crossover: after the selection is finished, the crossover algorithm is initiated. The crossover operation swaps certain parts of the two selected strings in a bit to capture the good parts of old chromosomes and create new ones.

Mutation: Using selection and crossover on their own will generate a large amount of different strings. However, there are two main problems with this:

- Depending on the initial population chosen, there may not be enough diversity in the initial strings to ensure the GA searches the entire problem space.
- The GA may converge on sub-optimum strings due to a bad choice of initial population

Algorithm:

- Initiate the strategy parameters
 - Create and initialize the initial gains
 - For each gain
 - Integrate the motion equations
 - Evaluate the objective function J

```

End
While stopping condition(s) not true do
  For i =1, n do
    Choose  $i \geq 2$ , new gains at random
      Create offspring through application of crossover operator
      Mutate offspring strategy parameters
      Integrate the motion equations
      Evaluate the objective function of new gains
      If value of objective function is less than epsilon
        Best gains
      End
    End
  End
  Select the new population
  t = t +1
End

```

The use of real-coded GAs with search operator find more suited than binary GAs in finding feasible gains from feasible parent gains. In this proposal, the use of real-coded GAs with simulated binary crossover (SBX) and a parameter-based mutation operator is implemented. The mutation probability, mutation parameter, crossover rate and crossover probability is selected depending on the speed of convergence of algorithm

3.3. Modified Genetic Algorithm and Applications

The modification of genetic algorithm in this thesis is based on the idea about an algorithm that is able to design optimally the parameters of controller in non-linear control systems. Depending on the state space approach, numerical algorithm for the ordinary differential equations (ODE) and classical genetic algorithm, an algorithm is proposed for designing the optimal controller for the nonlinear control system. On the other hand, with the rapid development of digital computer and sensor technology in recent years, PC-based control algorithm design is paid special attention by many researchers and engineers. So, depending on the minimum of objective function of output errors, consumption energy and PC-based design, the

proposed algorithm can be applied to automatically tune the parameters of controllers at time interval due to the changing factors in time and disturbances.

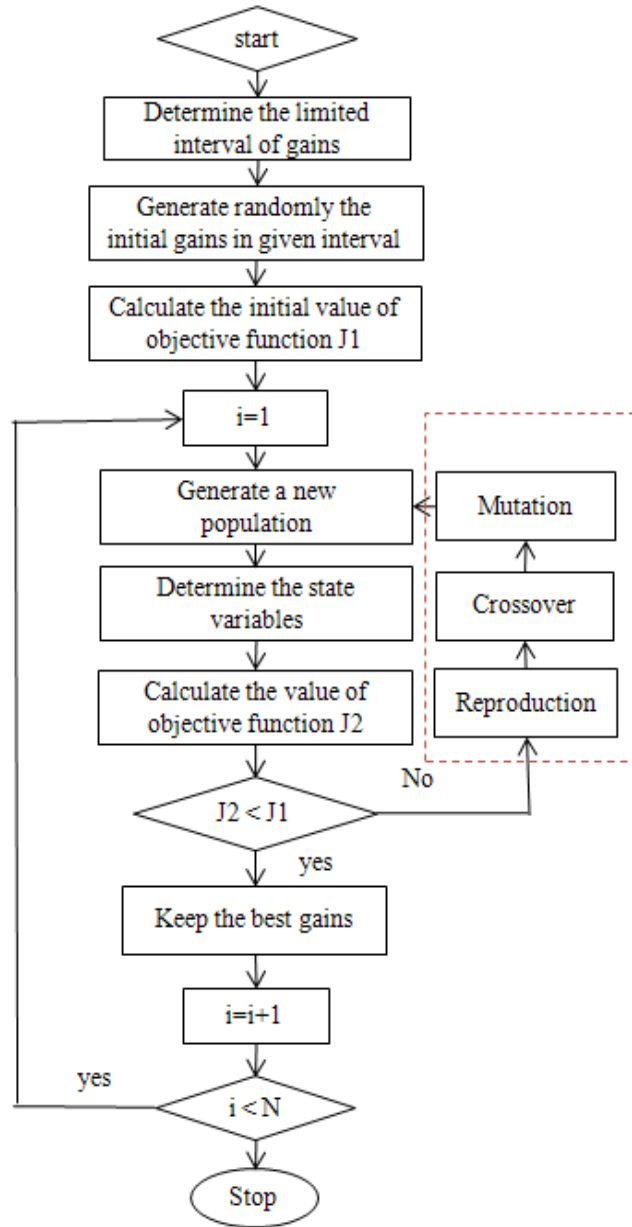


Figure 3.2: Block diagram of the MGA

Figure 3.2 is the block diagram of the MGA with the objective function shown in the Equation (3.1).

$$J = \beta_i \sum_{i=1}^N (e_i^2) + \eta_j \sum_{j=1}^M (\tau_j^2) \quad (3.1)$$

where N and M are the number of control variables and state errors, respectively. β_i, η_j are scale factors, $e_i(i=1, 2... N)$ is the error between the operating and reference points and $\tau_j(j=1, 2...M)$ is control variables.

In the next of the chapter, the effectiveness of proposed MGA will be implemented by numerical simulation. A PID controller design is employed for the third order system with the transfer function (3.2) and objective function (3.1) with parameters shown in Table 3.1.

$$G = \frac{4.228}{(s + 0.5)(s^2 + 1.64s + 8.456)} \quad (3.2)$$

Simulation results shown in Table 3.2 with ten times of simulations prove the convergence and reliability of the proposed algorithm. With ten times of simulations, it is clear that the third one is with the minimum value of objective function from Table 3.2. So, optimal gains are chosen in accordance with this case. Figure 3.3 shows the change in time of gains K_p , K_i , and K_d with 100 generations.

Table 3.1: Parameters of the MGA

Parameters	Values
A number of generation	N=100
Size of population	S=40
The probability of mutation	$p_m = 0.8$
The probability of crossover	$p_c = 0.5$
Scale factors	$\beta_1 = \eta_1 = 0.02$

Table 3.2: Simulation Results of the Third Order System

No.	K_p	K_I	K_D	Value of O.F.
1	1.416	0.9200	0.4335	0.0434
2	1.492	0.9897	0.5443	0.0433
3	1.157	0.7590	0.1175	0.0412
4	1.156	0.7731	0.1181	0.0412
5	1.318	0.8631	0.2949	0.0431
6	1.378	0.8999	0.3686	0.0433
7	1.449	0.9602	0.4746	0.0434
8	1.357	0.8789	0.3584	0.0432
9	1.353	0.8810	0.3483	0.0432
10	1.426	0.9361	0.4465	0.0434

In order to estimate the improvement of the proposed algorithm, the comparison of performance of system with Ziegler-Nichols (ZN) tuning method is employed. Figure 3.4 shows the step response of the third order system in two cases with MGA controlled and ZN controlled system.

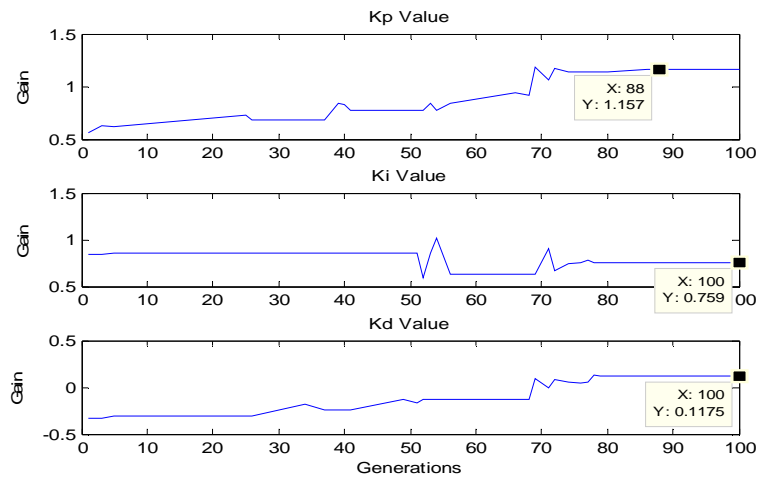


Figure 3.3: The change of PID gains in time

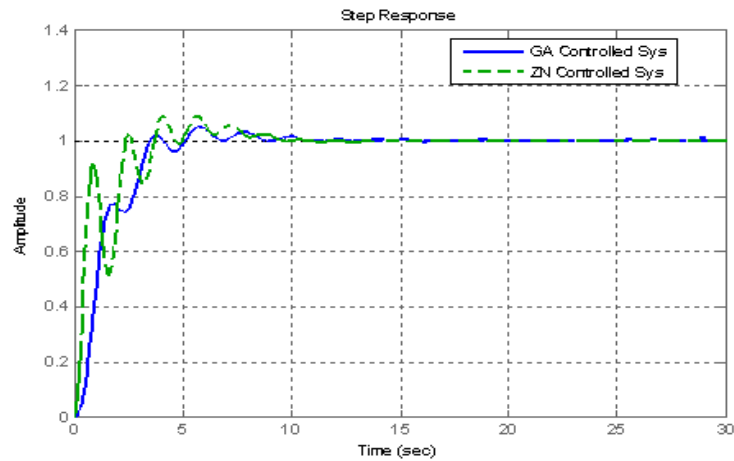


Figure 3.4: Step response of the third order system

3.4 Control System Design of Automatically Tuning Controller

Nowadays there are many applications in industry that require the manufacturing system with the flexible response and high precision due to the changing of operating condition. The concept of intelligent control and automation system is generated with the rapid development of digital computers which is able to detect the errors of system in the operating process due to the changing parameters and external disturbances and automatically recovering the errors to make plant stable and precise. In recent years, the PC-based control system and flexible automation system design is taken much attention by researchers and engineers and is a favor trend in designing the automation system. Basing on the rapid development of sensor technology, calculation speed of digital computers, and modified genetic

algorithm, an approach is proposed for designing the intelligent control system. Figure 3.5 shows the block diagram of control system of automatically tuning controller.

In this proposal, digital computers are considered as controllers. The use of sensors is to determine the output values of system. Depending on the reference values, output values and the objective function, the proposed algorithm calculates the convenient gains of controllers and automatically updates the gains after certain time intervals. The performance of the proposed algorithm is divided into two stages. The first one is to design the optimal gains of controllers by using on the initial parameters of system and the modified genetic algorithm shown in Figure 3.2. Due to the change of parameters and disturbances in operating process, the initial gains are not suitable any more. Thus, a gain tuning scheme needs to be employed at every time interval to make system stable and reliable. The second one has a function that will adjust automatically the gains by using the information about the difference between the output and reference and the value of objective function in Equation (3.1). The following is the algorithm diagram for control system design of automatically tuning controller scheme.

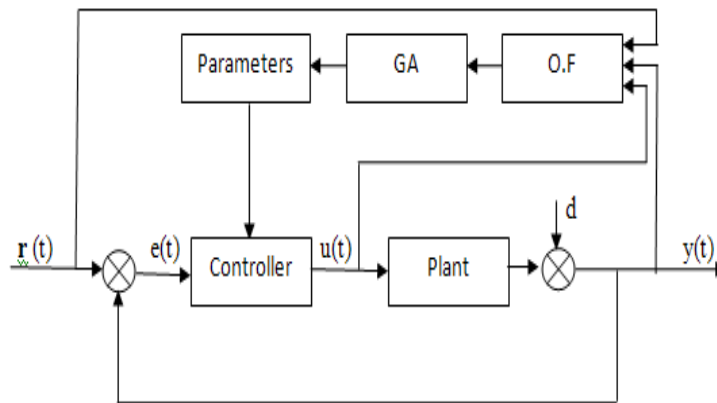


Figure 3.5: Control system design of automatically tuning controller scheme

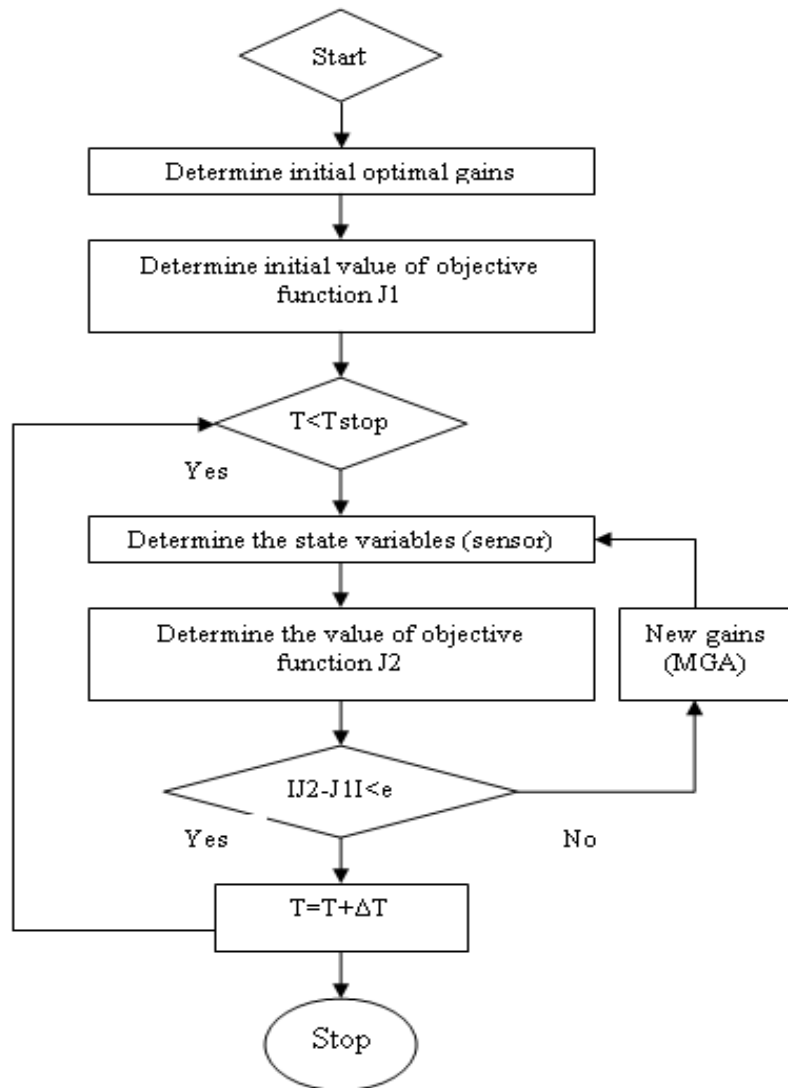


Figure 3.6: The algorithm diagram of automatically tuning controller scheme

In summary, the chapter summarized the GA and a modified genetic algorithm is proposed based on state space approach. The proposal is verified by numerical simulation of the third order system. And then algorithm of automatically tuning controller scheme of web control system is given. The applications of this proposal will be implemented in designing the R2R Web control system in chapter 5, 6, and 7.

4. R2R Web Control System for Printed Electronics

In this chapter, an outline and perspectives of R2R web control system is presented firstly and then a mathematical model obtained by using the Newton's second law and principle of mass conservation will be shown and finally an introduction of hardware and software design of R2R web control system are given.

4.1 Literature Survey

4.1.1. Concepts of R2R Web Control System

Figure 4.1 shows the R2R web system used to make the printed electronics devices. The term '*web*' is used to describe any long, thin, continuous and flexible materials such as paper, film and textiles. Web processing machinery is used extensively in industry because it is a cost effective method of material handling and processing. A simple example of a web process is a magnetic tape reader: The web in this case is the tape itself, which is transported from one roller (the unwinder) to another (the rewinder). A magnetic head reads the information on the tape as it is conveyed from one end to the other. Other examples of web handling machinery include textile manufacturing processes, printing presses and so forth. A R2R Web Based ESD is shown in Figure 4.1. The web is pulled from the unwinder to the rewinder via its tensile force (this is an internal force that is generated while the machine is operating). In manufacturing industry, the web typically undergoes various processing stages, each of which both requires a certain tension level in the material and also affects the tension in the web. Moreover, to increase throughput, manufacturers are running web processing machines at ever increasing speeds. These changes in industry have placed a high demand on more accurate control of the web's motion and tension.

R2R web control system at AMM laboratory consists of 27 idle rollers, an unwinder, a rewinder, an infeeder, an outfeeder, two dancer systems, four load cells, two ultrasonic sensors, two web guide systems and inkjet printing systems.



Figure 4.1: R2R web system based inkjet printing system at AMM Lab

In the next step, the concepts and functions of each part will be presented:

- The idle rollers are free movement without external action and used to guide the moving web around the load cell in a fixed angle. It is also used to support the oscillation of web in the presence of web weight. Thus, the arrangement of idle rollers is to increase the accuracy of printing processes.
- Unwinder consists of a roller supported and acted by the attached motor and roll of web materials that are used for printing goals. Also, unwinder is used to control the web tension in this span.
- Rewinder consists of a roller also supported and acted by the attached motor and roll of web that is rolled after the movement from unwinder and some processing sections. The rewinder is also used to control web velocity for single-span R2R web system and regulate the web tension for multi-span R2R web system.
- Infeeder is a system that consists of two rollers regulated by hydraulic system and one motor. Infeeder is used to control web velocity in multi-span R2R web system.

- Outfeeder is a system that consists of two rollers regulated by hydraulic system and one motor. Outfeeder is used to control web tension in that span in multi-span R2R web system.
- Dancer systems are used in two goals. The first one is to take up the slack during the start-up and the shutdown; it is also used to control the web tension with low speed in some applications.
- In order to control the web tension at spans, motors at the unwinder, the outfeeder, and the rewinder are used to produce control torques
- Load cells are used to feedback the web tensions during the operating process
- Web guide mechanism is used to control web lateral error.
- Ultrasonic sensors are used to measure the change of radii of unwinder and rewinder. These feedback signals are sent to the control board for convenient commands.
- Inkjet printing system is used for the printed electronics such as RFID, circuits, and solar cells and so on.
- Control panel is a combination of hardware and control software. It is also integrated with remote control for users. A PC is attached to help users to set the reference web velocity and tension. It is also used for other purposes such as inkjet system control, web guide system control and so on.

There are many tension related web problems such as deformation of web due to stretching or wrinkling, loss of registration while splicing or changing speed, slack web which can cause web breaks, wrap-ups around driven roller, variation of coating thickness, unwind or rewind core crushing, reduction of machine speed to accommodate web, handling problems, inconsistent repeat length, telescoping rolls, excessive waste of web material. In this dissertation, some assumptions are employed for simplifying the problem that is able to model and analysis.

4.1.2. Perspectives of Web Tension and Velocity Control

The first question arises what web tension is and how important it is. In generally, web tension is the longitudinal force being exerted on a process material often expressed in (N) or simply put how tight the material is pulled. Thus, a small variation of web tension leads to the poor quality of final products. In order to

improve the product quality with low production cost, many control algorithms have been proposed but most of them have been developed for linear systems. Through these models, there are two approaches in tension control in recent years:

- Open loop tension control that is no actual measured feedback value and a center wind application actual tension will vary directly with the diameter of the wound roll. A dancer can be used also to maintain constant tension, or the torque to the center-wind can be adjusted based on a measured diameter of the wound roll (diameter compensation)
- Closed loop or feedback tension control that uses a transducer or loadcell to measure actual web tension and then a torque of a center-wound roll is controlled based on the feedback value. Dancer systems can also be closed loop based on tension feedback

With the rapid development of mathematical tools and digital computers, nonlinear control systems are getting more attention. Depending on the mathematical model and experimental researches, some algorithms for a web tension and velocity control for an R2R web system have been proposed. Some proposals have achieved low cost and high quality through the implementation of observer techniques, the synthesis of an observer-based controller in place of tension transducer, and the estimation of friction, and rotational inertia of the rewinder and the unwinder. An important aspect in R2R web control system design is to fully understand the physical and mathematical models and to come up with disturbance rejection algorithms. In reality, one usually uses linearized models to design the control systems but due to the linearization, some crucial nonlinearity is ignored and as a result there is a discrepancy between the actual system performance and the simulated results (Ku-Chin, 2010).

In the recent years, many researchers have addressed in designing nonlinear feedback controllers by using the backstepping approach that have the advantages of avoiding the cancellation of benign dynamic nonlinearity, and not forcing the designed system to appear linear. The proposal (Shin K, 2009) shows that the web tension is a key factor to improve the web lateral error and register error. In this paper, the authors developed an integrated mathematical model of web tension and web lateral movement. The numerical simulation and experimental results prove the

reliability of the statement. Also, the rapid development of printed electronics technology, the web based printing accuracy is required with a micro-meter level in which the small variation leads to the bad quality of final product. Thus, precise web tension control model of R2R web control system is a key to achieve this goal. In the next section of the dissertation, some assumptions are proposed and a general mathematical model of nonlinear R2R web system is presented.

4.2 Mathematical Model Development of Roll-to-roll Web System

4.2.1 Assumptions

To obtain the governing equation that describes the variation of web tension in spans, we utilize the Newton's second law and the law of mass conservation with some assumptions as follows

- The tension variation is neglected where the roller contacts the web but is considered between two rollers
- The web has no permanent deformation due to applied tension
- The dynamics of loadcell and dancer dynamics is ignored
- The web thickness is quite small corresponding to the roller radius
- No slipping phenomena exists between web and nip rollers
- The density, the modulus of elasticity, and the cross-sectional area of web are constant

4.2.1 Development of Dynamic Equations

The control volume used in analysis is shown in Figure 4.2; it includes the region of embrace of the upstream roller and the free span, ending at the point of contact of the downstream roller (Gaby Saad, 2000).

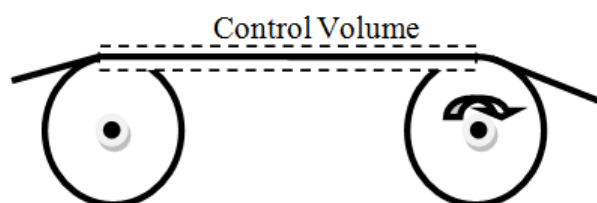


Figure 4.2: The control volume

It is a fact that there is a direct relationship between the force applied to an elastic material and the resulting amount of stretch. Assuming that the web is perfectly

elastic, the tension and the stretch are directly proportional. Engineering strain is defined as the ratio of material extension to the original length in the material (i.e., the percentage increase in length). The stress σ , is the ratio of internal force in the material (i.e., tension) to the cross-sectional area. For elastic materials, $\sigma = E\varepsilon$, where E is Young's modulus of elasticity.

Consider a portion of the web material of mass m and initial l_0 , shown in Figure 4.3

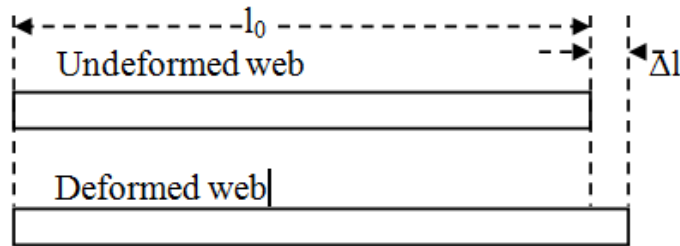


Figure 4.3: Deformation of web materials

By defining the linear density of the undeformed web as $\rho_u = \frac{m}{l_0}$, we see that once it is deformed to a length of $l = l_0 + \Delta l$, its linear density becomes

$$\rho = \frac{\rho_u}{1+\varepsilon}, \varepsilon = \frac{\Delta l}{l_0} \quad (4.1)$$

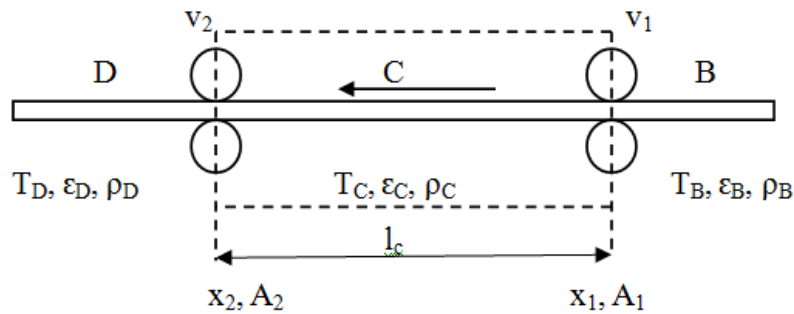


Figure 4.4: The relation between rollers and web in a zone

The relation between web tension and velocity is given in [21]. Consider the C zone shown in Figure 4.4 that is surrounded around by the dotted rectangular, the transmitting velocity and web tension have the following relation according to the mass conservation.

$$\frac{d}{dt} \left\{ \int_{x_1}^{x_2} \rho_C(x) A_C dx \right\} = \rho_B A_B v_1 - \rho_C A_C v_2 \quad (4.2)$$

where v : Tangent velocity, ρ : The density of web, A : Cross-sectional area of web.

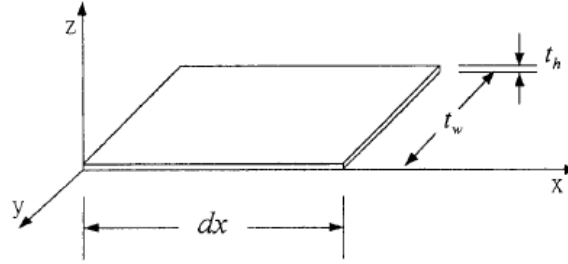


Figure 4.5: Isolated small element of web

By using the elastic theory for isolated small element in Figure 4.5 and the neglect of deformation of web in z and y direction, we have the following expressions:

$$dx_0 = (1 + \varepsilon_x)dx \quad (4.3)$$

where ε_x : Strain of web in x direction that is along the movement direction of web,
 dx_0 : Length of element before deformation

Substituting the Equation (4.3) into Equation (4.2) and according the assumption, we obtained:

$$\frac{d}{dt} [(1 - \varepsilon_C)l_C] = (1 - \varepsilon_B)v_1 - (1 - \varepsilon_C)v_2 \quad (4.4)$$

Where, shown in Figure 4.4, l_C is the web length between two nip rollers, ε_B is the web strain between the unwinder and the first nip rollers in the web transmitting direction. Therefore, the web velocity and web strain have the following relation.

$$l_C \frac{d}{dt} \varepsilon_C = v_2 - v_1 - v_2 \varepsilon_C + v_1 \varepsilon_B \quad (4.5)$$

It follows that from Hook's law, we have:

$$T_B = AE \varepsilon_B, T_C = AE \varepsilon_C \quad (4.6)$$

Where T and E represent web tension and the elastic modulus of web, respectively.

Then, the web tension dynamics of R2R web can be represented as:

$$\frac{d}{dt} [T_C] = \frac{AE}{l_C} [v_2 - v_1] - \frac{1}{l_C} [v_2 T_C - v_1 T_B] \quad (4.7)$$

In general of multispan R2R web system, consider the web velocity and tension at i^{th} span, the Equation (4.7) can be rewritten as follows:

$$\frac{dT_i}{dt} = \frac{AE}{l_i} [v_{i+1} - v_i] - \frac{1}{l_i} [v_{i+1} T_i - v_i T_{i+1}], i = 1, 2, \dots, N - 1 \quad (4.8)$$

where N is the number of web spans of R2R web system

In the next section, we formulate the relationship between the web velocity, tension, and torque that is generated by motors on rollers. It is assumed that there is no slippage between web and rollers and ignore of dry friction.

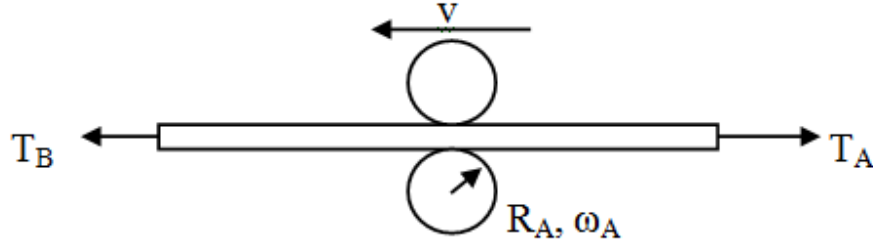


Figure 4.6: Relation between nip roller and web movement

As shown in Figure 4.6, the use of the Newton's second law, the web dynamics is obtained in the Equation (4.9):

$$J_A \frac{d\omega_A}{dt} = R_A(T_A - T_B) - B_A\omega_A + \tau_A \quad (4.9)$$

J_A : Total moment of inertia of the unwind roll and motor at startup; ω_A : Angular velocity of the roller; B_A : Coefficient of viscous friction; τ_A : Torque generated by motor at roller; R_A : Radius of roller.

By combining the Equations (4.8) and (4.9), the dynamic equations for i^{th} span are written as follows:

$$\begin{cases} \frac{dT_i}{dt} = \frac{AE}{l_i} [v_{i+1} - v_i] - \frac{1}{l_i} [v_{i+1}T_i - v_iT_{i+1}], i = 1, 2, \dots, N \\ J_i \frac{d\omega_i}{dt} = R_i(T_i - T_{i-1}) - B_i\omega_i + \tau_i \end{cases} \quad (4.10)$$

These equations are used to generate the motion equations of a multispan R2R web control system in the chapter 5, 6 and 7.

4.3 R2R Web Control System Design

In this section, a design introduction of the proposed R2R web control system is presented. Also, hardware and software scheme is briefly introduced.

4.3.1 Hardware Design

Figure 4.7 and 4.8 show the drawing of R2R web control system that is derived into four blocks:

- The first block consists of unwinder, web guide, nip system, two loadcells and rollers. This block has a function to handle the web tension at 1st span, velocity control for the whole system and lateral error for processing sections.
- The second block has two selections that can be installed with Inkjet Printing Units and Gravure/Offset Printing Units. This block is used to implement the web based printing technology.
- The third block is offset/gravure printing unit shown in Figure 4.8. This consists of offset gravure printing and dry units.
- The last block consists of rewinder, web guide, nip system, two loadcells and rollers. This block has a function to handle the web tension at 2nd and 3rd spans, and lateral error regulation for rewinding.

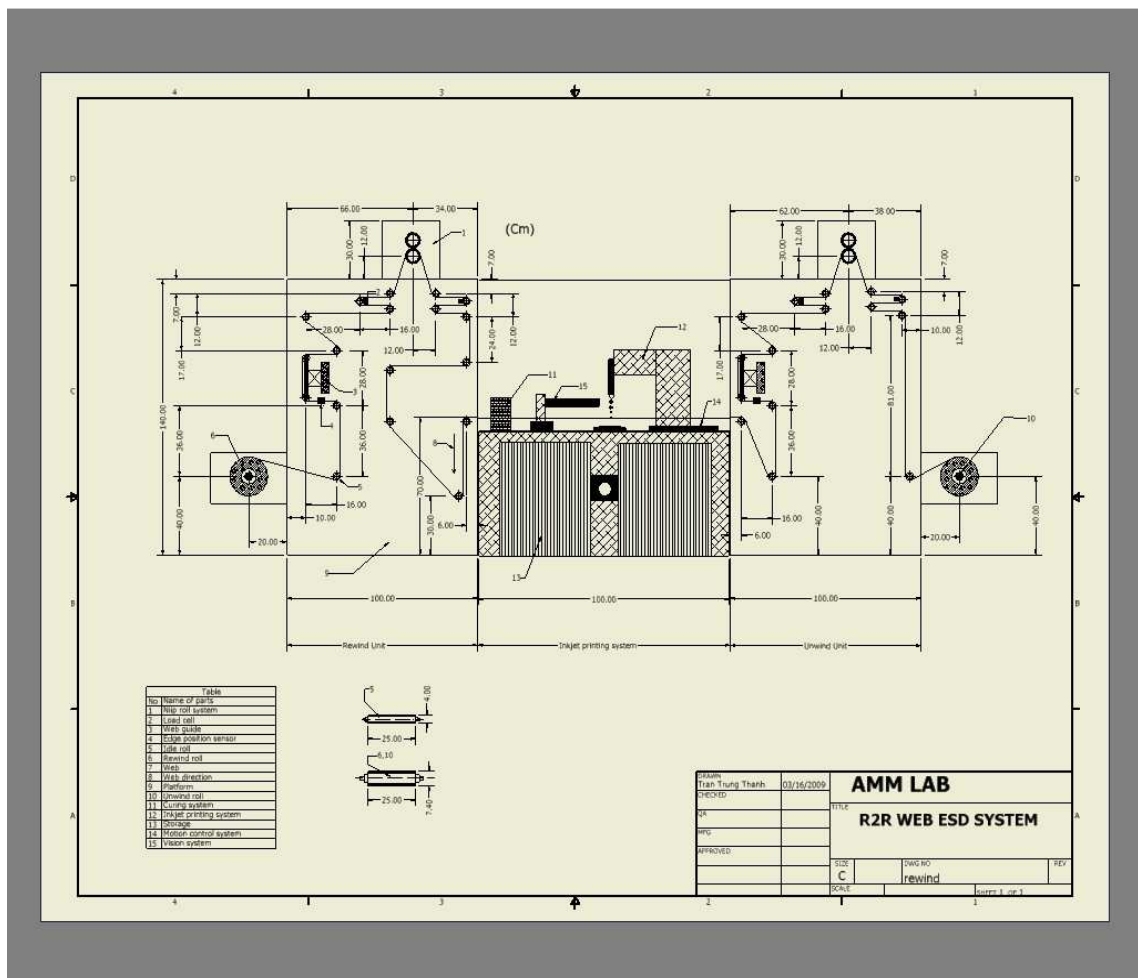


Figure 4.7: Drawing of R2R web ESD system

Table 4.1: Devices of R2R Web ESD at AMM Lab

No	Name of devices	No.	Type of devices	Company
1	Motor	4	HC-KFS43	BOSCH Group
2	Loadcells	4	CL Cantilevered Load Cells	MAGPOWR
3	Edge position sensor	2	DAC-004	FIFE company
4	Dancer system	2	On/Off	MAGPOWR
5	Ideal rollers	19	Small rollers	DGI
6	Nip roll system	2	On/Off Hydraulic Cylinder	DGI
7	Offset pivot guide	2	Symat 50 Offset Pivot Guide	FIFE company
8	Web materials	5	PET	DGI
9	Vision system	2	IEEE 1934 Camera	NI
10	PXI/ Real-time Controller	1	PXI 7813R reconfigurable I/O	NI
11	Motion control with I/O	2	Rexroth IndraDrive	NI
12	IndraDrive C	4	MR-J2S-40A	NI
13	Ultrasonic sensor	2	MIC+25/IU/TC	Migatron Corp.
14	FPGA module	4	DAQ I/O	NI

Table 4.1 shows the devices selected for building the R2R web control system at AMM lab, Jeju National University. Korea.

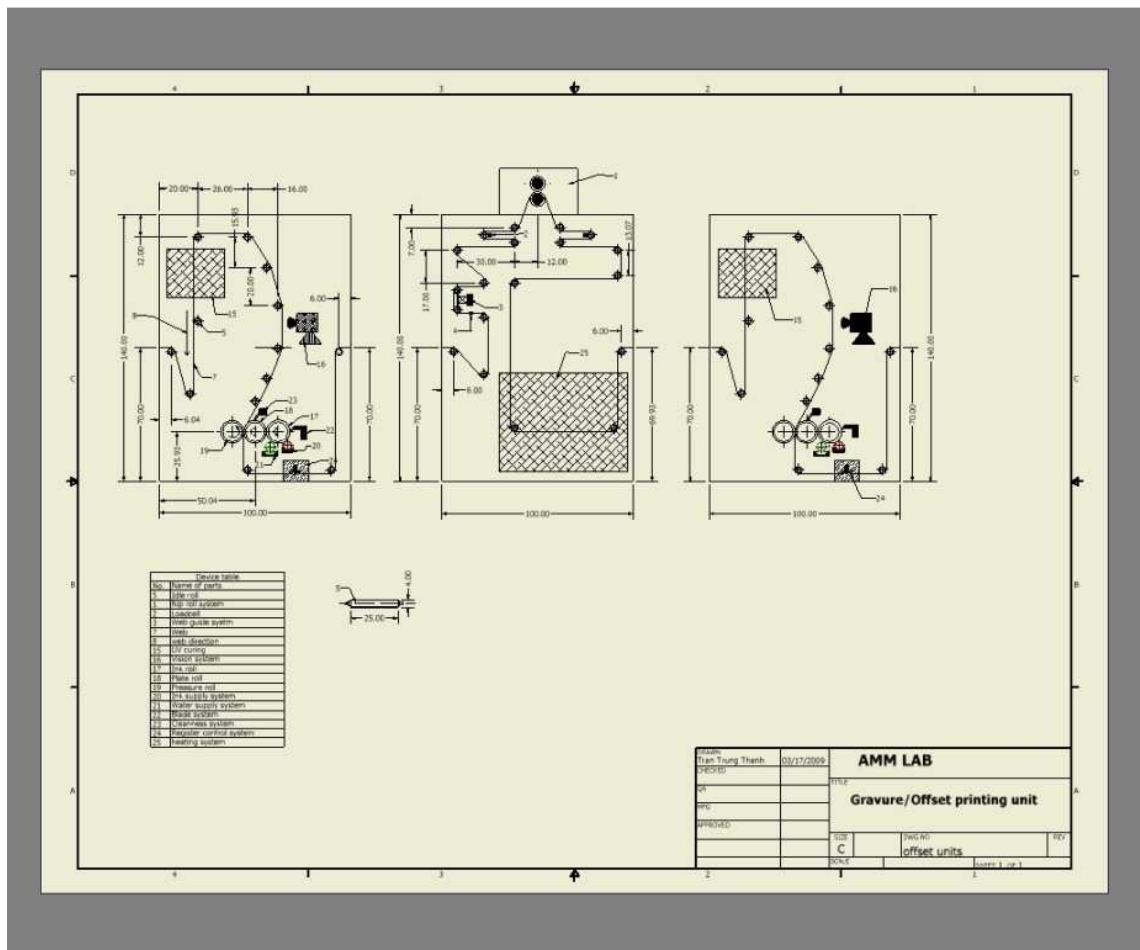


Figure 4.8: Drawing of gravure/offset printing units

4.3.2 Software Design

Figure 4.9 shows the block diagram for building the software for controlling the R2R web ESD system.

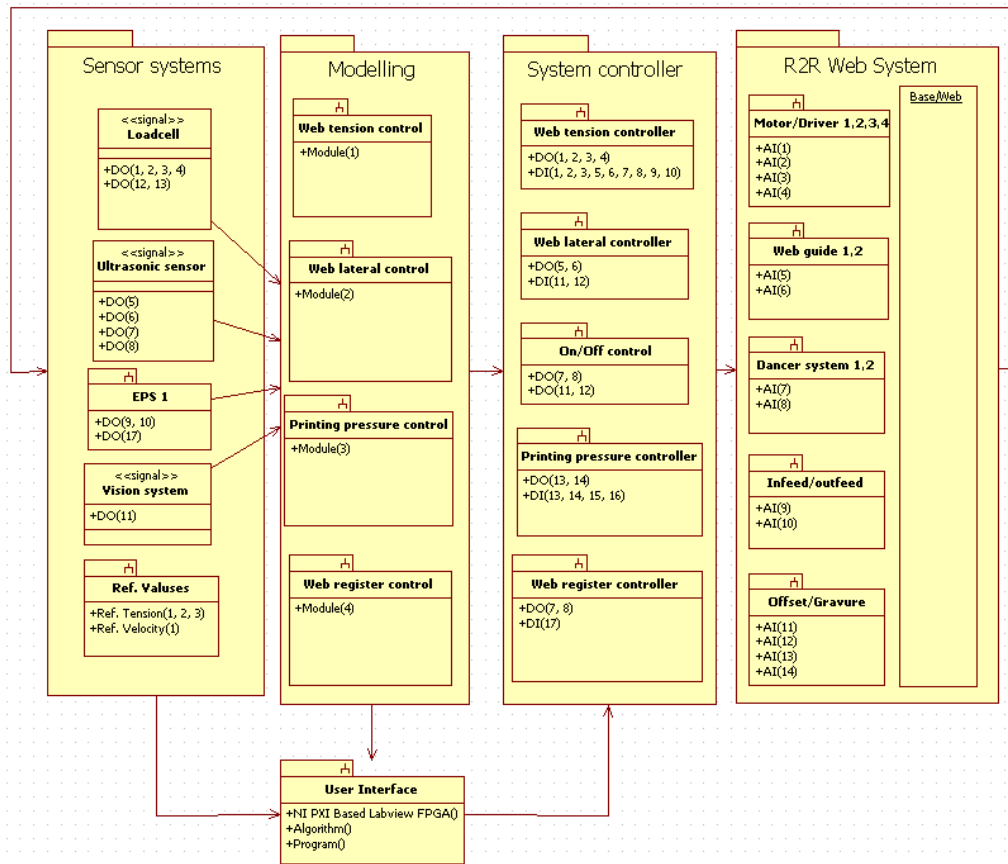


Figure 4.9: Block diagram for control Program

The block diagram consists of four modules:

- Sensor systems
- Modeling
- System controller
- R2R web system

Figure 4.10 shows the interface of control program of R2R ESD System. The software allows users handle the web tension and velocity at each span. Also, inkjet printing units is controlled by the motion control stages with three axes. On the other hand, the functions such as function generator, pump, and heater status are also regularized by software.

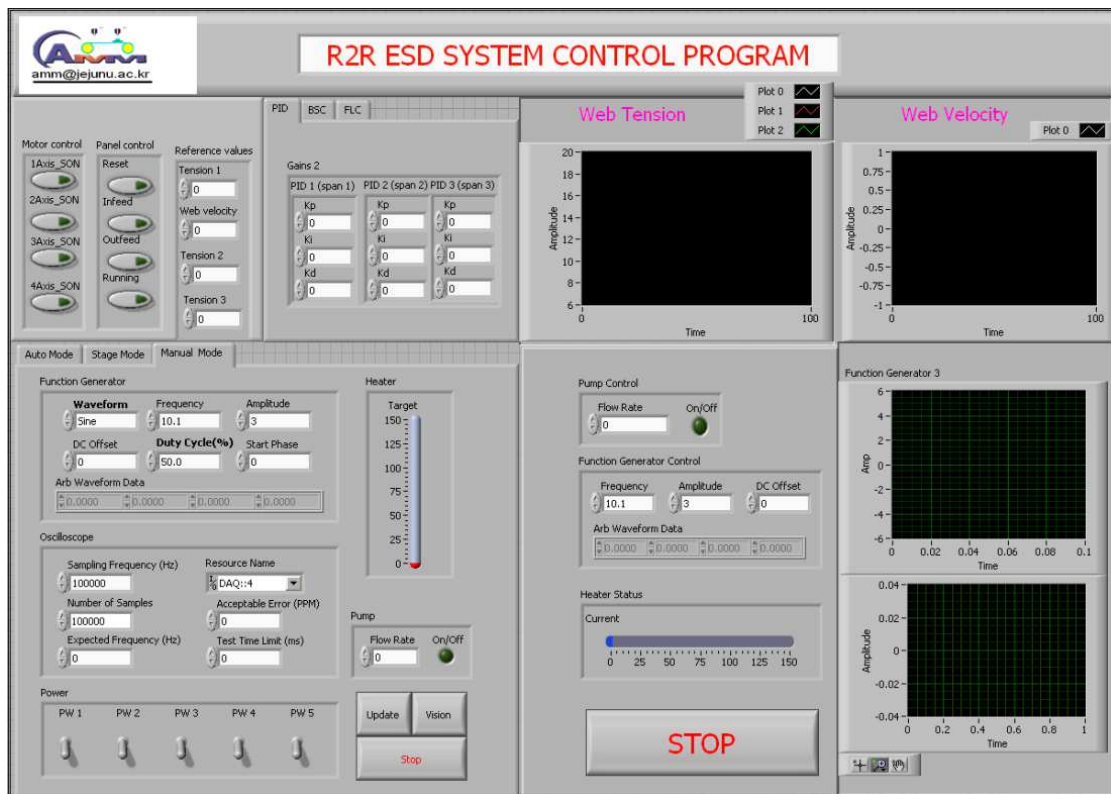


Figure 4.10: Interface of control program of R2R ESD System

The software also allows users to know about the system status of web velocity, web tension, and printing parameters. The sections of control algorithm of PID, Backstepping and Fuzzy Logic based algorithms are available to help users compare and analyze the experimental results.

In summary, this chapter introduces briefly about the concepts, definitions, and applications of R2R web control system in the first section and then a mathematical model of i^{th} span web dynamics is generated by using the Newton's second law and principle of mass conservation. Finally, the hardware and software scheme for R2R web ESD system is introduced.

5. Single-span R2R Web Velocity and Tension Control

In this chapter, a mathematical model for single-span R2R web control system is generated by using the mentioned theory in chapter 4. By rewriting the dynamics equations in affine form and using the feedback linearization theory and zero dynamics in chapter 2, a nonlinear feedback controller is obtained. For comparison and advantages of backstepping approach as compared to conventional approach, a procedure for formulating the backstepping controller and a backstepping based web tension and velocity control algorithm are proposed using the theory developed in chapter 2, chapter 3 and chapter 4 in the next section. After that a Labview FPGA Module based software design is introduced. Finally, numerical simulation and experimental results are addressed in the single-span R2R web control system. Those results will be discussed and compared to the existing developments in order to show advances and limitations of the proposed algorithm.

5.1 Mathematical Model of Single-span Roll-to-roll Web System

Figure 5.1 shows the two-span R2R web system that consists of unwinder, rewinder, infeed unit, and two loadcells, rollers, lateral control unit and dancer system. The idle rollers guide the moving web around the load cell in a fixed angle. In order to operate web, unwinder and rewinder motors are used with control torques τ_u and τ_r respectively. There are two dancers on unwind and rewind sides to take up the slack during start-up and shutdown

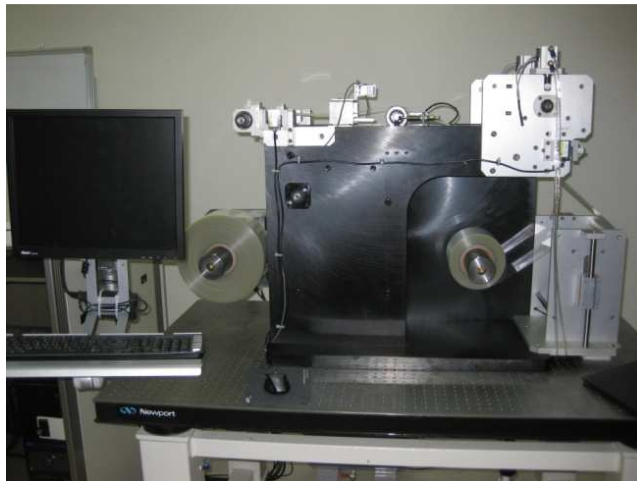


Figure 5.1: The R2R web system at AMM Laboratory

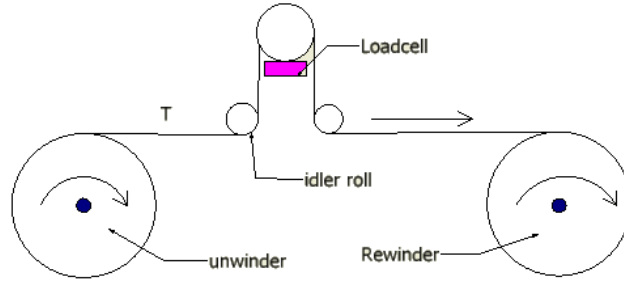


Figure 5.2: Model of single-span web control system

By using the dynamic equations in chapter 4 for one span R2R web system and some transformations, the nonlinear dynamic equations of single-span roll-to-roll web control system can be written as follows:

$$\dot{\omega}_u = \frac{R_u}{J_u} T - \frac{B_u}{J_u} \omega_u - \frac{1}{J_u} \tau_u \quad (5.1)$$

$$\dot{T} = -KR_u \omega_u - \frac{R_r}{L} T \omega_r + KR_r \omega_r \quad (5.2)$$

$$\dot{\omega}_r = -\frac{R_r}{J_r} T - \frac{B_r}{J_r} \omega_r + \frac{1}{J_r} \tau_r \quad (5.3)$$

The inertia change satisfies the following equations:

$$R_u(t) = R_{u0} - \frac{\theta_u h}{2\pi} \quad (5.4)$$

$$R_r(t) = R_{r0} + \frac{\theta_r h}{2\pi} \quad (5.5)$$

$$J_u = J_{u0} + \pi \rho w \frac{(R_u^4 - R_{u0}^4)}{2} \quad (5.6)$$

$$J_r = J_{r0} + \pi \rho w \frac{(R_r^4 - R_{r0}^4)}{2} \quad (5.7)$$

where J_{u0} : Total moment of inertia of the unwind roll and motor at start-up time;
 J_{r0} : Total moment of initial inertia of the rewind roll and motor at start-up time; J_u :
Total moment of inertia of the unwind roll and motor; J_r : Total moment of inertia of
the rewind roll and motor; ω_u : Angular velocity of the unwind roll; θ_u : Rotational
angle of the unwind roll; ω_r : Angular velocity of the rewind roll; θ_r : Rotational
angle of the rewind roll; R_{r0} : Initial radius of the rewind roll; R_{u0} : Initial radius of
the unwind roll; R_u : Operating radius of the unwind roll; R_r : Radius of the rewind
roll; h : The thickness of web; w : The width of web

5.2 Feedback Linearization based approach

5.2.1 State Space Feedback Controller Design

The nonlinear dynamic equations of single-span roll-to-roll web control system can be rewritten as in matrix form follows:

$$\begin{bmatrix} \dot{\omega}_u \\ \dot{T} \\ \dot{\omega}_r \end{bmatrix} = \begin{bmatrix} \frac{R_u}{J_u} T - \frac{B_u}{J_u} \omega_u \\ -KR_u \omega_u - \frac{R_r}{L} T \omega_r + KR_r \omega_r \\ -\frac{R_r}{J_r} T - \frac{B_r}{J_r} \omega_r \end{bmatrix} + \begin{bmatrix} -\frac{1}{J_u} & 0 \\ 0 & 0 \\ 0 & \frac{1}{J_r} \end{bmatrix} \begin{bmatrix} \tau_u \\ \tau_r \end{bmatrix} \quad (5.8)$$

The output equations are:

$$\begin{bmatrix} y_1 \\ y_2 \end{bmatrix} = \begin{bmatrix} T \\ \omega_r \end{bmatrix} \quad (5.9)$$

The Equations (5.8) and (5.9) is input-affine control system (2.10) and (2.11) in chapter 2. By using the concepts and theorems in chapter 2, we easily can transform the system (5.8) and (5.9) into the normal form of equation and zero dynamic form by using the local diffeomorphism in section 2.7.2 in chapter 2 and the obtained feedback controller is implemented to achieve the performance of the system.

We rewrite the Equations (5.8) and (5.9) in matrix form as:

$$\dot{x} = f(x) + g(x)u \quad (5.10)$$

$$y = h(x) \quad (5.11)$$

where $x = [\omega_u \ T \ \omega_r]^T$, $y = [y_1 \ y_2]^T$, $u = [\tau_u \ \tau_r]^T$

$$f(x) = \begin{bmatrix} \frac{R_u}{J_u} T - \frac{B_u}{J_u} \omega_u \\ -KR_u \omega_u - \frac{R_r}{L} T \omega_r + KR_r \omega_r \\ -\frac{R_r}{J_r} T - \frac{B_r}{J_r} \omega_r \end{bmatrix}, g_1 = \begin{bmatrix} -\frac{1}{J_u} \\ 0 \\ 0 \end{bmatrix}, g_2 = \begin{bmatrix} 0 \\ 0 \\ \frac{1}{J_r} \end{bmatrix}, h = \begin{bmatrix} T \\ \omega_r \end{bmatrix}$$

We firstly check if the problem is solvable of the state space exact linearization by using the Theorem 2.8 in chapter 2, indeed, we have the distribution $G_0 = \text{span}\{g_1, g_2\}$ has dimension $m=2$. Moreover, $[g_1, g_2] = 0 \in G_0$, thus G_0 is involutive.

We consider the $G_1 = \text{span}\{g_1, g_2, \text{ad}_f g_1, \text{ad}_f g_2\}$

where $\text{ad}_f g_1 = \begin{bmatrix} -B_u \\ 0 \\ 0 \end{bmatrix}$, $\text{ad}_f g_2 = \begin{bmatrix} 0 \\ 0 \\ B_r \end{bmatrix}$, $[g_1, \text{ad}_f g_1] = [g_1, \text{ad}_f g_2] = 0 \in G_1$

$$[g_2, \text{ad}_f g_1] = [g_2, \text{ad}_f g_2] = [\text{ad}_f g_1, \text{ad}_f g_2] = 0 \in G_1$$

It is easy to check $\dim(G_1) = 3$, and G_1 is involutive and also $\dim(G_2) = 3$ Thus,

Theorem 2.8 in chapter 2 verify that the state space exact linearization feedback problem is solvable. In order to find the feedback control law, Firstly, apply the definition 2.10 for the calculation of the relative degrees, we have:

$$L_{g_1}h_1 = 0, L_{g_1}h_2 = 0 \Rightarrow r_1 > 1$$

We check $L_f h_1 = -KR_u \omega_u - \frac{R_r}{L} T \omega_r + KR_r \omega_r, L_{g_1} L_f h_1 = \frac{KR_u}{J_u}, L_{g_2} L_f h_1(0) = \frac{KR_r}{J_r}$

Thus, the relative degree $r_1 = 2$

By do the same $L_{g_2}h_1 = 0, L_{g_2}h_2 = 1/j_r \Rightarrow r_2 = 1$

Consequently, the relative degree of the system is $r_1 = 2$ and $r_2 = 1$. It is easy to check the matrix:

$$\begin{bmatrix} L_{g_1}L_f h_1 & L_{g_2}L_f h_1 \\ L_{g_1}h_2 & L_{g_2}h_2 \end{bmatrix} = \begin{bmatrix} \frac{KR_u}{J_u} & -\frac{R_r}{J_r L} T + \frac{KR_r}{J_r} \\ 0 & 1 \end{bmatrix}$$

is nonsingular with every state vector.

By transformations, having

$$\begin{cases} z_1 = h_1 = T \\ z_2 = L_f h_1 = -KR_u \omega_u - \frac{R_r}{L} T \omega_r + KR_r \omega_r \\ z_3 = h_2 = \omega_r \end{cases} \quad (5.12)$$

The input-affine control system is rewritten as normal form of equations:

$$\begin{cases} \dot{z}_1 = z_2 \\ \dot{z}_2 = b_1(z) + a_{11}(z) + a_{12}(z)\tau_u \\ z_3 = b_2(z) + a_{22}\tau_r \end{cases} \quad (5.13)$$

where $b_1(z_1, z_2, z_3) = -\frac{R_r}{L} \left(\frac{B_r}{J_r} + \frac{B_u}{J_u} \right) z_1 z_3 - \frac{R_r}{L} z_2 z_3 + \frac{R_r R_r}{L J_r} z_1^2 + \left(-KR_r \frac{R_r}{J_r} - \frac{R_u}{J_u} KR_u \right) z_1 - \frac{B_u}{J_u} z_2 + KR_r \left(-\frac{B_r}{J_r} + \frac{B_u}{J_u} \right) z_3; a_{11}(z_1, z_2, z_3) = \frac{KR_u}{J_u}, a_{12}(z_1, z_2, z_3) = -\frac{R_r}{L} \frac{1}{J_r} z_1 + \frac{KR_r}{J_r}, b_2 = -\frac{R_r}{J_r} z_1 - \frac{B_r}{J_r} z_3, a_{22} = \frac{1}{J_r}$

The exact linearization feedback control laws for (4.20 are:

$$\begin{cases} \tau_u = \frac{(v_1 - b_1(z) + a_{11}(z))}{a_{12}} \\ \tau_r = \frac{(v_2 - b_2(z))}{a_{22}} \end{cases} \quad (5.14)$$

where v_1 and v_2 are new inputs for a linear system (5.15) and (5.16) and are chosen by using the classical design theory.

Thus, by coordinate transformations (5.12) and a state feedback (5.14), the original system (5.9) and (5.9) are rewritten in a new coordinate as follows:

$$\begin{bmatrix} \dot{z}_1 \\ \dot{z}_2 \\ \dot{z}_3 \end{bmatrix} = \begin{bmatrix} 0 & 1 & 0 \\ 0 & 0 & 0 \\ 0 & 0 & 0 \end{bmatrix} \begin{bmatrix} z_1 \\ z_2 \\ z_3 \end{bmatrix} + \begin{bmatrix} 0 & 0 \\ 1 & 0 \\ 0 & 1 \end{bmatrix} \begin{bmatrix} v_1 \\ v_2 \end{bmatrix} \quad (5.15)$$

5.2.2 Numerical Simulation

The simulation condition is set up with the zero initial conditions and the desired web tension $T_{ref} = 0.5$ (Kgf). The PI controller is designed using the frequency domain design with the gains $k_{pu} = 0.00013$, $k_{iu} = 0.0017$ and $k_{pr} = 0.047$, $k_{ir} = 0.375$. The feedback gains (5.16) are designed for (5.15) by using the pole placement method.

$$K = \begin{bmatrix} 0.02488 & -4.88658 & -0.009328 \\ -0.03731 & 7.329874 & 0.013992 \end{bmatrix} \quad 16)$$

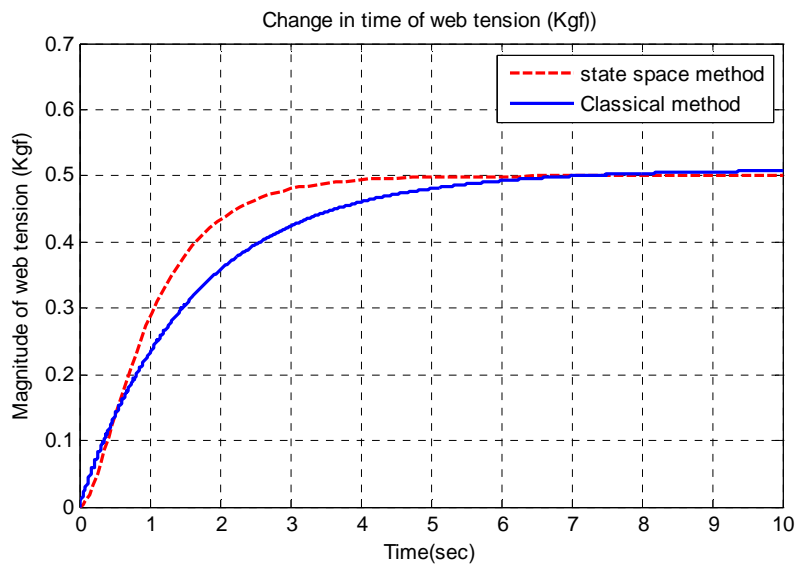


Figure 5.3: Comparison of web tension response in two cases: state space based design and PI based design methods

The solid line shows time response of web tension by using the classical method. The dash line represents the time response of web tension by using the state space exact linearization.

From the above analysis and results in Figure 5.3, some comments are made:

- Many limitations such as the requirement of a complex coordinate transformation that is a hard work for the MIMO nonlinear control system and zero dynamics must also be considered as control design.
- After using the classical design, the resultant feedback controllers need to be

returned the original coordinate. Thus, the coordinate transformation must have the inverse form. From the Equation (5.12), we realize that finding the inverse form is a very hard job and this is impossible in this case.

- Web tension response of state space based design is improved as compared to the PI controller based design.
- For the printed electronics technology, we want to design the time response of web tension with no overshoot and settling time less than 2 second. The result in Figure 5.3 shows that the trade-off between overshoot and settling time of both methods is conflicted.

To get over this obstacle, in the next section, the author proposes the backstepping based design approach for nonlinear R2R web control system using the theory developed in the chapter 2.

5.3 Backstepping Approach of Single-span R2R Web Control System

In this section, a procedure for formulating the backstepping controller for the nonlinear single-span R2R web control system is given and then a backstepping controller based algorithm for single-span R2R web system is proposed.

5.3.1 Back-stepping Controller Design

By putting the $k_1 = \frac{R_u}{J_u}$, $k_2 = -\frac{B_u}{J_u}$, $k_3 = -\frac{1}{J_u}$, $k_4 = -KR_u$, $k_5 = -\frac{R_r}{L}$, $k_6 = KR_r$, $k_7 = -\frac{R_r}{J_r}$, $k_8 = -\frac{B_r}{J_r}$, $k_9 = \frac{1}{J_r}$, the Equations (4.8) and (4.9) and some transformations, the non-linear dynamic equations of single-span roll-to-roll web control system can be written as follows:

$$\dot{T} = k_4\omega_u + k_5T\omega_r + k_6\omega_r \quad (5.17)$$

$$\dot{\omega}_u = k_1T + k_2\omega_u + k_3\tau_u \quad (5.18)$$

$$\dot{\omega}_r = k_7T + k_8\omega_r + k_9\tau_r \quad (5.19)$$

It is assumed that the exact state space linearization problem in sense of Theorem 2.8 is solvable. Since the complete system (5.17) - (5.19) is divided into three subsystems with the first one consisting of the Equation (5.17) and the second one consisting of the Equations (5.17) and (5.18) and the third subsystem is complete system. After applying the modified backstepping method mentioned in chapter 2 with each subsystem, A Control Lyapunov Function (CLF) is given out such that the derivative of this function is a negative definite function. Depending on this

criterion, the resulted controllers called the backstepping controller are proven to be globally asymptotical stable using the CLF and theorem 2.12 in chapter 2.

The following is the procedure to get the backstepping controller with desired tension T_{ref} and desired angular velocity of rewind roll ω_{ref} . By adding the new variables:

$$\bar{T} = T - T_{ref} \quad (5.20)$$

$$\bar{\omega}_u = \omega_u - \alpha(T, \omega_r) \quad (5.21)$$

$$\bar{\omega}_r = \omega_r - \omega_{ref} \quad (5.22)$$

Where

T_{ref} : The desired tension of web, ω_{ref} : The desired angular velocity of web, $\alpha(T, \omega_r)$:

An unknown function called the stabilizing function that will be determined later.

Step 1: Taking time derivative of the Equation (5.20) and combining with the Equations (5.17), (5.21) and (5.22) result as follows:

$$\dot{\bar{T}} = \dot{T} - \dot{T}_{ref} = k_4(\bar{\omega}_u + \alpha(T, \omega_r)) + k_5(\bar{T} + T_{ref})(\bar{\omega}_r - \omega_{ref}) + k_6(\bar{\omega}_r - \omega_{ref}) \quad (5.23)$$

A CLF $V_1(\bar{T})$ can be chosen such that when applied, its time derivative becomes a negative definite function:

$$V_1(\bar{T}) = \frac{1}{2}\bar{T}^2 \quad (5.24)$$

In order to make the Equation (5.23) asymptotically stable. In other words, the web tension T tends to T_{ref} , it is necessary to choose $\alpha(T, \omega_r)$ virtual control law such that the first derivative in time of the CLF of the Equation (5.23) is a negative definite function. Finally $\alpha(T, \omega_r)$ virtual control law can be written as follows:

$$\alpha(T, \omega_r) = \frac{1}{k_3}(-c_1(T - T_{ref}) - (k_1T + k_2)\omega_r) \quad (5.25)$$

where c_1 is a positive gain

Step 2: Taking time derivative of the Equation (5.21) and combining with the Equations (5.18), the Equation (5.21) is rewritten as follows:

$$\dot{\bar{\omega}}_u = k_1(\omega_u + \alpha(T, \omega_r)) + k_2(\bar{T} + T_{ref}) + k_3\tau_u - \dot{\alpha}(T, \omega_r) \quad (5.26)$$

A CLF $V_2(\bar{T}, \bar{\omega}_u)$ can be chosen as follows:

$$V_2(\bar{T}, \bar{\omega}_u) = V_1(\bar{T}) + \frac{1}{2}\bar{\omega}_u^2 \quad (5.27)$$

In order to make the Equation (5.26) asymptotically stable, it is necessary to choose the τ_u control law such that time derivative of the CLF of the Equation (5.27) is a negative definitive function. Combining with the Equations (5.17), (5.18), and (5.26), the τ_u control law is chosen as follows:

$$\tau_u = \frac{1}{k_3}(-c_2(\omega_u - \alpha) - k_2T - k_1\omega_u + \dot{\alpha}) \quad (5.28)$$

where c_2 is the positive gain and

$$\dot{\alpha} = \frac{1}{k_3}(-(c_1 + k_1\omega_r)(k_1\omega_r T + k_2\omega_r + k_3\omega_u) - (k_1T + k_2)(k_7T + k_8\omega_r + k_9\tau_r)) \quad (5.29)$$

Step 3: Taking time derivative of the Equation (5.22) and combination with the Equations (5.19), (5.20) and (5.21), the Equation (5.19) is rewritten as follows:

$$\dot{\bar{\omega}}_r = k_7(\bar{T} + T_{ref}) + k_8(\bar{\omega}_r + \omega_{ref}) + k_9\tau_r \quad (5.30)$$

A CLF $V_3(\bar{T}, \bar{\omega}_u, \bar{\omega}_r)$ can be chosen as follows:

$$V_3(\bar{T}, \bar{\omega}_u, \bar{\omega}_r) = V_2(\bar{T}, \bar{\omega}_u) + \frac{1}{2}\bar{\omega}_r^2 \quad (5.31)$$

In order to make the Equation (5.30) asymptotically stable, it is necessary to choose the τ_r control law such that the first derivative of the CLF of the Equation (5.31) is a negative definite function. Combining with the CLF of the Equations (5.31) and (5.30), the τ_r control law is chosen as:

$$\tau_r = \frac{1}{k_9}(-c_3(\omega_r - \omega_{ref}) - k_7T - k_8\omega_r) \quad (5.32)$$

where c_3 is a positive gain

Thus, by choosing $\alpha(T, \omega_r)$, τ_u and τ_r shown in the Equations (5.25), (5.28) and (5.32), respectively. There exist a CLF

$$V(T, \omega_u, \omega_r) = \frac{1}{2}(T - T_{ref})^2 + \frac{1}{2}(\omega_u - \alpha)^2 + \frac{1}{2}(\omega - \omega_{ref})^2 \quad (5.33)$$

Such that the Lie Derivative of V with respect to the Equations (5.17), (5.18) and (5.19) is a negative definitive function. So, the backstepping controllers shown in the Equations (4.39) and (4.40) are proven with globally asymptotical stability using the Control Lyapunov Function (CLF) and theorem 2.8 in chapter 2.

$$\tau_u = \frac{1}{k_6}(-c_2(\omega_u - \alpha) - k_4T - k_5\omega_u + \dot{\alpha}) \quad (5.34)$$

$$\tau_r = \frac{1}{k_9}(-c_3(\omega_r - \omega_{ref}) - k_7T - k_8\omega_r) \quad (5.35)$$

where $\alpha = \frac{1}{k_3}(-c_1(T - T_{ref}) - (k_1T + k_2)\omega_r)$

$$\dot{\alpha} = \frac{1}{k_3}(-(c_1 + k_1\omega_r)(k_1\omega_rT + k_2\omega_r + k_3\omega_u) - (k_1T + k_2)(k_7T + k_8\omega_r + k_9\tau_r))$$

The positive gains c_1, c_2, c_3 in the Equations (5.34) and (5.35) can be determined optimally by using the modified genetic algorithm in chapter 3. The parameters c_1, c_2, c_3 are obtained by optimizing the objective function (5.36).

$$J = \beta_1 \sum_{i=1}^N (\tau_u^2)_i + \beta_2 \sum_{i=1}^N (\tau_r^2)_i + \beta_3 \sum_{i=1}^N (\Delta T^2)_i + \beta_4 \sum_{i=1}^N (\Delta \omega_r^2)_i \quad (5.36)$$

where N is an integer number of iterations in control simulations, $\beta_1, \beta_2, \beta_3, \beta_4$ are scale factors, $\Delta T = T - T_{ref}$ is the error between the operating and reference tension and $\Delta \omega_r = \omega_r - \omega_{ref}$ is the error between the operating and reference angular velocity of rewinder.

Table 5.1: Parameters for the MGA for R2R web system

Parameters	Values
A number of generation	N=100
Size of population	S=10
The probability of mutation	$p_m=0.8$
The probability of crossover	$p_c=0.3$
Scale factors	$\beta_1 = \beta_2 = 0.4, \beta_3 = \beta_4 = 1.5$

5.3.2 Backstepping Based Control Algorithm

Figure 5.5 shows the block diagram of two-span roll-to-roll web control system algorithm using the back-stepping controllers. In this algorithm, the FPGA module based on PCI shown in Figure 5.4a depends on the input data to generate the control signals of torques to keep web velocity and tension with prescribed reference values in the presence of inertia change and viscous friction. These values are determined by the backstepping controllers

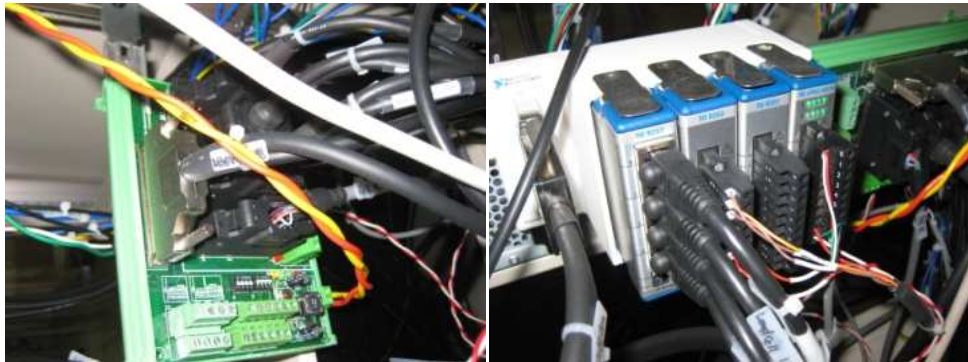


Figure 5.4: FPGA module of input/outputs

The feedback signals are obtained by using load cells, ultrasonic and FPGA module of Input/Outputs as shown in Figure 5.4b. Using the Labview programming language, control software is given out for the two-span roll-to-roll web system. With the rapid development of digital computer, the algorithm will be developed with the function that can detect errors and automatically recover the errors of control system due to disturbances and changing parameters.

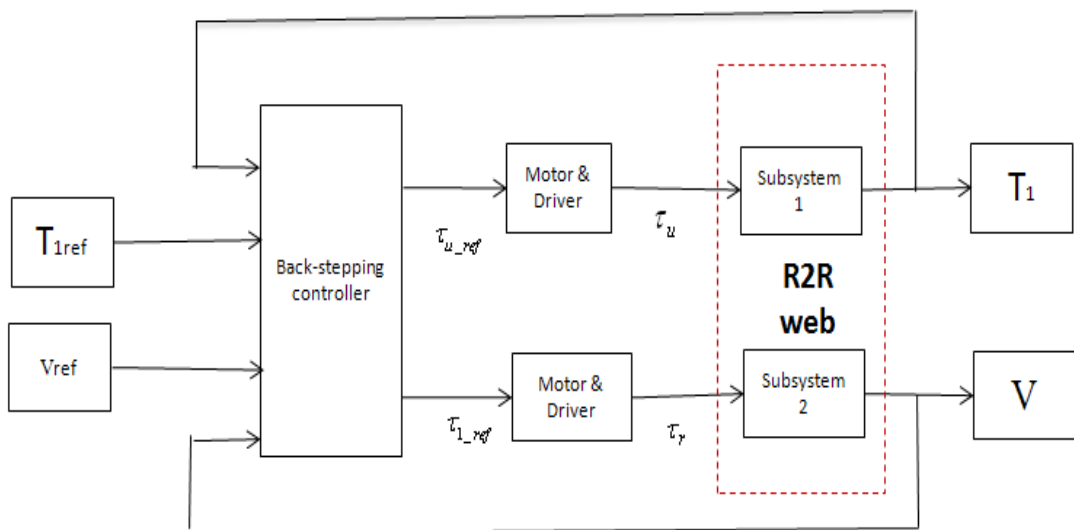


Figure 5.5: Block diagram of web tension and velocity control system

5.4 Numerical Simulation

5.4.1 Simulation Condition and Parameters

The simulation parameters of single-span roll-to-roll web control system are shown in Table 5.1. The simulation condition is set up with the zero initial conditions. Simulation is implemented in two cases:

Case 1: The desired web tension is $T_{ref} = 10$ (N) and the desired angular velocity change is 0.5 (rad/s).

Case 2: The change of desired web tension is shown in the Figure 5.6 and the desired angular velocity change is 0.15 (rad/s).

In order to observe the effectiveness of proposed algorithm using backstepping controller, one complements with the initial vicious friction and inertia change of rewinding and unwinding rolls in time. Furthermore, incorporating the sudden change in web tension in time as mentioned in the following the Figure 5.6.

Table 5.2: Simulation Parameters of Single-span R2R Web control system

Parameters	Values	Units
Radius of the unwind roll	0.177	(m)
Radius of the rewind roll	0.127	(m)
Total moment of initial inertia of unwinder and motor	0.0017072	(kg/m/s)
Total moment of initial inertia of rewinder and motor	0.0015072	(kg/m/s)
Total length of web	2.9	(m)
PET material E	$2.5 \cdot 10^9$	(N/m ²)
Coefficient of vicious friction of unwind roll	0.00002533	(kg-m-s/rad)
Coefficient of vicious friction of unwind roll	0.00002533	(kg-m-s/rad)
The thickness of web	0.00002	(m)
The width of web	0.2	(m)

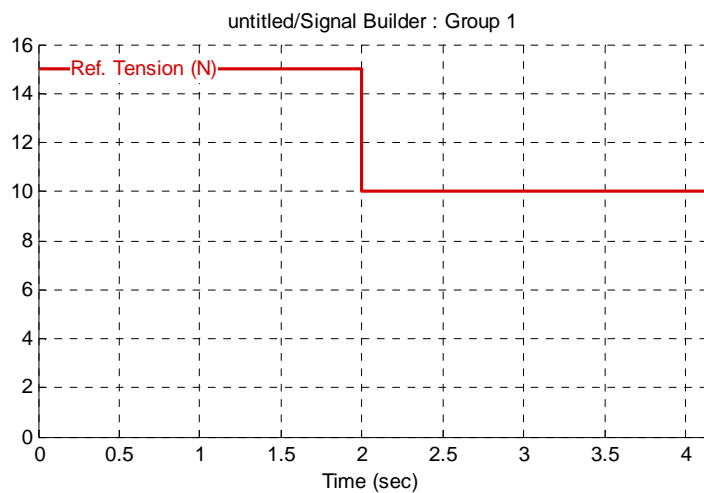


Figure 5.6: Prescribed web tension of sudden change in time

5.4.2 Simulation results

Figure 5.5 shows the simulation diagram of single-span roll-to-roll web control system using the backstepping controllers. PI/PID based algorithm is investigated intensively and applied widely in industry. By depending on the classical methods, many tools have been developed and applied for designing the PI/PID controller. Nowadays, with the rapid development of digital computer, many algorithms are proposed for designing optimally the controller. In this paper, the modified genetic algorithm is used to determine optimally the parameters of controllers. The algorithm diagram shown in chapter 3 is employed for the objective function (5.36) with parameters shown in Table 5.1. The application of the proposed algorithm in the Figure 5.5 of the backstepping controllers shown in the Equations (5.34) and (5.35), the simulation outcomes can be implemented by using the Matlab/Simulink tool. The optimal gains $c_1, c_2,$ and c_3 obtained by using the modified genetic algorithm in chapter 3 are shown below:

$$c_1 = 10.12, c_2 = 10.00, \text{ and } c_3 = 18.25$$

Case 1: The simulation results are employed with zero initial condition and the desired web tension $T_{ref} = 10$ (N) and the desired angular velocity change is 0.5 rad/s. The following is simulation results.

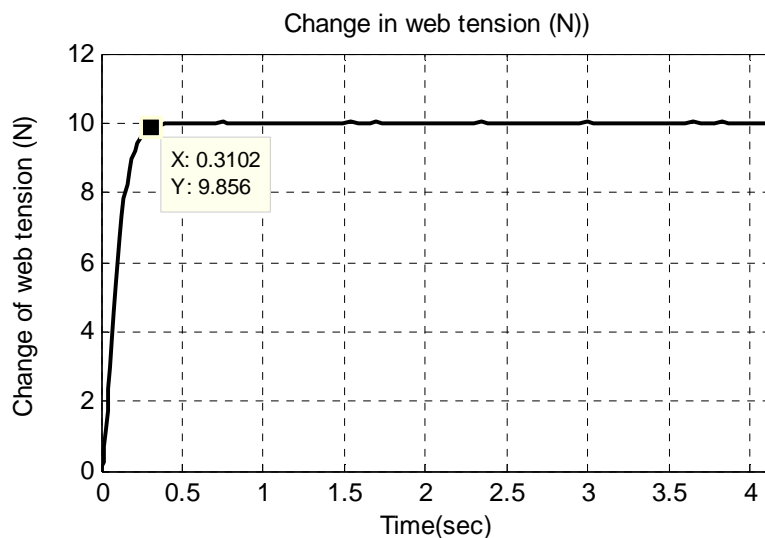


Figure 5.7: The tension change in time in case 1

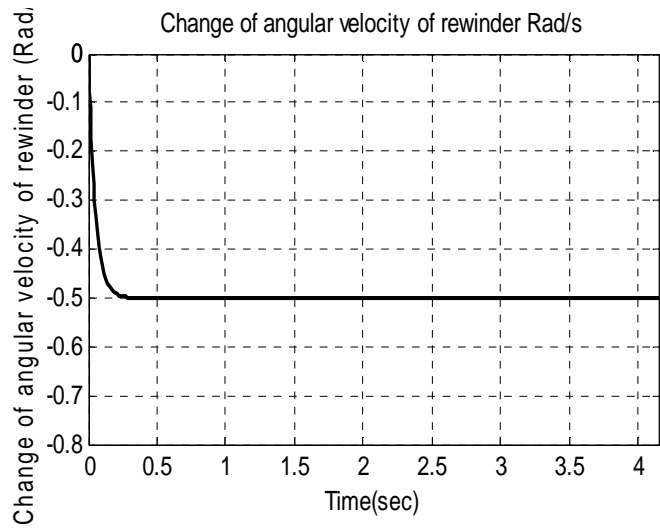


Figure 5.8: The angular velocity change in time of rewinder in case 1

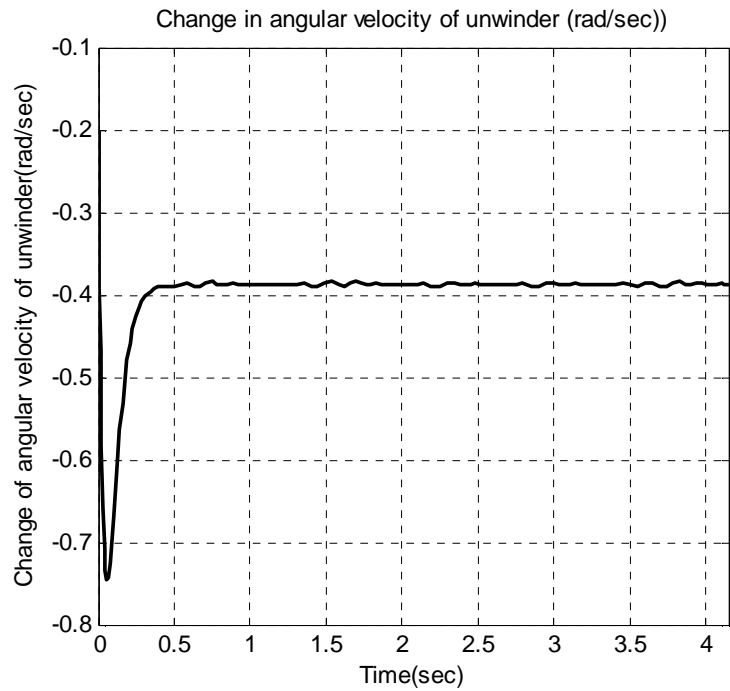


Figure 5.9: The angular velocity change in time of unwinder in case 1

Case 2: The simulation results are employed with zero initial condition and the desired web tension T_{ref} is shown in Figure 5.6 and the desired angular velocity change is 0.15 rad/s. The following is simulation results.

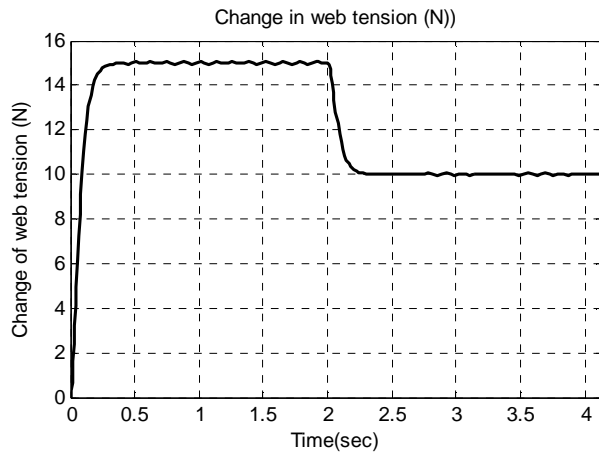


Figure 5.10: The tension change in time in case 2

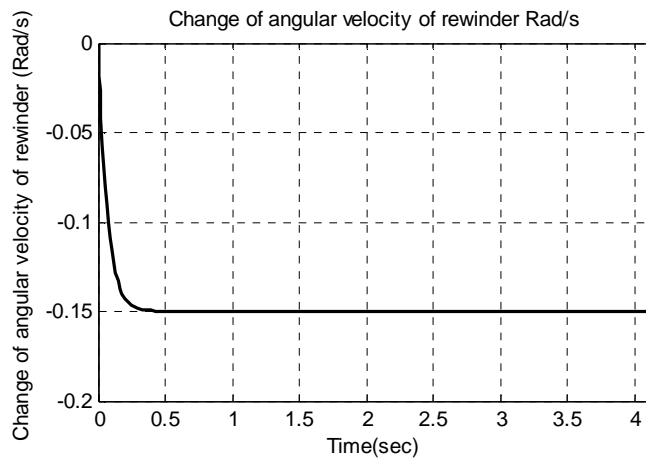


Figure 5.11: The angular velocity change in time of rewinder in case 2

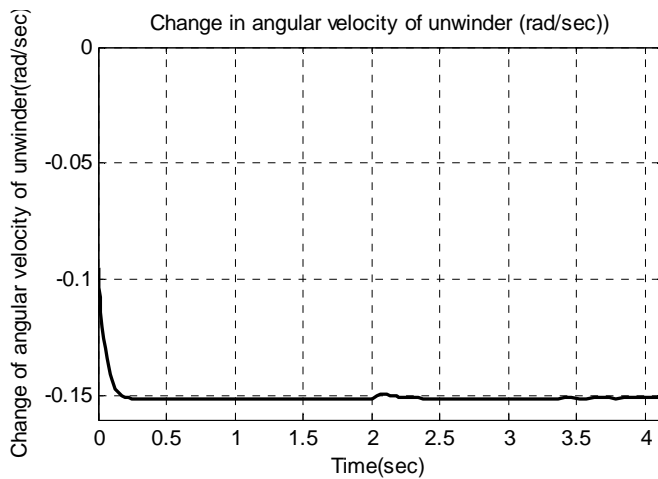


Figure 5.12: The angular velocity change in time of unwinder in case 2

The goal is to design the precise control algorithm that is required to keep web tension and web velocity at prescribed reference values, satisfy the performance

By using the diagram in Figure 5.13, the above mentioned mathematical model and Labview language, tension control program for R2R web system is given out as shown Figure 5.14. In this program, the reference web velocity and tension can be changed arbitrarily by users. The control program displays the change of web tension and change of angular velocity of rewinder and unwinder as shown in Figure 5.5. The change of gains in backstepping is also available to help user understand and tune the gains to get the reference response of system in the presence of disturbance.

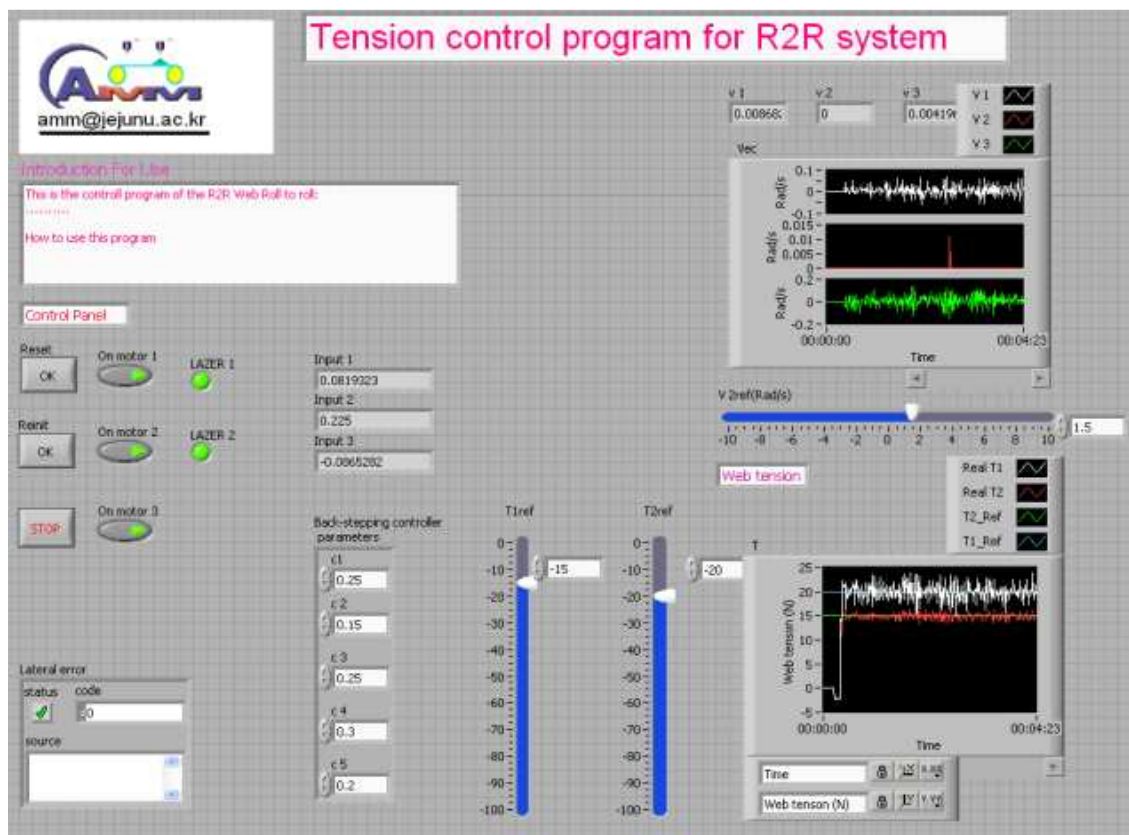


Figure 5.14: Tension control program of R2R web system

Case 1: The desired web tension $T_{ref} = 10$ (N) and the desired angular velocity change is 0.5 rad/s. The following is the experimental results.

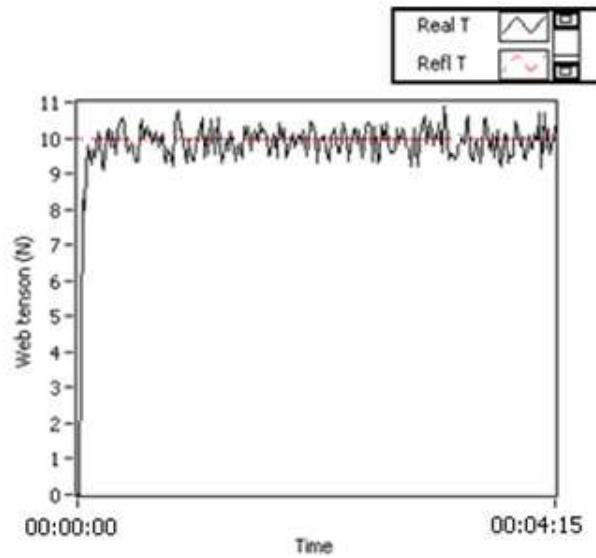


Figure 5.15: The change of web tension in time of experimental study

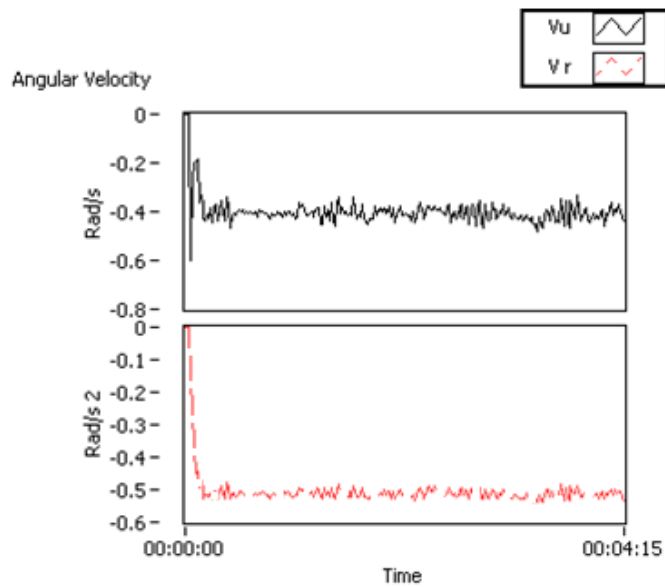


Figure 5.16: The change of angular velocity of rewinder and unwinder of experimental study

The dash line in Figure 5.15 is the reference web tension and the solid one is the response of web tension in time. The response of reference angular velocity is the dash line as shown in Figure 5.16. From the above results, it is clear that the time response of web tension and velocity is with no overshoot and the experimental results of the proposed algorithm are validated to the numerical simulation.

Case 2: In order to test the proposed algorithm in the different operating conditions, the change of desired web tension in time is shown in Figure 5.5 is applied.

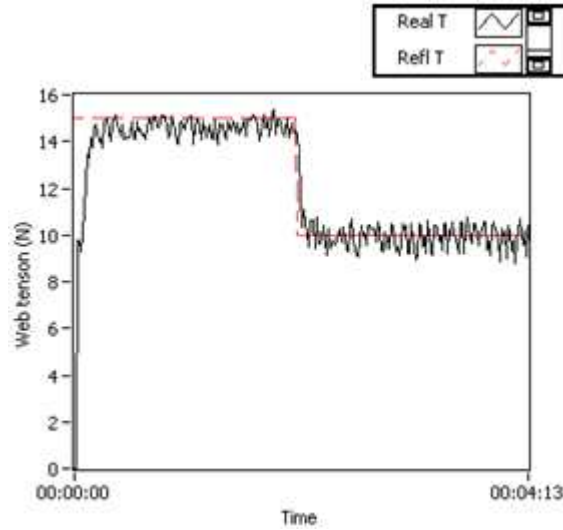


Figure 5.17: The change of web tension in time of experimental study

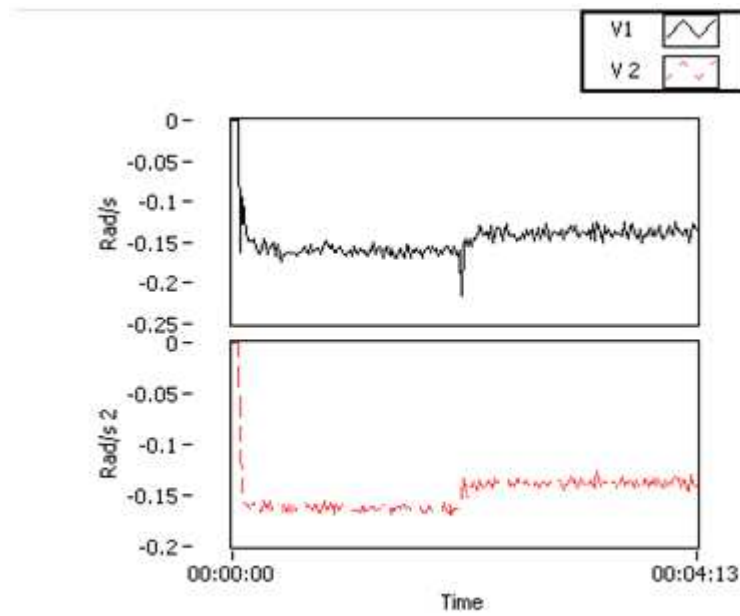


Figure 5.18: The change of angular velocity of rewinder and unwinder of experimental study

The dash line in Figure 5.17 is the reference web tension and the solid one is the response of web tension in time. The response of reference angular velocity is the dash line as shown in Figure 5.18. From the above, it is clear that the proposed algorithm is flexible with different operating conditions. By comparing the

experimental results in Figure 5.17 to the simulation ones in Figure 5.10 and also the experimental outcomes in Figure 5.15 to the simulation one in Figure 5.7, that proves that the proposed algorithm are reliable and high precision.

5. 6. Analysis and discussions

In this chapter, a mathematical model for single-span R2R web system is firstly generated using the dynamic equations in chapter 4. By using the concepts in chapter 2, we conclude that the relative degree (vector) is well-defined and the state space exact linearization problem is solvable. The numerical simulation is implemented for this approach and compared to PI based approach. As shown in the above comments, the time response of web tension is not able to meet the performance specifications. Thus, the idea of backstepping based approach comes up to get over this obstacle. In the next section, the backstepping controllers are formulating using the proposed theory in chapter 2. After that a new precise control algorithm is proposed for nonlinear single-span roll-to-roll web tension and velocity control system by using the backstepping controller with optimal gains determined by using the MGA in chapter 3. The efficiency of this method is proven by the simulation results in Matlab/Simulink and the experimental results. The following are some conclusions:

- The simulation results with gains optimally determined by using the modified genetic algorithm give a better response in web tension and velocity that is with no overshoot and short settling time.
- By comparing the simulation and experimental results, it is proven that the proposed algorithm is reliable and highly accurate.
- The proposed algorithm based on the backstepping controllers can be obtained the stability with every positive gain.

Also, from the obtained results, it is clear that the proposed algorithm using the backstepping controller obtained the desired performance specifications of the high stability under the presence of inertia change of the unwinder and rewinder and viscous friction. With the rapid development of sensors and electronic devices, the proposed control algorithm of backstepping controllers can result in a control system with high precision and are useful for applications with high digital computational system.

Chapter 6 Two-span R2R Web Tension and Velocity Control

In this chapter, a mathematical model is developed for the nonlinear two-span R2R web control system and the procedure for checking if the state space exact feedback problem is solvable is implemented. In the next section, a procedure for formulating the backstepping controller and a backstepping based web tension and velocity control algorithm are proposed using the theory developed in chapter 2 and chapter 3. After that a Labview FPGA based software design is introduced. Finally, numerical simulation and experimental results are addressed in two-span R2R web control system. Those results will be discussed and compared to the existing developments in order to show advances and limitations of the proposed algorithm.

6.1 Mathematical Model of Two-span R2R Web Control System

Figure 6.1 shows a two-span R2R web control system consisting of an unwinder, a rewinder, an infeeder, a dancer system, two load cells, rollers, and a web lateral control system. The idle rollers guide the moving web around the load cell in a fixed angle. In order to control the web tension at span 1 and span 2, motors at the unwinder and the rewinder are used to produce control torques τ_u and τ_r respectively to keep web tensions at the desired values and the infeeder is used for web velocity control. The dancer system put on the unwinder side is to take up the slack during the start-up and the shutdown. On the other hand, two load cells are used to feedback the web tension during the operating process and a web guide mechanism is used to control any web lateral error.

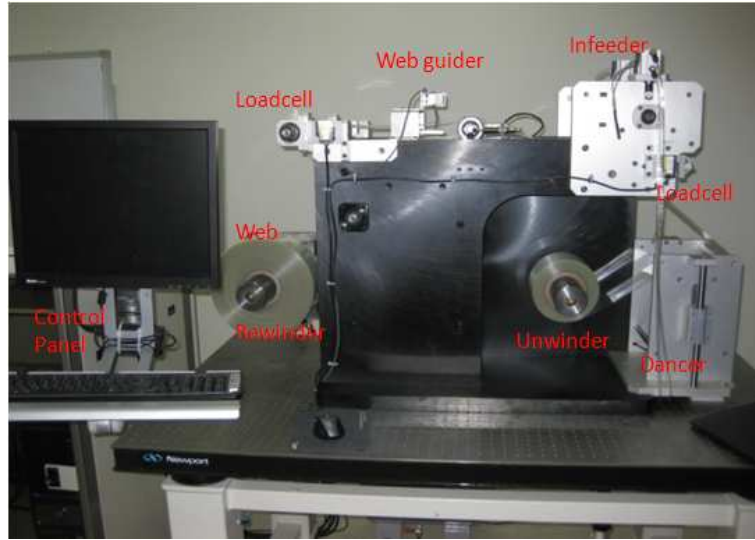


Figure 6.1: Two-span R2R web control system

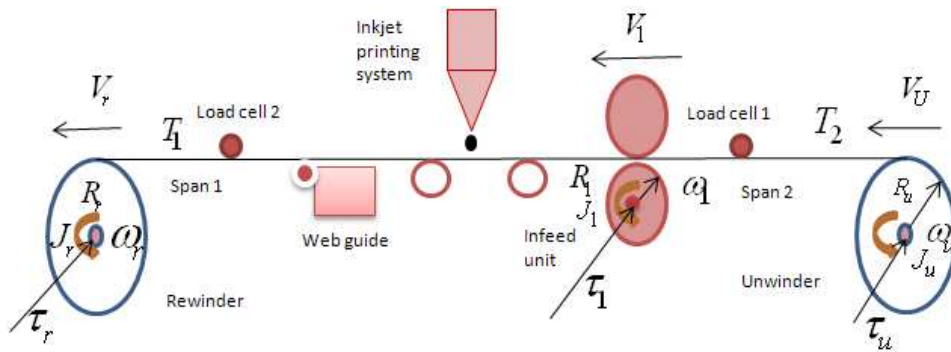


Figure 6.2: Model of two-span R2R web control system

By using the theory for formulating the governing equations for the R2R web control system in chapter 4, the nonlinear dynamic equations of two-span R2R web control system can be written as follows:

$$\dot{\omega}_i = k_7 T_2 + k_8 T_1 + k_9 \omega_i + k_{10} \tau_i \quad (6.1)$$

$$\dot{T}_1 = k_1 \omega_i T_1 + k_2 \omega_i + k_3 \omega_u \quad (6.2)$$

$$\dot{\omega}_u = k_4 T_1 + k_5 \omega_u + k_6 \tau_u \quad (6.3)$$

$$\dot{T}_2 = k_{11} \omega_i T_1 + k_{12} \omega_r T_2 + k_{13} \omega_r + k_{14} \omega_i \quad (6.4)$$

$$\dot{\omega}_r = k_{15} T_2 + k_{16} \omega_r + k_{17} \tau_r \quad (6.5)$$

We rewrite equations (6.1)-(6.5) in vector form:

$$\begin{bmatrix} \dot{\omega}_1 \\ \dot{T}_1 \\ \dot{\omega}_u \\ \dot{T}_2 \\ \dot{\omega}_r \end{bmatrix} = \begin{bmatrix} k_7 T_2 + k_8 T_1 + k_9 \omega_1 \\ k_1 \omega_1 T_1 + k_2 \omega_1 + k_3 \omega_u \\ k_4 T_1 + k_5 \omega_u \\ k_{11} \omega_1 T_1 + k_{12} \omega_r T_2 + k_{13} \omega_r + k_{14} \omega_1 \\ k_{15} T_2 + k_{16} \omega_r \end{bmatrix} + \begin{bmatrix} k_{10} \tau_1 \\ 0 \\ k_6 \tau_u \\ 0 \\ k_{17} \tau_r \end{bmatrix} \quad (6.6)$$

with output

$$\begin{bmatrix} y_1 \\ y_2 \\ y_3 \end{bmatrix} = \begin{bmatrix} \omega_1 \\ T_1 \\ T_2 \end{bmatrix} \quad (6.7)$$

where

$$\begin{aligned} k_1 &= -R_1 / L_1, k_2 = EAR_1 / L_1, k_3 = -EAR_u / L_1, k_4 = R_u / J_u, k_5 = -B_u / J_u, k_6 = 1 / J_u, k_7 = R_1 / J_1 \\ k_8 &= -R_1 / J_1, k_9 = -B_1 / J_1, k_{10} = 1 / J_1, k_{11} = R_1 / L_2, k_{12} = -R_r / L_2, k_{13} = EAR_r / L_2, k_{14} = -EAR_1 / L_2 \\ k_{15} &= -R_r / j_r, k_{16} = -B_r / J_r, k_{17} = 1 / j_r \end{aligned}$$

T_1 = web tensions of span 1, T_2 = web tensions of span2, ω_u = angular velocity of unwinder, ω_1 = angular velocity of infeed, ω_r = angular velocity of rewinder, J_u = inertia moment of unwinder and motor at unwinder, J_1 = inertia moment of roller 1 and motor at roller 1, J_r = inertia moment of winder and motor at winder, R_u = radius of unwinder, R_1 = radius of infeed roller 1, R_r = radii of rewinder, L_1 = the length of span1, L_2 = the length of span 2, E: Young's module of web materials, A: Area of cross-section, τ_u = control torque generated by the motor at unwinder, τ_1 = control torque generated by the motor at infeed roller 1, τ_r = control torque generated by the motor at rewinder, ρ = the density of the web, h = the thickness of web.

6.2. Backstepping Controller Design

The first step of the BSC design is to check if the conditions in Theorem 2.7 in chapter 2 are satisfied, i.e. the control system can be decoupled by a coordinate transformation and the BSC and then a systematic procedure is given for obtaining the BSC for the two-span R2R web control system. From the Equation (6.6) and Equation (6.7), it is easy to show that the Equation (6.6) and Equation (6.7) are in the form (2.21) and (2.22) in chapter 2 with the following:

$$\left. \begin{aligned} f_1 &= k_7 T_2 + k_8 T_1 + k_9 \omega_1 \\ f_2 &= k_1 \omega_1 T_1 + k_2 \omega_1 + k_3 \omega_u \\ f_3 &= k_4 T_1 + k_5 \omega_u \\ f_4 &= k_{11} \omega_1 T_1 + k_{12} \omega_r T_2 + k_{13} \omega_r + k_{14} \omega_1 \\ f_5 &= k_{15} T_2 + k_{16} \omega_r \end{aligned} \right\} \quad (6.8)$$

$$\left. \begin{aligned} g_1 &= k_{10} \\ g_2 &= 0 \\ g_3 &= k_6 \\ g_4 &= 0 \\ g_5 &= k_{17} \end{aligned} \right\} \quad (6.9)$$

and the output equations

$$\left. \begin{aligned} h_1 &= \omega_1 \\ h_2 &= T_1 \\ h_3 &= T_2 \end{aligned} \right\} \quad (6.10)$$

In our application, we have $k = 0$, $m = 3$ and $r_1 = 1$, $r_2 = r_3 = 2$, thus

Because $L_f^0 h_1 = h_1$, $L_f^0 h_2 = h_2$, $L_f^0 h_3 = h_3$, and $L_{g_2} L_f^0 h_i(x) = L_{g_4} L_f^0 h_i = 0$ due to $g_2 = 0$, $g_4 = 0$

We have, $L_{g_1} L_f^0 h_1(x) = L_{g_1} h_1(x)$, $L_{g_2} L_f^0 h_1(x) = L_{g_2} h_1(x)$, $L_{g_3} L_f^0 h_1(x) = L_{g_3} h_1(x)$

$$(L_{g_1} L_f^0 h_1(x), L_{g_3} L_f^0 h_1, L_{g_5} L_f^0 h_1(x)) \neq (0, 0, 0)$$

At $x = [\omega_1 \quad T_1 \quad \omega_u \quad T_2 \quad \omega_r] = [0 \quad 0 \quad 0 \quad 0 \quad 0]$

Thus, we can conclude that the input-output decoupling problem is solvable by the state feedback law. The next step is to show the details of the BSC design for the two-span R2R web control system.

The given problem is to design the controller that is required to keep web tension and web velocity at prescribed reference values, to satisfy the performance specifications with no overshoot and settling time of 0.2 second and to obtain the high precision and stability. By using the above developed theory, the complete system (6.1) - (6.5) is divided into five subsystems. The first one consists of the Equation (6.1), the second one consists of the Equation (6.1) and Equation (6.2), the third one consists of the Equations (6.1), (6.2) and (6.3), the fourth one consists of the Equations (6.1), (6.2) (6.3) and (6.4), and the last one consists of the whole system. After applying the modified backstepping method with each subsystem as shown above, the resulting controller called the backstepping controller is proven to achieve globally asymptotical stability using a CLF and Theorem 2.8. The following

is the procedure to get the BSC with desired tensions at span 1 and 2 of T_{1ref} , T_{2ref} respectively and desired angular velocity of infeed roll

Step 1: By considering the first subsystem and putting:

$$\zeta_1 = \omega_1 - \omega_{1ref} \quad (6.11)$$

Taking the derivative both sides in time and combining with the Equation (6.11), we have:

$$\dot{\zeta}_1 = \dot{\omega}_1 = k_7 T_2 + k_8 T_1 + k_9 (\zeta_1 + \omega_{1ref}) + k_{10} \tau_1 \quad (6.12)$$

For Equation (6.12), a CLF $V(\zeta_1)$ can be chosen such that when the control law is applied, its time derivative becomes negative definite or mathematically

$$V_1(\zeta_1) = \frac{1}{2} \zeta_1^2 \quad (6.13)$$

By taking the derivative in time of the Equation (6.13) and combining with the Equation (6.12) results in;

$$\dot{V}_1 = \zeta_1 \dot{\zeta}_1 = \zeta_1 (k_7 T_2 + k_8 T_1 + k_9 \omega_1 + k_{10} \tau_1) \quad (6.14)$$

To meet the asymptotically stable condition in the sense of Lyapunov in Theorem 2.12 for the Equation (6.12), the controller τ_1 can be chosen as follows;

$$\begin{aligned} -c_1 \zeta_1 &= k_7 T_2 + k_8 T_1 + k_9 \omega_1 + k_{10} \tau_1 \\ \Rightarrow \tau_1 &= \frac{1}{k_{10}} (-c_1 (\omega_1 - \omega_{1ref}) - k_7 T_2 - k_8 T_1 - k_9 \omega_1) \end{aligned} \quad (6.15)$$

Where c_1 is the positive gain

By doing so, we have:

$$\dot{V}_1 = \zeta_1 \dot{\zeta}_1 = -c_1 \zeta_1^2 < 0 \quad \forall \zeta_1 \neq 0 \quad (6.16)$$

Step 2: by choosing the state feedbacks (6.15) and a change of state transformations (6.11), the second subsystem can be rewritten as follows:

$$\left. \begin{aligned} \dot{\zeta}_1 &= -c_1 \zeta_1 \\ \dot{T}_1 &= k_1 (\zeta_1 + \omega_{1ref}) T_1 + k_2 (\zeta_1 + \omega_{1ref}) + k_3 \omega_u \end{aligned} \right\} \quad (6.17)$$

By putting

$$\zeta_2 = T_1 - T_{1ref} \quad (6.18)$$

the second subsystem can be rewritten as follows:

$$\left. \begin{aligned} \dot{\zeta}_1 &= -c_1 \zeta_1 \\ \dot{\zeta}_2 &= k_1 (\zeta_1 + \omega_{1ref}) (\zeta_2 + T_{1ref}) + k_2 (\zeta_1 + \omega_{1ref}) + k_3 \omega_u \end{aligned} \right\} \quad (6.19)$$

Now, ω_u is regarded as a control input to the subsystem (6.19). So, ω_u can be chosen to make the subsystem (6.19) globally asymptotically stable. A CLF $V_2(\zeta_1, \zeta_2)$ can be

chosen such that it makes the subsystem (6.19) asymptotically global stable with a virtual control law, i.e.

$$V_2(\zeta_1, \zeta_2) = V_1 + \frac{1}{2}\zeta_2^2 \quad (6.20)$$

By taking the derivative of Equation (6.20) in time and combining with Equation (6.19) results in;

$$\dot{V}_2 = -c_1\zeta_1^2 - \zeta_2(k_1(\zeta_1 + \omega_{1ref})(\zeta_2 + T_{1ref}) + k_2(\zeta_1 + \omega_{1ref}) + k_3\omega_u) \quad (6.21)$$

By satisfying the asymptotically global stable condition in the sense of Lyapunov in Theorem 2.12 of the Equation (6.21), a virtual control law α_2 can be chosen as follows;

By choosing:

$$\begin{aligned} -c_2\zeta_2 &= k_1(\zeta_1 + \omega_{1ref})(\zeta_2 + T_{1ref}) + k_2(\zeta_1 + \omega_{1ref}) + k_3\omega_u \\ \Rightarrow \alpha_2 &= \frac{1}{k_3}(-c_2(T_1 - T_{1ref}) - k_1\omega_1T_1 - k_2\omega_1) \equiv \omega_u \end{aligned} \quad (6.22)$$

Where c_2 is the positive gain

By doing so, we have:

$$\dot{V}_2 = -c_1\zeta_1^2 - c_2\zeta_2^2 < 0 \quad \forall \zeta_1, \zeta_2 \neq 0 \quad (6.23)$$

By choosing the state feedbacks (6.15), (6.22) and a change of state transformations (6.11) and (6.18), the third subsystem can be rewritten as follows:

$$\left. \begin{aligned} \dot{\zeta}_1 &= -c_1\zeta_1 \\ \dot{\zeta}_2 &= -c_2\zeta_2 \\ \dot{\omega}_u &= k_4(\zeta_2 + \omega_{1ref}) + k_5\omega_u + k_6\tau_u \end{aligned} \right\} \quad (6.24)$$

Step 3: By putting

$$\zeta_3 = \omega_u - \alpha_2 \quad (6.25)$$

The third subsystem can be rewritten as follows:

$$\left. \begin{aligned} \dot{\zeta}_1 &= -c_1\zeta_1 \\ \dot{\zeta}_2 &= -c_2\zeta_2 \\ \dot{\zeta}_3 &= k_4(\zeta_2 + T_{1ref}) + k_5(\zeta_3 + \alpha_2) - \dot{\alpha}_2 + k_6\tau_u \end{aligned} \right\} \quad (6.26)$$

where $\dot{\alpha}_2$ is determined by the equation (6.22) or

$$\begin{aligned} \dot{\alpha}_2 &= \frac{1}{k_3}(-(c_2 + k_1\omega_1)(k_1\omega_1T_1 + k_2\omega_1 + k_3\omega_u) + (k_1T_1 + k_2)(k_7T_2 + k_8T_1 \\ &\quad + k_9\omega_1 + k_{10}\tau_1)) \end{aligned}$$

So, τ_u can be chosen to make the subsystem (6.26) globally asymptotically stable. A CLF $V_3(\zeta_1, \zeta_2, \zeta_3)$ can be chosen arbitrarily such that it makes the subsystem (6.26) asymptotically stable with a virtual control law, i.e.

$$V_3(\zeta_1, \zeta_2, \zeta_3) = V_2(\zeta_1, \zeta_2) + \frac{1}{2}\zeta_3^2 \quad (6.27)$$

Taking the derivative of the Equation (6.27) in time and combining with the Equation (6.26) result in;

$$\dot{V}_3 = -c_1\zeta_1^2 - c_2\zeta_2^2 + \zeta_3(k_4(\zeta_2 + T_{1ref}) + k_5(\zeta_3 + \alpha_2) - \dot{\alpha}_2 + k_6\tau_u) \quad (6.28)$$

To satisfy the asymptotically stable condition in the sense of Lyapunov in Theorem 2.12 for Equation (6.28), a control law τ_u can be chosen as follows;

$$\begin{aligned} -c_3\zeta_3 &= k_4(\zeta_2 + T_{1ref}) + k_5(\zeta_3 + \alpha_2) - \dot{\alpha}_2 + k_6\tau_u \\ \Rightarrow \tau_u &= \frac{1}{k_6}(-c_3(\omega_u - \alpha_2) - k_4T_1 - k_5\omega_u + \dot{\alpha}_2) \end{aligned} \quad (6.29)$$

where c_3 is the positive gain

By doing so, we have:

$$\dot{V}_3 = -c_1\zeta_1^2 - c_2\zeta_2^2 - c_3\zeta_3^2 < 0 \quad \forall \zeta_1, \zeta_2, \zeta_3 \neq 0 \quad (6.30)$$

By choosing the state feedbacks (6.15), (6.22) and (6.29) and a change of state transformations (6.11), (6.18) and (6.25), the fourth subsystem can be rewritten as follows:

$$\left. \begin{aligned} \dot{\zeta}_1 &= -c_1\zeta_1 \\ \dot{\zeta}_2 &= -c_2\zeta_2 \\ \dot{\zeta}_3 &= -c_3\zeta_3 \\ \dot{T}_2 &= k_{11}(\zeta_1 + \omega_{1ref})(\zeta_2 + T_{1ref}) + k_{12}\omega_r T_2 + k_{13}\omega_r + k_{14}(\zeta_1 + \omega_{1ref}) \end{aligned} \right\} \quad (6.31)$$

Step 4: by putting

$$\zeta_4 = T_2 - T_{2ref} \quad (6.32)$$

The fourth subsystem can be rewritten as follows:

$$\left. \begin{aligned} \dot{\zeta}_1 &= -c_1\zeta_1 \\ \dot{\zeta}_2 &= -c_2\zeta_2 \\ \dot{\zeta}_3 &= -c_3\zeta_3 \\ \dot{\zeta}_4 &= k_{11}(\zeta_1 + \omega_{1ref})(\zeta_2 + T_{1ref}) + k_{12}\omega_r(\zeta_4 + T_{2ref}) + k_{13}\omega_r + k_{14}(\zeta_1 + \omega_{1ref}) \end{aligned} \right\} \quad (6.33)$$

Now, ω_r is regarded as a control input in subsystem (6.33). So, ω_r can be chosen to make the subsystem (6.33) globally asymptotically stable. A CLF $V_4(\zeta_1, \zeta_2, \zeta_3, \zeta_4)$

can be chosen such that it makes the subsystem (6.33) asymptotically stable with a virtual control law, i.e.

$$V_4(\zeta_1, \zeta_2, \zeta_3, \zeta_4) = V_3 + \frac{1}{2}\zeta_4^2 \quad (6.34)$$

Taking the derivative of the Equation (6.34) in time and combining with the Equation (6.33) result in;

$$\begin{aligned} \dot{V}_4 = & -c_1\zeta_1^2 - c_2\zeta_2^2 - c_3\zeta_3^2 + \zeta_4(k_{11}(\zeta_1 + \omega_{1ref})(\zeta_2 + T_{1ref}) + k_{12}\omega_r(\zeta_4 + \\ & T_{2ref}) + k_{13}\omega_r + k_{14}(\zeta_1 + \omega_{1ref})) \end{aligned} \quad (6.35)$$

To satisfy the asymptotically stable condition in the sense of Lyapunov in Theorem 2.12 for Equation (6.35), a virtual control law α_3 can be chosen as follows;

$$\begin{aligned} -c_4\zeta_4 = & k_{11}(\zeta_1 + \omega_{1ref})(\zeta_2 + T_{1ref}) + k_{12}\omega_r(\zeta_4 + T_{2ref}) + k_{13}\omega_r \\ & + k_{14}(\zeta_1 + \omega_{1ref}) \\ \Rightarrow \alpha_3 = & \frac{1}{k_{12}T_2 + k_{13}}(-c_4(T_2 - T_{2ref}) - k_{11}\omega_1T_1 - k_{14}\omega_1) \equiv \omega_r \end{aligned} \quad (6.36)$$

where c_4 is the positive gain

By doing so, we have:

$$\dot{V}_4 = -c_1\zeta_1^2 - c_2\zeta_2^2 - c_3\zeta_3^2 - c_4\zeta_4^2 < 0 \quad \forall \zeta_1, \zeta_2, \zeta_3, \zeta_4 \neq 0 \quad (6.37)$$

By choosing the state feedbacks (6.15), (6.22), (6.29) and (6.36) and a change of state transformations (6.11), (6.18), (6.25), and (6.32) the complete system can be rewritten as follows:

$$\left. \begin{aligned} \dot{\zeta}_1 &= -c_1\zeta_1 \\ \dot{\zeta}_2 &= -c_2\zeta_2 \\ \dot{\zeta}_3 &= -c_3\zeta_3 \\ \dot{\zeta}_4 &= -c_4\zeta_4 \\ \dot{\omega}_r &= k_{15}(\zeta_4 + T_{2ref}) + k_{16}\omega_r + k_{17}\tau_r \end{aligned} \right\} \quad (6.38)$$

Step 5: by putting

$$\zeta_5 = \omega_r - \alpha_3 \quad (6.39)$$

The complete system can be rewritten as follows:

$$\left. \begin{aligned} \dot{\zeta}_1 &= -c_1\zeta_1 \\ \dot{\zeta}_2 &= -c_2\zeta_2 \\ \dot{\zeta}_3 &= -c_3\zeta_3 \\ \dot{\zeta}_4 &= -c_4\zeta_4 \\ \dot{\zeta}_5 &= k_{15}(\zeta_4 + T_{2ref}) + k_{16}(\zeta_5 + \alpha_3) - \dot{\alpha}_3 + k_{17}\tau_r \end{aligned} \right\} \quad (6.40)$$

where $\dot{\alpha}_3$ is determined by (6.36) or

$\dot{\alpha}_3$

$$= \frac{1}{(k_{12}T_2 + k_{13})^2} \left\{ \begin{array}{l} [-c_4(k_1\omega_1T_1 + k_{12}\omega_rT_2 + k_{13}\omega_r + k_{14}\omega_1) \\ -k_{11}\omega_1(k_{11}\omega_1T_1 + k_2\omega_1 + k_3\omega_u) \\ -(k_{11}T_1 + k_{14})(k_7T_2 + k_8T_1 + k_9\omega_1 + k_{10}\tau_1)][k_{12}T_2 + k_{13}] - \\ (-c_4(T_2 - T_{2ref}) - k_{11}\omega_1T_1 - k_{14}\omega_1) \\ (k_{11}\omega_1T_1 + k_{12}\omega_rT_2 + k_{13}\omega_r + k_{14}\omega_1)k_{12} \end{array} \right\}$$

Thus, τ_r can be chosen to make the subsystem (6.40) globally asymptotically stable. A CLF $V_5(\zeta_1, \zeta_2, \zeta_3, \zeta_4, \zeta_5)$ can be chosen such that it makes complete system asymptotically stable with the control law;

$$V_5(\zeta_1, \zeta_2, \zeta_3, \zeta_4, \zeta_5) = V_4 + \frac{1}{2}\zeta_5^2 \quad (6.41)$$

Taking the derivate of the Equation (6.41) in time and combining with the Equation (6.40) result in;

$$\dot{V}_5(\zeta_1, \zeta_2, \zeta_3, \zeta_4, \zeta_5) = -c_1\zeta_1^2 - c_2\zeta_2^2 - c_3\zeta_3^2 - c_4\zeta_4^2 + \zeta_5(k_{15}(\zeta_4 + T_{2ref}) + k_{16}(\zeta_5 + \alpha_3) - \dot{\alpha}_3 + k_{17}\tau_r) \quad (6.42)$$

To satisfy the asymptotically stable condition in a sense of Lyapunov in Theorem 2.12 for Equation (6.42), a control law τ_r can be chosen as follows;

$$\begin{aligned} -c_5\zeta_5 &= k_{15}(\zeta_4 + T_{2ref}) + k_{16}(\zeta_5 + \alpha_3) - \dot{\alpha}_3 + k_{17}\tau_r \\ \Rightarrow \tau_r &= \frac{1}{k_{17}}(-c_5(\omega_r - \alpha_3) - k_{15}T_2 - k_{16}\omega_r + \dot{\alpha}_3) \end{aligned} \quad (6.43)$$

where c_5 is the positive gain

By doing so, we have:

$$\dot{V}_5 = -c_1\zeta_1^2 - c_2\zeta_2^2 - c_3\zeta_3^2 - c_4\zeta_4^2 - c_5\zeta_5^2 < 0 \quad \forall \zeta_1, \zeta_2, \zeta_3, \zeta_4, \zeta_5 \neq 0 \quad (6.44)$$

Thus, there exists a CLF of the Eq. (69) and the state feedbacks (6.15), (6.22), (6.29), (6.36) and (6.43) and a change of state transformations (6.11), (6.18), (6.25), (6.32) and (6.39) the complete system can be rewritten as follows:

$$\left. \begin{array}{l} \dot{\zeta}_1 = -c_1\zeta_1 \\ \dot{\zeta}_2 = -c_2\zeta_2 \\ \dot{\zeta}_3 = -c_3\zeta_3 \\ \dot{\zeta}_4 = -c_4\zeta_4 \\ \dot{\zeta}_5 = -c_5\zeta_5 \end{array} \right\} \quad (6.45)$$

By the backstepping approach shown above, the backstepping controller of the system is given as follows

$$\left. \begin{aligned} \tau_1 &= \frac{1}{k_{10}} (-c_1(\omega_1 - \omega_{1ref}) - k_7 T_2 - k_8 T_1 - k_9 \omega_1) \\ \tau_u &= \frac{1}{k_6} (-c_3(\omega_u - \alpha_2) - k_4 T_1 - k_5 \omega_u + \dot{\alpha}_2) \\ \tau_r &= \frac{1}{k_{17}} (-c_5(\omega_r - \alpha_3) - k_{15} T_2 - k_{16} \omega_r + \dot{\alpha}_3) \end{aligned} \right\} \quad (6.46)$$

where c_1, c_2, c_3, c_4 , and c_5 are positive gains and determined by the modified genetic algorithms (MGA), and $\alpha_2, \alpha_3, \dot{\alpha}_2$, and $\dot{\alpha}_3$ are determined in the equations (6.34), (6.37), (6.42), (6.44) and (6.36). The positive gains c_1, c_2, c_3, c_4 , and c_5 in the (6.46) can be determined optimally by using the MGA by objective function (6.47).

$$J = \beta_1 \sum_{i=1}^N (\tau_u^2)_i + \beta_2 \sum_{i=1}^N (\tau_w^2)_i + \beta_3 \sum_{i=1}^N (\Delta T_1^2)_i + \beta_4 \sum_{i=1}^N (\Delta T_2^2)_i \quad (6.47)$$

where N is an integer number of iterations in control simulations, $\beta_1, \beta_2, \beta_3, \beta_4$ are scale factors, $\Delta T_i = T_i - T_{i ref}$ is the errors between the operating and reference tensions of span 1 and 2. The detailed explanation of the genetic algorithm and the MGA are developed by the authors in (Kyung-Hyun Choi and Thanh T. Tran, 2009) in chapter 3. The use of real-coded GAs with search operator find more suited than binary GAs in finding feasible gains from feasible parent gains. In this paper, the use of real-coded GAs with simulated binary crossover (SBX) and a parameter-based mutation operator is implemented. The mutation probability, mutation parameter, crossover rate and crossover probability is selected depending on the speed of convergence of algorithm as mentioned in chapter 3.

6.3 Backstepping Based Control Algorithm design

Figure 6.3 shows the block diagram of the two-span R2R web control system algorithm using the BSC. In this algorithm, the FPGA module based on PC shown in Figure 6.3 depends on the input data to generate the control signals of torques to keep web velocity and tension at prescribed reference values due to the presence of inertia change and viscous friction. This torques at rewinder, infeeder and unwinder are generated by the BSC (6.46). Load cells in channel 1 are used for web tension feedbacks of span 1 and 2, ultrasonic sensors are used to determine the radius change in time and encoders are used for velocity feedback of motors 1, 2, and 3. The FPGA module of Input/Outputs shown in Figure 5.3 depends on input signals to generate

the output signals. Using the Labview programming language, control software is given out for the two-span R2R web system as shown in Figure 6.8. With the rapid development of digital computers, the algorithm will be developed with the function that can detect errors and automatically recover the errors of the control system due to disturbances and changing parameters

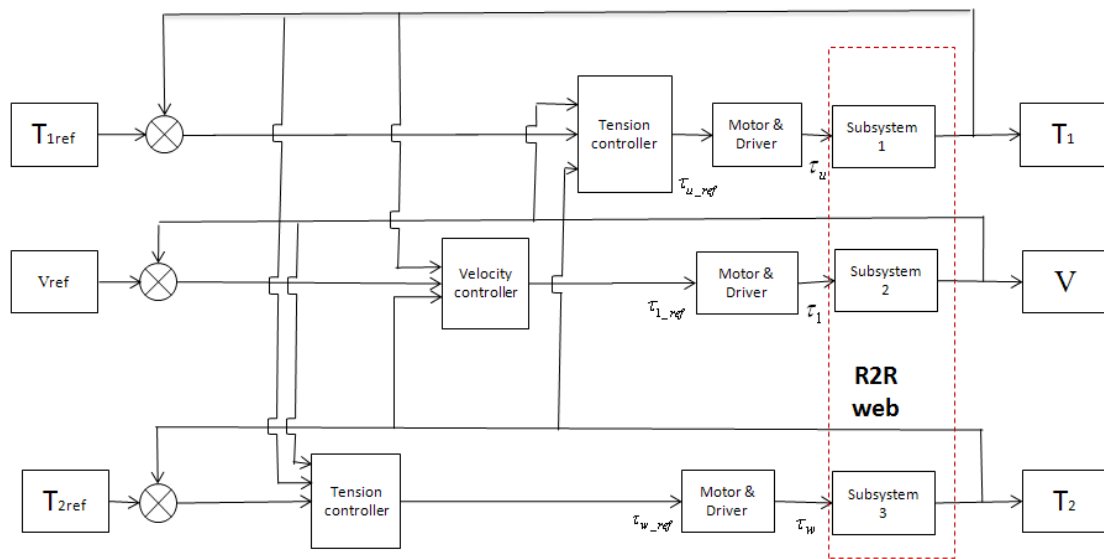


Figure 6.3: Block diagram of two-span R2R web tension and velocity control system

6.4 Numerical Simulation

6.4.1 Simulation Condition and Parameters

The simulation parameters of the two-span R2R web control system are shown in Table 6.1. The simulation condition is set up with the zero initial conditions, the desired web tension of $T_{1ref} = 20$ (N) and $T_{2ref} = 15$ (N) and the desired angular velocity of the infeeders of 0.5 (rad/s). In order to observe the effectiveness of the proposed algorithm of the BSC, one compensates the initial friction and inertia change of the rewinding and unwinding rollers in time. By using the feedback signals of loadcells for web tension at span 1, span 2 and of encoders for angular velocities at rewinder and unwinder, the backstepping controllers in Equation (6.46) will generate the reference torques to keep web tension and velocity at desired values.

Table 6.1: Simulation Parameter of Two-span R2R Web system

Parameters	values	units
Initial radius of the unwinder (R_u)	0.1455	(m)
Initial radius of the winder (R_r)	0.0483	(m)
Radius of the roller 1 (R_1)	0.02535	(m)
Total moment of inertia of motor at unwinder (J_{u0})	0.000707	(kg-m)
Total moment of inertia of motor at roller 1 (J_{10})	0.0001	(kg-m- s^2)
Total moment of inertia of motor at Winder (J_{r0})	0.000707	(kg-m- s^2)
Total length of span 1 (L_1)	1.490	(m)
Total length of span 2(L_2)	1.335	(m)
Coefficient of vicious friction at unwinder (B_u)	0.00002533	(kg-m-s/rad)
Coefficient of vicious friction at winder (B_r)	0.00002533	(kg-m-s/rad)
Coefficient of vicious friction at roll 1 (B_1)	0.00002533	(kg-m-s/rad)
The thickness of web (h)	0.0002	(m)
The width of web (w)	0.12	(m)
Young's module (E)	$2.7 \cdot 10^9$	(N/m^2)
Area of cross-section (A)	0.000013	m^2

6.4.2 Simulation results

The backstepping based control algorithm of backstepping controllers in Equations (6.46) is implemented in Matlab/Simulink. The optimal gains obtained by the MGA in chapter 3 are shown in Equation (6.48):

$$c_1 = 9.12, c_2 = 19.00, c_3 = 14.23, c_4 = 11.2, c_5 = 12.3 \quad (6.48)$$

The simulation results are presented in Figure 6.4 and Figure 6.5:

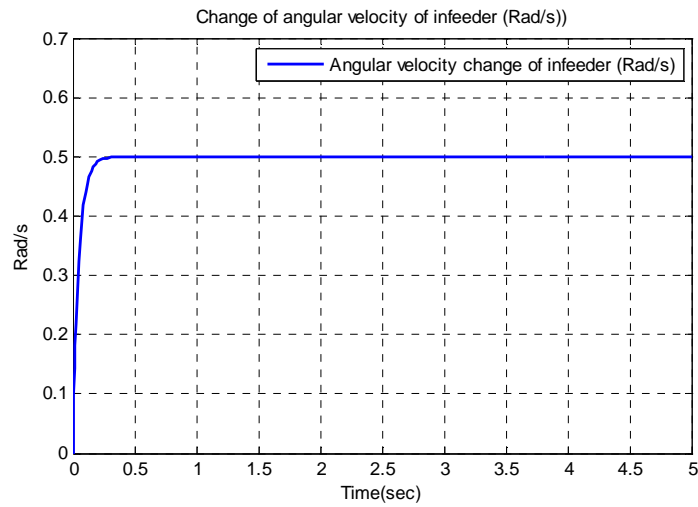


Figure 6.4: The angular velocity change in time of infeeders

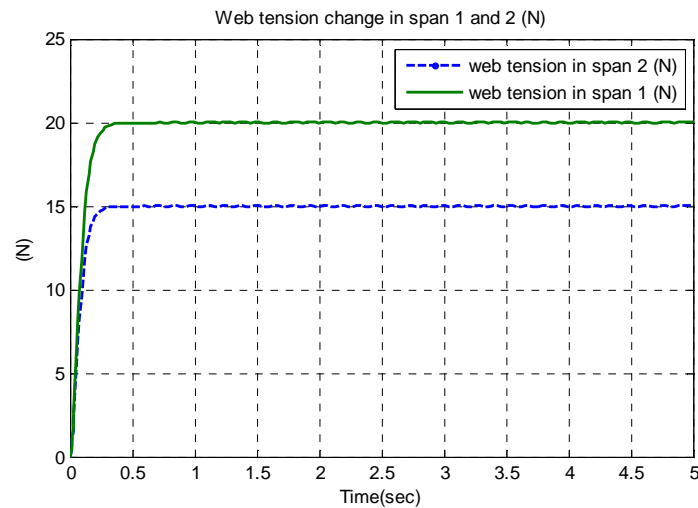


Figure 6.5: The tension change in time of span 1 and 2

Figures 6.4 and Figure 6.5 show the angular velocity change of the infeeders and the web tension change in web span 1 and web span 2 in time, respectively. From the simulation results, the following comments can be made:

- The time response of R2R web system of the BSC with optimal gains determined by the MGA has no overshoot and yields settling time of 0.2 second. This is validated by examining the Equations (6.45) that are the dynamic equations in new coordinates. Time response of these equations is always asymptotically global stable at the origin every positive gain and no overshoot or web tension and velocity is a well-tracking with positive gains.
- The proposed algorithm based on the BSC achieved the high precision, high stability and met the performance specifications.

6.5 Experimental Implementation

6.5.1 Experimental setup

Figure 6.6 shows the diagram of the two-span R2R web control system for experimental study. In order to operate the web, the unwinder, infeeder unit and rewinder motors HC-KFS43 and Driver (MR-J2S-40A) with torque control mode (0~8 V) are used. The two load cells are used to measure the web tensions at span 1 and span 2 of the system and an ultrasonic sensor MIC+25/IU/TC is used to determine the change in the radii in time. The system with NI FPGA board (PCI 7811R reconfigurable I/O) is integrated with input/output equipments to receive and send out the input and output signals. Depending on the input, the control program shown in Figure 6.7 with the proposed algorithm generates the torques to keep web velocity and tension at prescribed values.

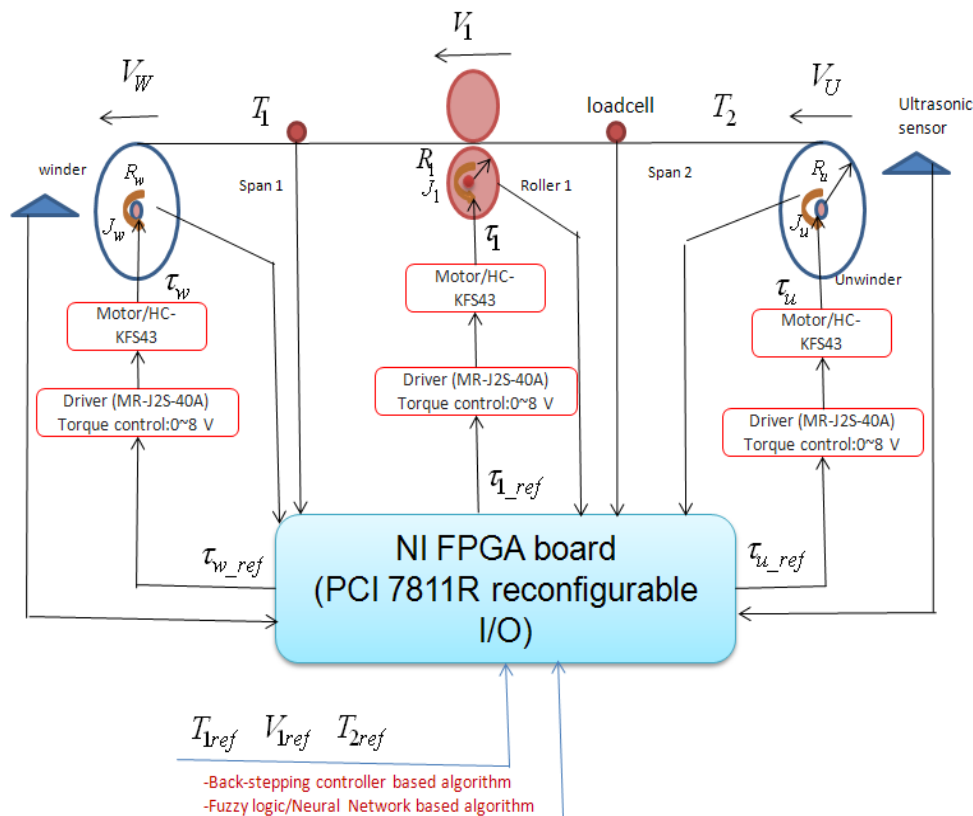


Figure 6.6: Block diagram of experimental study of two-span R2R web system

Using the diagram in Figure 6.6, the aforementioned mathematical model and the Labview language of Labview FPGA module, the web tension and velocity control program for R2R web system is shown in Figure 6.7. In this program, the

reference web tension and velocity and tension can be changed arbitrarily by users. The control program displays the change of web tension and change of angular velocity of rewinder and unwinder as shown in Figure 6.7. The change of gains in the BSC is also available to help the users understand and tune the gains to get the reference response of system in the presence of disturbance.

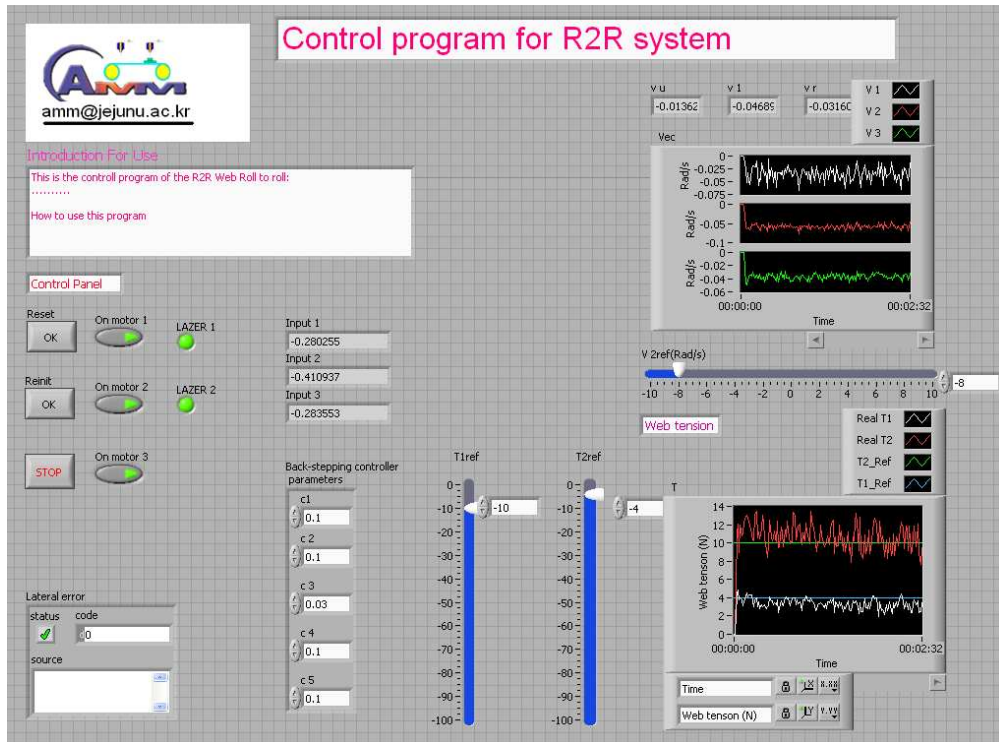


Figure 6.7: Tension control program of R2R web system

6.5.2 Experimental results

The desired web tensions of $T_{1ref} = 20$ (N), $T_{2ref} = 15$ (N) and the desired angular velocity change are 0.5 (rad/s). The experimental results are given in Figure 6.8 and Figure 6.9.

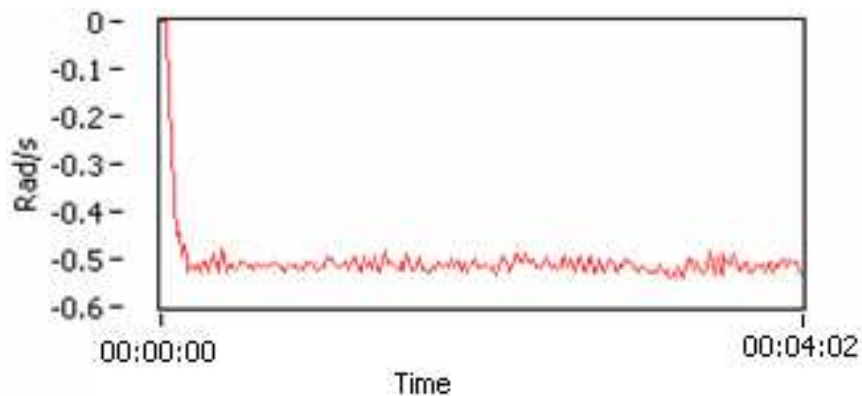


Figure 6.8: Angular velocity change of infeed roller

Figure 6.8 shows the time change of angular velocity of the infeder. It can be observed that the system response with low velocity shows no overshoot and good tracking to the command that is expected in the proposed theory. The minus sign represents the opposite direction of the motor.

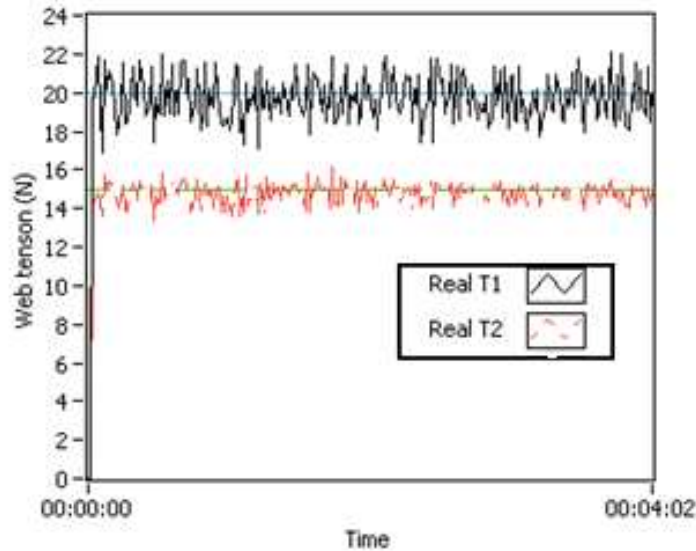


Figure 6.9: Web tension change in time of span 1 and 2

Figure 6.9 shows the web tension change in span 1 and span 2 respectively. The dash line shows the time response of web tension in span 2 and the solid line shows the time response of the web tension in span 1. The big variation of web tension in span 1 is due to the static charge existence in the unwinder. The static charge is removed by high voltage. Thus, the variation of web tension in span 2 is small. It is clear that the web tensions approach the reference values in short time with no overshoots.

From the above simulation results, the following comments can be made:

- The time responses of web tension and velocity of the proposed algorithm have no overshoot and fast response that is coincided with conclusions of the proposed theory.
- The large variations of web tension in time in span 1 due to the static charge can be eliminated when a specified device with high voltage is installed. The web tension in span 2 is proven this.

- By comparing with the simulation results in section 6.4, the experimental results validate the proposed algorithm. Also, the experimental results prove with high reliability.

6.6 Analysis and Discussions

In this chapter, a mathematical model is generated by using the theory in chapter 4. This system is with three inputs and three outputs and has a well-defined relative degree vector. By the coordinate transformations and feedback, it is proven that the exact state space linearization fails and thus backstepping based approach is proposed. The backstepping controllers are formulated using the chapter 2 and then a new precise control algorithm is proposed for a nonlinear two-span R2R web tension and velocity control system. The optimal gains of the BSC are determined by the MGA in chapter 3. The efficiency of this method is validated by the numerical simulation in Matlab/Simulink and the experimental results. The following conclusions are drawn:

- The time response of web tension and velocity of the optimal gains gives a zero overshoot and less settling time as proven in chapter 2. Also, tension and velocity commands are well-tracking.
- The simulation and experimental results show that the proposed algorithm is reliable and highly accurate.
- The proposed algorithm based on the BSC achieves asymptotically global stability with positive gains

Also, from the obtained results, it follows that the proposed algorithm using the BSC meets the desired performance specifications of the high stability in the presence of inertia change of the unwinder and rewinder and viscous friction. With the rapid development of sensors and electronic devices, the proposed control algorithm of the BSC results in a control system with high precision and is useful for applications with high digital computational system.

Chapter 7 Three-span R2R Web Tension and Velocity Control

In this chapter, a mathematical model for three-span R2R web control system obtained by using the results in chapter 4 will be shown. For comparison and advantages of backstepping approach as compared to conventional approach, a procedure for obtaining the backstepping controller and a backstepping based web tension and velocity control algorithm are proposed using the theory developed in chapter 2 and chapter 3. After that a Labview FPGA based software design is introduced. Finally, numerical simulation and experimental results are addressed in three-span R2R web system. Those results will be discussed and compared to show advances and limitations of the proposed algorithm.

7.1 Mathematical Model

The given problem is to design the controller that is required to keep web tension and web velocity at prescribed reference values, satisfy the performance specifications and obtain the high precision and stability. In recent years, almost all proposals are employed by using the PI or PID controllers with linear control system. However, some nonlinearity is ignored. The actual system performance is different from the simulated results. In this section, the idea of precise controller design for the nonlinear three-span web R2R system is implemented basing on the development of the theory of nonlinear control system.

Figure 7.1 shows a three-span R2R web system used to make the printed electronics devices such as RFID, solar cells. Figure 7.2 is the model of the three-span R2R web system that consists of an unwinder, a rewinder, an infeeder, an outfeeder, two dancer systems, four load cells, rollers, and web lateral control systems. The idle rollers guide the moving web around the load cell in a fixed angle. In order to control the web tension at span 1, span 2 and span 3, motors at the unwinder, the outfeeder, and the rewinder are used to produce control torques τ_u, τ_2 and τ_r , respectively to keep web tensions at the desired values and the infeeder is used for web velocity control. The dancer systems are used to take up the slack during the start-up and the shutdown. On the other hand, three load cells are used to feedback the web tensions during the operating process and a web guide mechanism

is used to control web lateral error. It is assumed that no web slippage occurs, the web has no permanent deformation due to applied tension, and the load cell dynamics is ignored. The given problem is to design the control inputs to the unwinder motor, the rewinder motor, and each of the driven rollers to maintain web velocity and tension at prescribed values in the presence of disturbances

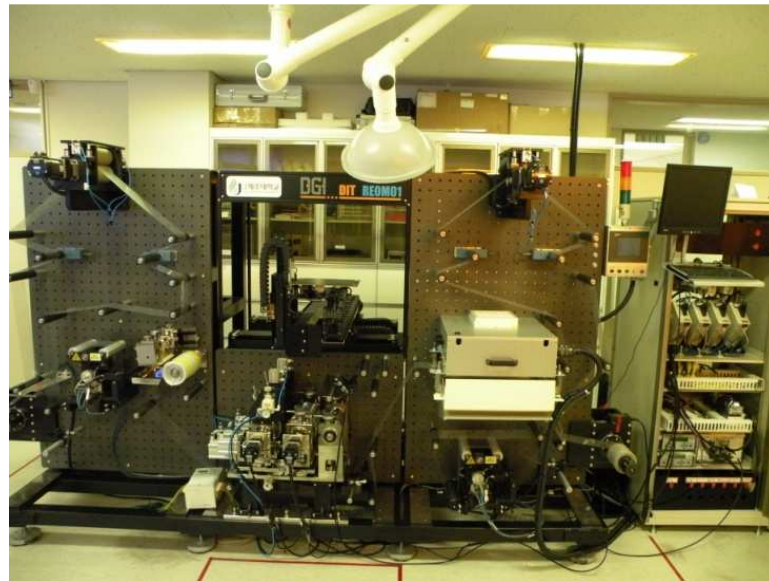


Figure 7.1: Three-span R2R web control system for printed electronics

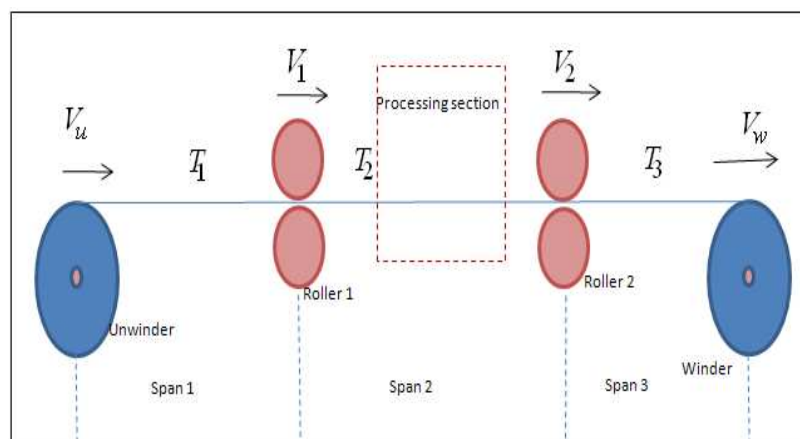


Figure 7.2: Model of three-span R2R web control system

By using Newton's second law at each span as shown in section 4.2 in chapter 4, we have:

$$\dot{\omega}_u = -\frac{B_u}{J_u}\omega_u + \frac{r_u}{J_u}T_1 - \frac{1}{J_u}\tau_u \quad (7.1)$$

$$\dot{\omega}_1 = -\frac{B_1}{J_1}\omega_1 - \frac{r_1}{J_1}T_1 + \frac{r_1}{J_1}T_2 + \frac{1}{J_1}\tau_1 \quad (7.2)$$

$$\dot{\omega}_2 = -\frac{B_2}{J_2}\omega_2 - \frac{r_2}{J_2}T_2 + \frac{r_2}{J_2}T_3 + \frac{1}{J_2}\tau_2 \quad (7.3)$$

$$\dot{\omega}_r = -\frac{B_r}{J_r}\omega_r - \frac{r_r}{J_r}T_3 + \frac{1}{J_r}\tau_r \quad (7.4)$$

and the use of principle of conservation of mass with aforementioned assumptions,

$$\dot{T}_1 = -\frac{r_1}{L_1}\omega_1T_1 + \frac{AEr_1}{L_1}\omega_1 - \frac{AEr_u}{L_1}\omega_u \quad (7.5)$$

$$\dot{T}_2 = \frac{r_1}{L_2}\omega_1T_1 - \frac{r_2}{L_2}\omega_2T_2 + \frac{AEr_2}{L_2}\omega_2 - \frac{AEr_1}{L_2}\omega_1 \quad (7.6)$$

$$\dot{T}_3 = \frac{r_2}{L_3}\omega_2T_2 - \frac{r_r}{L_3}\omega_rT_3 + \frac{AEr_r}{L_3}\omega_r - \frac{AEr_2}{L_3}\omega_2 \quad (7.7)$$

By combining the above equations and noting that $k_1 = -\frac{B_1}{J_1}$, $k_2 = -\frac{r_1}{J_1}$, $k_3 = \frac{r_1}{J_1}$,

$$k_4 = \frac{1}{J_1}, k_5 = -\frac{r_1}{L_1}, k_6 = \frac{AEr_1}{L_1}, k_7 = -\frac{AEr_u}{L_1}, k_8 = -\frac{B_u}{J_u}, k_9 = \frac{r_u}{J_u}, k_{10} = -\frac{1}{J_u},$$

$$k_{11} = \frac{r_1}{L_2}, k_{12} = -\frac{r_2}{L_2}, k_{13} = \frac{AEr_2}{L_2}, k_{14} = -\frac{AEr_1}{L_2}, k_{15} = -\frac{B_2}{J_2}, k_{16} = -\frac{r_2}{J_2}, k_{17} =$$

$$\frac{r_2}{J_2}, k_{18} = \frac{1}{J_2}, k_{19} = \frac{r_2}{L_3}, k_{20} = -\frac{r_r}{L_3}, k_{21} = \frac{AEr_r}{L_3}, k_{22} = -\frac{AEr_2}{L_3}, k_{23} = -\frac{B_r}{J_r}, k_{24} =$$

$$-\frac{r_r}{J_r}, k_{25} = \frac{1}{J_r}$$

The web nonlinear dynamic equations (7.1)-(7.7) of a three-span R2R web control system can be rearranged and rewritten as follows:

$$\dot{\omega}_1 = k_1\omega_1 + k_2T_1 + k_3T_2 + k_4\tau_1 \quad (7.8)$$

$$\dot{T}_1 = k_5\omega_1T_1 + k_6\omega_1 + k_7\omega_u \quad (7.9)$$

$$\dot{\omega}_u = k_8\omega_u + k_9T_1 + k_{10}\tau_u \quad (7.10)$$

$$\dot{T}_2 = k_{11}\omega_1T_1 + k_{12}\omega_2T_2 + k_{13}\omega_2 + k_{14}\omega_1 \quad (7.11)$$

$$\dot{\omega}_2 = k_{15}\omega_2 + k_{16}T_2 + k_{17}T_3 + k_{18}\tau_2 \quad (7.12)$$

$$\dot{T}_3 = k_{19}\omega_2T_2 + k_{20}\omega_rT_3 + k_{21}\omega_r + k_{22}\omega_2 \quad (7.13)$$

$$\dot{\omega}_r = k_{23}\omega_r + k_{24}T_3 + k_{25}\tau_r \quad (7.14)$$

We rewrite equations (7.8)-(7.14) in vector form:

$$\begin{bmatrix} \dot{\omega}_1 \\ \dot{T}_1 \\ \dot{\omega}_u \\ \dot{T}_2 \\ \dot{\omega}_2 \\ \dot{T}_3 \\ \dot{\omega}_r \end{bmatrix} = \begin{bmatrix} k_1\omega_1 + k_2T_1 + k_3T_2 \\ k_5\omega_1T_1 + k_6\omega_1 + k_7\omega_u \\ k_8\omega_u + k_9T_1 \\ k_{11}\omega_1T_1 + k_{12}\omega_2T_2 + k_{13}\omega_2 + k_{14}\omega_1 \\ k_{15}\omega_2 + k_{16}T_2 + k_{17}T_3 \\ k_{19}\omega_2T_2 + k_{20}\omega_rT_3 + k_{21}\omega_r + k_{22}\omega_2 \\ k_{23}\omega_r + k_{24}T_3 \end{bmatrix} + \begin{bmatrix} k_4\tau_1 \\ 0 \\ k_{10}\tau_u \\ 0 \\ k_{18}\tau_2 \\ 0 \\ k_{25}\tau_r \end{bmatrix} \quad (7.15)$$

with output equations

$$\begin{bmatrix} y_1 \\ y_2 \\ y_3 \end{bmatrix} = \begin{bmatrix} \omega_1 \\ T_1 \\ T_2 \\ T_3 \end{bmatrix} \quad (7.16)$$

T_1, T_2, T_3 : Web tensions of span 1, span2, span 3, respectively, $\omega_u, \omega_1, \omega_2, \omega_r$: Angular velocities at motor of unwinder, roller 1, and roller 2, and rewinder, respectively, J_u, J_1, J_2, J_r : Inertia moments of unwind roll and unwinder motor, roller 1 and roll motor, roller 2 and roll motor, rewinder, and motor, respectively, r_u, r_1, r_2, r_r : Radii of unwind roll, roller 1, roller 2, and rewind roll, respectively, L_1, L_2, L_3 : The length of span1, span 2, span 3, respectively, B_u, B_1, B_2, B_r : The coefficients of viscous friction of unwind roll, roller 1, roller 2, and rewind roll, respectively, $\tau_u, \tau_1, \tau_2, \tau_r$: Control torques generated by the unwinder motor, roller 1 motor, roller 2 motor, and winder motor, respectively, E: The Young modulus of materials, A: The area of web cross-section, h: The thickness of web.

7.2 Backstepping Control Design

It is the same as in two-span R2R web system. The system has a well-defined relative degree at the origin and it is easy to check that the state space exact linearization problem is solvable. Thus, backstepping based design for the system is presented. In the next section, the backstepping controller design is based on the idea of using the CLF, backstepping technique, and assumption about decentralization i.e. Backstepping controller is obtained by choosing the control torques for each of subsystems such that the time derivative of CLF is a negative definitive function. An algorithm for designing the backstepping controller of a nonlinear single-span and two-span R2R web control system has been proposed by the authors in chapter 4 and 5. In this chapter, the above results will be applied and extended for the three-span R2R web control system consisting of the Equations (7.8)-(7.14). We suppose that

the complete system Equations (7.8)-(7.14) is divided into seven subsystems. The first one consists of the first Equation (6.8). The second one consists of the two Equations (7.8) and (7.9). The third one consists of the three Equations (7.8), (7.9) and (7.10). The fourth one consists of the four Equations (7.8), (7.9), (7.10), and (7.11). The fifth one consists of the five Equations (7.8), (7.9), (7.10), (7.11), and (7.12). The sixth one consists of the six Equations (7.8), (7.9), (7.10), (7.11), (7.12), and (7.13). Finally, the last one is a complete system of the Equations (7.8)-(7.14). After applying the modified backstepping method with each subsystem mentioned in chapter II and applications with results in chapter 3, the resulting controller called the backstepping controller is proven to achieve globally asymptotical stability using a CLF and Theorem 2.12 in chapter 2. The next step is the detail of backstepping controller design for three-span R2R system of desired tensions at span 1, span 2, and 3 of T_{1ref} , T_{2ref} , and T_{3ref} respectively and desired angular velocity of infeed roll ω_{1ref} .

Step 1: Consider the first subsystem and put:

$$\zeta_1 = \omega_1 - \omega_{1ref} \quad (7.17)$$

By taking the derivative both sides in time and combining with Equation (7.17), we have:

$$\dot{\zeta}_1 = \dot{\omega}_1 = k_1(\zeta_1 + \omega_{1ref}) + k_2T_1 + k_3T_2 + k_4\tau_1 \quad (7.18)$$

For the Equation (7.18), a CLF $V_1(\zeta_1)$ can be chosen such that when the control law is applied, its time derivative becomes negative definite or mathematically

$$V_1(\zeta_1) = \frac{1}{2}\zeta_1^2 \quad (7.19)$$

Taking the derivative in time of the Equation (7.19) and combining with the Equation (7.18) results in:

$$\dot{V}_1(\zeta_1) = \zeta_1\dot{\zeta}_1 = \zeta_1(k_1(\zeta_1 + \omega_{1ref}) + k_2T_1 + k_3T_2 + k_4\tau_1) \quad (7.20)$$

To meet the asymptotically stable condition in the sense of Lyapunov for the Equation (7.20), the controller τ_1 can be chosen as follows;

$$\begin{aligned} -c_1\zeta_1 &= k_1(\zeta_1 + \omega_{1ref}) + k_2T_1 + k_3T_2 + k_4\tau_1 \\ \Rightarrow \tau_1 &= \frac{1}{k_4}(-c_1(\omega_1 - \omega_{1ref}) - k_3T_2 - k_2T_1 - k_1\omega_1) \end{aligned} \quad (7.21)$$

where c_1 is the positive gain

By doing so, we have:

$$\dot{V}_1(\zeta_1) = \zeta_1 \dot{\zeta}_1 = -c_1 \zeta_1^2 < 0 \quad \forall \zeta_1 \neq 0 \quad (7.22)$$

Step 2: by choosing the state feedbacks (7.21) and a change of state transformations (7.17), the second subsystem can be rewritten as follows:

$$\left. \begin{aligned} \dot{\zeta}_1 &= -c_1 \zeta_1 \\ \dot{T}_1 &= k_5 \omega_1 T_1 + k_6 (\zeta_1 + \omega_{1ref}) + k_7 \omega_u \end{aligned} \right\} \quad (7.23)$$

By putting

$$\zeta_2 = T_1 - T_{1ref} \quad (7.24)$$

The second subsystem can be rewritten as follows:

$$\left. \begin{aligned} \dot{\zeta}_1 &= -c_1 \zeta_1 \\ \dot{\zeta}_2 &= k_5 (\zeta_1 + \omega_{1ref}) (\zeta_2 + T_{1ref}) + k_6 (\zeta_1 + \omega_{1ref}) + k_7 \omega_u \end{aligned} \right\} \quad (7.25)$$

Now, ω_u is regarded as a control input to the system (7.25). So, ω_u can be chosen to make the subsystem (7.25) globally asymptotically stable. A CLF $V_2(\zeta_1, \zeta_2)$ can be chosen such that it makes the subsystem (7.25) asymptotically stable with the virtual control law, i.e.

$$V_2(\zeta_1, \zeta_2) = V_1(\zeta_1) + \frac{1}{2} \zeta_2^2 \quad (7.26)$$

By taking the derivative of the Equation (7.26) in time and combining with the Equation (7.25) result in:

$$\dot{V}_2(\zeta_1, \zeta_2) = -c_1 \zeta_1^2 - \zeta_2 (k_5 (\zeta_1 + \omega_{1ref}) (\zeta_2 + T_{1ref}) + k_6 (\zeta_1 + \omega_{1ref}) + k_7 \omega_u) \quad (7.27)$$

By satisfying the asymptotically stable condition in the sense of Lyapunov in chapter 2 for the Equation (7.27), a virtual control law α_2 can be chosen as follows;

$$\begin{aligned} -c_2 \zeta_2 &= k_5 (\zeta_1 + \omega_{1ref}) (\zeta_2 + T_{1ref}) + k_6 (\zeta_1 + \omega_{1ref}) + k_7 \omega_u \\ \Rightarrow \alpha_2 &= \frac{1}{k_7} (-c_2 (T_1 - T_{1ref}) - k_5 \omega_1 T_1 - k_6 \omega_1) \equiv \omega_u \end{aligned} \quad (7.28)$$

Where c_2 is the positive gain

By doing so, we have:

$$\dot{V}_2(\zeta_1, \zeta_2) = -c_1 \zeta_1^2 - c_2 \zeta_2^2 < 0 \quad \forall \zeta_1, \zeta_2 \neq 0 \quad (7.29)$$

By choosing the state feedbacks (7.21) and (7.28) and a change of state transformations (7.17) and (7.24), the third subsystem can be rewritten as follows:

$$\left. \begin{aligned} \dot{\zeta}_1 &= -c_1 \zeta_1 \\ \dot{\zeta}_2 &= -c_2 \zeta_2 \\ \dot{\omega}_u &= k_8 \omega_u + k_9 (\zeta_2 + T_{1ref}) + k_{10} \tau_u \end{aligned} \right\} \quad (7.30)$$

Step 3: By putting

$$\zeta_3 = \omega_u - \alpha_2 \quad (7.31)$$

The third subsystem can be rewritten as follows:

$$\left. \begin{aligned} \dot{\zeta}_1 &= -c_1 \zeta_1 \\ \dot{\zeta}_2 &= -c_2 \zeta_2 \\ \dot{\zeta}_3 &= k_8(\zeta_3 + \alpha_2) + k_9(\zeta_2 + T_{1ref}) - \dot{\alpha}_2 + k_{10} \tau_u \end{aligned} \right\} \quad (7.32)$$

where $\dot{\alpha}_2$ is determined by the following

$$\begin{aligned} \dot{\alpha}_2 &= \frac{1}{k_7} \left(-(c_2 + k_1 \omega_1)(k_5 \omega_1 T_1 + k_6 \omega_1 + k_7 \omega_u) - (k_5 T_1 + k_6)(k_3 T_2 + k_2 T_1 \right. \\ &\quad \left. + k_1 \omega_1 + k_4 \tau_1) \right) \end{aligned}$$

So, τ_u can be chosen to make the subsystem (7.32) globally asymptotically stable. A CLF $V_3(\zeta_1, \zeta_2, \zeta_3)$ can be chosen such that it makes the subsystem (7.32) asymptotically stable with a virtual control law:

$$V_3(\zeta_1, \zeta_2, \zeta_3) = V_2(\zeta_1, \zeta_2) + \frac{1}{2} \zeta_3^2 \quad (7.33)$$

Taking the derivative of the Equation (7.33) in time and combining with Eq. (7.32) result in;

$$\dot{V}_3(\zeta_1, \zeta_2, \zeta_3) = -c_1 \zeta_1^2 - c_2 \zeta_2^2 + \zeta_3(k_8(\zeta_3 + \alpha_2) + k_9(\zeta_2 + T_{1ref}) - \dot{\alpha}_2 + k_{10} \tau_u) \quad (7.34)$$

To satisfy the asymptotically stable condition in the sense of Lyapunov in chapter 2 for the Equation (7.34), a control law τ_u can be chosen as follows;

$$\begin{aligned} -c_3 \zeta_3 &= k_8(\zeta_3 + \alpha_2) + k_9(\zeta_2 + T_{1ref}) - \dot{\alpha}_2 + k_{10} \tau_u \\ \Rightarrow \tau_u &= \frac{1}{k_{10}} (-c_3(\omega_u - \alpha_2) - k_9 T_1 - k_8 \omega_u + \dot{\alpha}_2) \end{aligned} \quad (7.35)$$

where c_3 is the positive gain

By doing so, we have:

$$\dot{V}_3(\zeta_1, \zeta_2, \zeta_3) = -c_1 \zeta_1^2 - c_2 \zeta_2^2 - c_3 \zeta_3^2 < 0 \quad \forall \zeta_1, \zeta_2, \zeta_3 \neq 0 \quad (7.36)$$

By choosing the state feedbacks (7.21), (7.28) and (7.35) and a change of state transformations (7.17), (7.24) and (7.31), the fourth subsystem can be rewritten as follows:

$$\left. \begin{aligned} \dot{\zeta}_1 &= -c_1 \zeta_1 \\ \dot{\zeta}_2 &= -c_2 \zeta_2 \\ \dot{\zeta}_3 &= -c_3 \zeta_3 \\ \dot{T}_2 &= k_{11}(\zeta_1 + \omega_{1ref})(\zeta_2 - T_{1ref}) + k_{12} \omega_2 T_2 + k_{13} \omega_2 + k_{14}(\zeta_1 + \omega_{1ref}) \end{aligned} \right\} \quad (7.37)$$

Step 4: by putting

$$\zeta_4 = T_2 - T_{2ref} \quad (7.38)$$

The fourth subsystem can be rewritten as follows:

$$\left. \begin{aligned} \dot{\zeta}_1 &= -c_1 \zeta_1 \\ \dot{\zeta}_2 &= -c_2 \zeta_2 \\ \dot{\zeta}_3 &= -c_3 \zeta_3 \\ \dot{\zeta}_4 &= k_{11}(\zeta_1 + \omega_{1ref})(\zeta_2 - T_{1ref}) + k_{12}\omega_2(\zeta_4 + T_{2ref}) + k_{13}\omega_2 + k_{14}(\zeta_1 + \omega_{1ref}) \end{aligned} \right\} \quad (7.39)$$

Now, ω_2 is regarded as a control input in system (7.39). So, ω_2 can be chosen to make the subsystem (7.39) globally asymptotically stable. A CLF $V_4(\zeta_1, \zeta_2, \zeta_3, \zeta_4)$ can be chosen such that it makes subsystem (7.39) asymptotically stable with the virtual control law;

$$V_4(\zeta_1, \zeta_2, \zeta_3, \zeta_4) = V_3(\zeta_1, \zeta_2, \zeta_3) + \frac{1}{2}\zeta_4^2 \quad (7.40)$$

Taking the derivative of the Equation (7.40) in time and combining with the Equation (7.39) result in;

$$\begin{aligned} \dot{V}_2 &= -c_1\zeta_1^2 - c_2\zeta_2^2 - c_3\zeta_3^2 + \zeta_4(k_{11}(\zeta_1 + \omega_{1ref})(\zeta_2 - T_{1ref}) + k_{12}\omega_2(\zeta_4 + \\ &T_{2ref}) + k_{13}\omega_2 + k_{14}(\zeta_1 + \omega_{1ref})) \end{aligned} \quad (7.41)$$

By satisfying the asymptotically stable condition in the sense of Lyapunov in chapter 2 for the Equation (7.41), a virtual control law α_3 can be chosen as follows;

$$\begin{aligned} -c_4\zeta_4 &= k_{11}(\zeta_1 + \omega_{1ref})(\zeta_2 - T_{1ref}) + k_{12}\omega_2(\zeta_4 + T_{2ref}) + k_{13}\omega_2 \\ &+ k_{14}(\zeta_1 + \omega_{1ref}) \\ \Rightarrow \alpha_3 &= \frac{1}{k_{12}T_2 + k_{13}}(-c_4(T_2 - T_{2ref}) - k_{11}\omega_1 T_1 - k_{14}\omega_1) \equiv \omega_2 \end{aligned} \quad (7.42)$$

where c_4 is the positive gain

By doing so, we have:

$$\dot{V}_4 = -c_1\zeta_1^2 - c_2\zeta_2^2 - c_3\zeta_3^2 - c_4\zeta_4^2 < 0 \quad \forall \zeta_1, \zeta_2, \zeta_3, \zeta_4 \neq 0 \quad (7.43)$$

By choosing the state feedbacks (7.21), (7.28), (7.35) and (7.42) and a change of state transformations (7.17), (7.24) (7.31) and (7.38), the fifth subsystem can be rewritten as follows:

$$\left. \begin{aligned} \dot{\zeta}_1 &= -c_1\zeta_1 \\ \dot{\zeta}_2 &= -c_2\zeta_2 \\ \dot{\zeta}_3 &= -c_3\zeta_3 \\ \dot{\zeta}_4 &= -c_4\zeta_4 \end{aligned} \right\} \quad (7.44)$$

$$\dot{\omega}_2 = k_{15}\omega_2 + k_{16}(\zeta_4 + T_{2ref}) + k_{17}T_3 + k_{18}\tau_2$$

Step 5: by putting

$$\zeta_5 = \omega_2 - \alpha_3 \quad (7.45)$$

The fifth system can be rewritten as follows:

$$\left. \begin{aligned} \dot{\zeta}_1 &= -c_1\zeta_1 \\ \dot{\zeta}_2 &= -c_2\zeta_2 \\ \dot{\zeta}_3 &= -c_3\zeta_3 \\ \dot{\zeta}_4 &= -c_4\zeta_4 \end{aligned} \right\} \quad (7.46)$$

$$\dot{\zeta}_5 = k_{15}(\zeta_5 + \alpha_3) + k_{16}(\zeta_4 + T_{2ref}) + k_{17}T_3 - \dot{\alpha}_3 + k_{18}\tau_2$$

Where $\dot{\alpha}_3$ is determined as follows:

$$\dot{\alpha}_3 = \frac{1}{(k_{12}T_2 + k_{13})^2} \left\{ \begin{aligned} &[-c_4(k_{11}\omega_1T_1 + k_{12}\omega_2T_2 + k_{13}\omega_2 + k_{14}\omega_1) \\ &\quad - k_{11}\omega_1(k_5\omega_1T_1 + k_6\omega_1 + k_7\omega_u) \\ &-(k_{11}T_1 + k_{14})(k_3T_2 + k_2T_1 + k_1\omega_1 + k_4\tau_1)][k_{12}T_2 + k_{13}] - \\ &\quad (-c_4(T_2 - T_{2ref}) - k_{11}\omega_1T_1 - k_{14}\omega_1) \\ &\quad (k_{11}\omega_1T_1 + k_{12}\omega_2T_2 + k_{13}\omega_2 + k_{14}\omega_1)k_{12} \end{aligned} \right\}$$

Thus, τ_2 can be chosen to make the subsystem (7.46) globally asymptotically stable.

A CLF $V_5(\zeta_1, \zeta_2, \zeta_3, \zeta_4, \zeta_5)$ can be chosen such that it makes subsystem (7.46) asymptotically stable with the control law;

$$V_5(\zeta_1, \zeta_2, \zeta_3, \zeta_4, \zeta_5) = V_4(\zeta_1, \zeta_2, \zeta_3, \zeta_4) + \frac{1}{2}\zeta_5^2 \quad (7.47)$$

Taking derivative of the Equation (7.47) in time and combining with the terms of the Equation (7.46) result in;

$$\dot{V}_5(\zeta_1, \zeta_2, \zeta_3, \zeta_4, \zeta_5) = -c_1\zeta_1^2 - c_2\zeta_2^2 - c_3\zeta_3^2 - c_4\zeta_4^2 + \zeta_5(k_{15}(\zeta_5 + \alpha_3) + k_{16}(\zeta_4 + T_{2ref}) + k_{17}T_3 - \dot{\alpha}_3 + k_{18}\tau_2) \quad (7.48)$$

By satisfying the asymptotically stable condition in the sense of Lyapunov in chapter 2 for the Equation (7.48), a control law τ_2 can be chosen as follows;

$$\begin{aligned} -c_5\zeta_5 &= k_{15}(\zeta_5 + \alpha_3) + k_{16}(\zeta_4 + T_{2ref}) + k_{17}T_3 - \dot{\alpha}_3 + k_{18}\tau_2 \\ \Rightarrow \tau_2 &= \frac{1}{k_{18}}(-c_5(\omega_2 - \alpha_3) - k_{15}\omega_2 - k_{16}T_2 - k_{17}T_3 + \dot{\alpha}_3) \end{aligned} \quad (7.49)$$

Where c_5 is the positive gain

By doing so, we have:

$$\dot{V}_5 = -c_1\zeta_1^2 - c_2\zeta_2^2 - c_3\zeta_3^2 - c_4\zeta_4^2 - c_5\zeta_5^2 < 0 \quad \forall \zeta_1, \zeta_2, \zeta_3, \zeta_4, \zeta_5 \neq 0 \quad (7.50)$$

By choosing the state feedbacks (7.21), (7.28), (7.35) (7.42) and (7.49) and a change of state transformations (7.17), (7.24) (7.31), (7.38) and (7.45), the sixth subsystem can be rewritten as follows:

$$\left. \begin{aligned} \dot{\zeta}_1 &= -c_1\zeta_1 \\ \dot{\zeta}_2 &= -c_2\zeta_2 \\ \dot{\zeta}_3 &= -c_3\zeta_3 \\ \dot{\zeta}_4 &= -c_4\zeta_4 \\ \dot{\zeta}_5 &= -c_5\zeta_5 \\ \dot{T}_3 &= k_{19}(\zeta_5 + \alpha_3)(\zeta_4 + T_{2ref}) + k_{20}\omega_r T_3 + k_{21}\omega_r + k_{22}(\zeta_5 + \alpha_3) \end{aligned} \right\} \quad (7.51)$$

Step 6: by putting

$$\zeta_6 = T_3 - T_{3ref} \quad (7.52)$$

The sixth subsystem can be rewritten as follows:

$$\left. \begin{aligned} \dot{\zeta}_1 &= -c_1\zeta_1 \\ \dot{\zeta}_2 &= -c_2\zeta_2 \\ \dot{\zeta}_3 &= -c_3\zeta_3 \\ \dot{\zeta}_4 &= -c_4\zeta_4 \\ \dot{\zeta}_5 &= -c_5\zeta_5 \\ \dot{\zeta}_6 &= k_{19}(\zeta_5 + \alpha_3)(\zeta_4 + T_{2ref}) + k_{20}\omega_r(\zeta_6 + T_{3ref}) + k_{21}\omega_r + k_{22}(\zeta_5 + \alpha_3) \end{aligned} \right\} \quad (7.53)$$

Now, ω_r is regarded as a control input in the system (7.53). So, ω_r can be chosen arbitrarily to make the subsystem (7.53) globally asymptotically stable. A CLF $V_6(\zeta_1, \zeta_2, \zeta_3, \zeta_4, \zeta_5, \zeta_6)$ can be chosen such that it makes subsystem (7.53) asymptotically stable with the virtual control law;

$$V_6(\zeta_1, \zeta_2, \zeta_3, \zeta_4, \zeta_5, \zeta_6) = V_5(\zeta_1, \zeta_2, \zeta_3, \zeta_4, \zeta_5) + \frac{1}{2}\zeta_6^2 \quad (7.54)$$

Taking the derivative of the Equation (7.54) in time and combining with the Equation (7.53) result in;

$$\dot{V}_6(\zeta_1, \zeta_2, \zeta_3, \zeta_4, \zeta_5, \zeta_6) = -c_1\zeta_1^2 - c_2\zeta_2^2 - c_3\zeta_3^2 - c_4\zeta_4^2 - c_5\zeta_5^2 + \zeta_6(k_{19}(\zeta_5 + \alpha_3)(\zeta_4 + T_{2ref}) + k_{20}\omega_r(\zeta_6 + T_{3ref}) + k_{21}\omega_r + k_{22}(\zeta_5 + \alpha_3)) \quad (7.55)$$

By satisfying the asymptotically stable condition in the sense of Lyapunov in chapter 2, a virtual control law α_3 can be chosen as follows;

$$-c_6\zeta_6 = k_{19}(\zeta_5 + \alpha_3)(\zeta_4 + T_{2ref}) + k_{20}\omega_r(\zeta_6 + T_{3ref}) + k_{21}\omega_r + k_{22}(\zeta_5 + \alpha_3)$$

$$\alpha_4 = \frac{1}{k_{20}T_3 + k_{21}}(-c_6(T_3 - T_{3ref}) - k_{19}\omega_2T_2 - k_{22}\omega_2) \equiv \omega_r \quad (7.56)$$

Where c_6 is the positive gain

By doing so, we have:

$$\dot{V}_6 = -c_1\zeta_1^2 - c_2\zeta_2^2 - c_3\zeta_3^2 - c_4\zeta_4^2 - c_5\zeta_5^2 + c_6\zeta_6^2 < 0 \quad \forall \zeta_1, \zeta_2, \zeta_3, \zeta_4, \zeta_5, \zeta_6 \neq 0 \quad (7.57)$$

By choosing the state feedbacks (7.21), (7.28), (7.35) (7.42) (7.49) and (7.56) and a change of state transformations (7.17), (7.24) (7.31), (7.38) (7.45) and (7.52), the complete system can be rewritten as follows:

$$\left. \begin{aligned} \dot{\zeta}_1 &= -c_1\zeta_1 \\ \dot{\zeta}_2 &= -c_2\zeta_2 \\ \dot{\zeta}_3 &= -c_3\zeta_3 \\ \dot{\zeta}_4 &= -c_4\zeta_4 \\ \dot{\zeta}_5 &= -c_5\zeta_5 \\ \dot{\zeta}_6 &= -c_6\zeta_6 \\ \dot{\omega}_r &= k_{23}\omega_r + k_{24}(\zeta_6 + T_{3ref}) + k_{25}\tau_r \end{aligned} \right\} \quad (7.58)$$

Step 7: by putting

$$\zeta_7 = \omega_r - \alpha_4 \quad (7.59)$$

The complete system can be rewritten as follows:

$$\left. \begin{aligned} \dot{\zeta}_1 &= -c_1\zeta_1 \\ \dot{\zeta}_2 &= -c_2\zeta_2 \\ \dot{\zeta}_3 &= -c_3\zeta_3 \\ \dot{\zeta}_4 &= -c_4\zeta_4 \\ \dot{\zeta}_5 &= -c_5\zeta_5 \\ \dot{\zeta}_6 &= -c_6\zeta_6 \\ \dot{\zeta}_7 &= k_{23}(\zeta_7 + \alpha_4) + k_{24}(\zeta_6 + T_{3ref}) - \dot{\alpha}_4 + k_{25}\tau_r \end{aligned} \right\} \quad (7.60)$$

Where $\dot{\alpha}_4$ is determined as follows:

$$\dot{\alpha}_4 = \frac{1}{(k_{20}T_3 + k_{21})^2} \left\{ \begin{aligned} &[-c_6(k_{19}\omega_2T_2 + k_{20}\omega_rT_3 + k_{21}\omega_r + k_{22}\omega_2) \\ &-k_{19}\omega_2(k_{11}\omega_1T_1 + k_{12}\omega_2T_2 + k_{13}\omega_2 + k_{14}\omega_1) \\ &-(k_{19}T_2 + k_{22})(k_{15}\omega_2 + k_{16}T_2 + k_{17}T_3 + k_{18}\tau_2)][k_{20}T_3 + k_{21}] - \\ &(-c_6(T_3 - T_{3ref}) - k_{19}\omega_2T_2 - k_{20}\omega_2)(k_{19}\omega_2T_2 + k_{20}\omega_rT_3 \\ &+ k_{21}\omega_r + k_{22}\omega_2)k_{20} \end{aligned} \right\}$$

Thus, τ_r can be chosen arbitrarily to make the subsystem (7.60) globally asymptotically stable. A CLF $V_7(\zeta_1, \zeta_2, \zeta_3, \zeta_4, \zeta_5, \zeta_6, \zeta_7)$ can be chosen such that it makes complete system (7.60) asymptotically stable with the control law;

$$V_7(\zeta_1, \zeta_2, \zeta_3, \zeta_4, \zeta_5, \zeta_6, \zeta_7) = V_6(\zeta_1, \zeta_2, \zeta_3, \zeta_4, \zeta_5, \zeta_6) + \frac{1}{2}\zeta_7^2 \quad (7.61)$$

Taking the time derivative of the Equation (7.61) in time and combining with Equation (7.60) result in;

$$\begin{aligned} \dot{V}_7(\zeta_1, \zeta_2, \zeta_3, \zeta_4, \zeta_5, \zeta_6, \zeta_7) = & -c_1\zeta_1^2 - c_2\zeta_2^2 - c_3\zeta_3^2 - c_4\zeta_4^2 - c_5\zeta_5^2 - c_6\zeta_6^2 + \\ & \zeta_7(k_{23}(\zeta_7 + \alpha_4) + k_{24}(\zeta_6 + T_{3ref}) - \dot{\alpha}_4 + k_{25}\tau_r) \end{aligned} \quad (7.62)$$

By satisfying the asymptotically global stable condition in the sense of Lyapunov in chapter 2 for the Equation (7.62), a control law τ_r can be chosen as follows;

$$\begin{aligned} -c_7\zeta_7 &= k_{23}(\zeta_7 + \alpha_4) + k_{24}(\zeta_6 + T_{3ref}) - \dot{\alpha}_4 + k_{25}\tau_r \\ \Rightarrow \tau_r &= \frac{1}{k_{25}}(-c_7(\omega_r - \alpha_4) - k_{23}\omega_r - k_{24}T_3 + \dot{\alpha}_4) \end{aligned} \quad (7.63)$$

Where c_7 is the positive gain

By doing so, we have:

$$\dot{V}_7 = -c_1\zeta_1^2 - c_2\zeta_2^2 - c_3\zeta_3^2 - c_4\zeta_4^2 - c_5\zeta_5^2 - c_6\zeta_6^2 - c_7\zeta_7^2 < 0 \quad \forall \zeta_1, \zeta_2, \zeta_3, \zeta_4, \zeta_5, \zeta_6, \zeta_7 \neq 0 \quad (7.64)$$

Thus, there exists a CLF (7.62) and the state feedbacks (7.21), (7.28), (7.35) (7.42) (7.49), (7.56) and (7.63) and a change of state transformations (7.17), (7.24) (7.31), (7.38) (7.45), (7.52), and (7.59), the complete system can be rewritten as follows:

$$\left. \begin{aligned} \dot{\zeta}_1 &= -c_1\zeta_1 \\ \dot{\zeta}_2 &= -c_2\zeta_2 \\ \dot{\zeta}_3 &= -c_3\zeta_3 \\ \dot{\zeta}_4 &= -c_4\zeta_4 \\ \dot{\zeta}_5 &= -c_5\zeta_5 \\ \dot{\zeta}_6 &= -c_6\zeta_6 \\ \dot{\zeta}_7 &= -c_7\zeta_7 \end{aligned} \right\} \quad (7.65)$$

By examining the system (7.65), it is clear that the system is asymptotically global stable and converges to zero with positive gains and the response of the system has no overshoots. The desired settling time and rising time of system are obtained by tuning the gains $c_1, c_2, c_3, c_4, c_5, c_6,$ and c_7 . Thus, the stability and performance specifications on the system (7.15)-(7.16) are achieved with the BSC.

By the backstepping based approach shown above, the backstepping controllers of equations (7.1)-(7.7) system are given as follows.

$$\left. \begin{aligned} \tau_1 &= \frac{1}{k_4} (-c_1(\omega_1 - \omega_{1ref}) - k_3 T_2 - k_2 T_1 - k_1 \omega_1) \\ \tau_u &= \frac{1}{k_{10}} (-c_3(\omega_u - \alpha_2) - k_9 T_1 - k_8 \omega_u + \dot{\alpha}_2) \\ \tau_2 &= \frac{1}{k_{18}} (-c_5(\omega_2 - \alpha_3) - k_{15} \omega_2 - k_{16} T_2 - k_{17} T_3 + \dot{\alpha}_3) \\ \tau_r &= \frac{1}{k_{25}} (-c_7(\omega_r - \alpha_4) - k_{23} \omega_r - k_{24} T_3 + \dot{\alpha}_4) \end{aligned} \right\} \quad (7.66)$$

where $c_1, c_2, c_3, c_4, c_5, c_6, c_7$ are the positive gains and determined by modified genetic algorithm in chapter 3 and $T_{1ref}, T_{2ref}, T_{3ref}, V_{ref}$ are the prescribed reference values. By using the proposed algorithm, the positive gains $c_1, c_2, c_3, c_4, c_5, c_6, c_7$ of backstepping controller (7.66) are optimally determined by using the modified genetic algorithm in chapter 3 to obtain the desired performance specifications with objective function shown in the (7.67).

$$J = \beta_1 \sum_{i=1}^N (\tau_u^2)_i + \beta_2 \sum_{i=1}^N (\Delta T_k^2)_i + \beta_3 \sum_{i=1}^N (\Delta V_j^2)_i \rightarrow \text{Min}_{C_m} \quad (7.67)$$

$$u = 1, 2, 3, 4; k = 1, 2, 3; j = 1, 2, 3, 4; m = \overline{1, 7};$$

Where N is an integer number of iterations in control simulations, $\beta_1, \beta_2, \beta_3$ are scale factors. $\Delta T_k = T_k - T_{kref}$ is the error between the operating and reference tension. $\Delta V_j = V_j - V_{jref}$ is the error between the operating and velocity of web and. τ_u ($u = 1, 2, 3, 4$) are toques at unwind motor, the rewind motor, and each of the driven rollers

7.3 Backstepping Based Control Algorithm Design

Figure 7.3 shows the algorithm diagram of a three-span R2R web control system using the backstepping controllers. In this algorithm, digital computer is considered as a controller that generates the desired control torque to keep web velocity and tension with prescribed reference values due to the presence of inertia change and viscous friction. Load cell, encoder, tachometer, and ultrasonic sensors are used to gain the feedback signals. Control software depending on all feedback signals of

velocity, tension and the control laws in the Equations (7.66) calculates the required toques to keep the desired performance specifications. Simulation is complemented in Matlab/Simulink R2008b

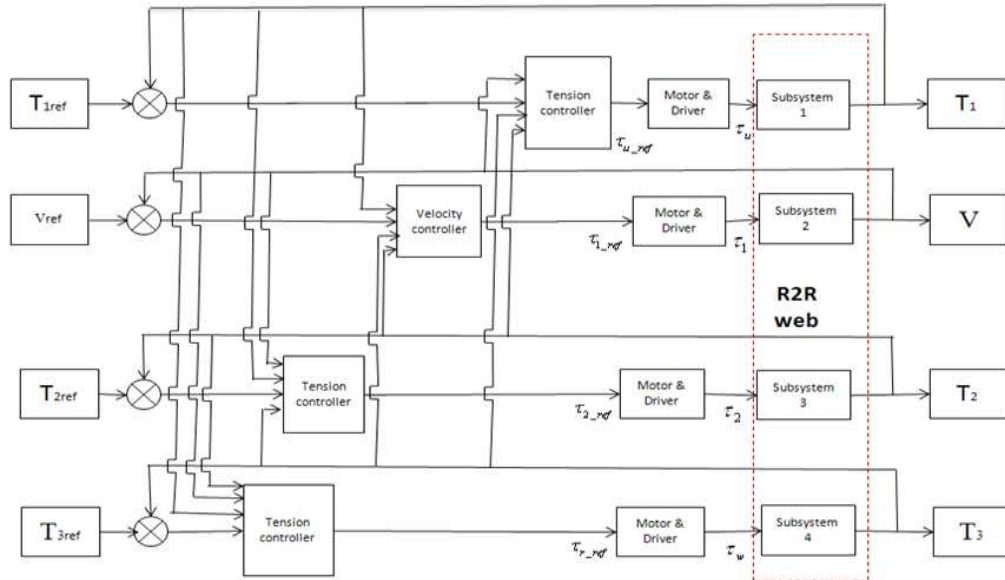


Figure 7.3: Algorithm diagram for three-span R2R web system

7.4 Numerical Simulation

7.4.1 Simulation Condition and Parameters

The simulation parameters of a three-span R2R web control system are shown in Table 7.1. The optimal gains of backstepping controllers are determined by using the MGA in chapter 3 with design parameters in chapter 3. The simulation is set up with the zero initial conditions, the prescribed reference web tension are presented in the Equation (7.68):

$$T_{1ref} = 12 \text{ (N)}, T_{2ref} = 10 \text{ (N)}, T_{3ref} = 8 \text{ (N)} \quad (7.68)$$

The desired angular velocity of the infeeder is set up with 0.8 (rad/sec). In order to observe the effectiveness of proposed algorithm using backstepping controllers, Numerical simulation is complemented with the initial viscous friction and inertia change of rewinder and unwinder in time. The outcomes of this study prove the reliability throughout simulation results in Matlab/Simulink and comparison with the experimental results.

Table 7.1: Simulation Parameters of Three-span R2R Web Control System

Parameters	Values	units
Radius of the unwind roll	0.355	(m)
Radius of the roller 1	0.05	(m)
Radius of the roller 2	0.05	(m)
Radius of the rewind roll	0.096	(m)
Inertial moment of the unwinder and motor	0.06006	(kgm ²)
Inertial moment of the infeed and motor	0.00750	(kgm ²)
Inertial moment of the outfeeder and motor	0.00750	(kgm ²)
Inertial moment of the winder and motor	0.02377	(kgm ²)
The length of span 1	2.360	(m)
The length of span 2	7.335	(m)
The length of span 3	2.632	(m)
The thickness of web	0.0001	(m)
The width of web	0.2	(m)
PET's Young module	2.5*10 ⁹	N/m ²
Density of web (PET)	1.4*10 ³	Kg/m ³

7.4.2 Simulation results

The BSC based algorithm in the Equations (7.66) is implemented in Matlab/Simulink and the control scheme for a three-span R2R web velocity and tension control system is shown in Figure 7.3, the simulation results employed with the presence of inertia change and viscous friction can be obtained with the optimal gains $c_1 = 9.6, c_2 = 8.7, c_3 = 8.9, c_4 = 7.5, c_5 = 7.3, c_6 = 9.4, c_7 = 6.6$

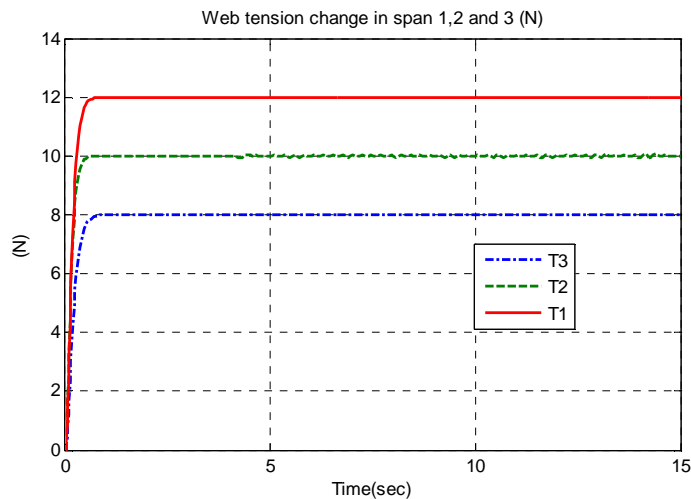


Figure 7.4: Web tension change in span 1, 2 and 3 (N)

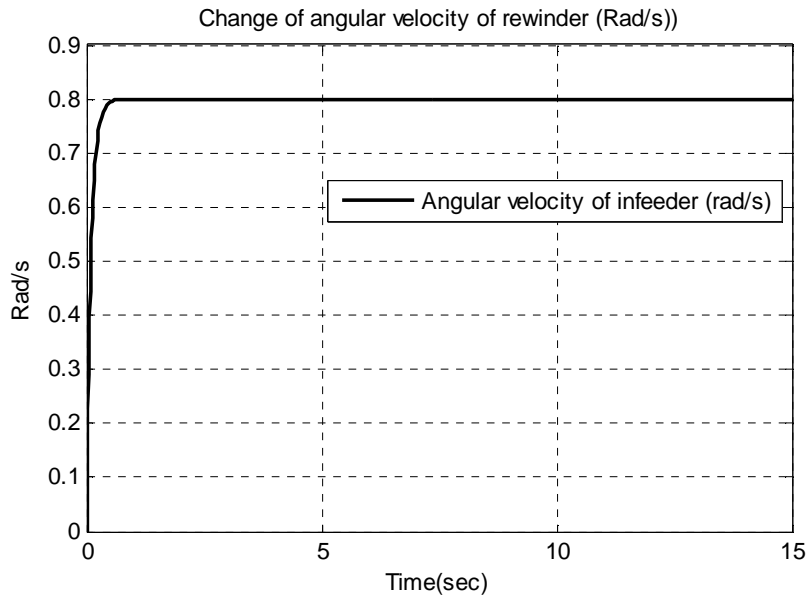


Figure 7.5: The angular velocity change in time of infeeder

The proposed theory is expected that the time response of web tension and velocity is with no zero overshoot and fast response. In Figure 7.4, the solid, dash and double dash lines show the web tension change in span 1, span 2 and span 3 in time, respectively. Figure 7.5 shows the angular velocity change in time of the infeeder.

From the above results and comments, the following comments can be made:

- The time response of web tension in spans and web velocity of three-span R2R web system of the BSC with optimal gains determined by the MGA has no overshoot and yields settling time of 0.2 second that is coincided to the expected results .
- The proposed algorithm based on the BSC achieved the precision, high stability and met the performance specifications.

7.5 Experimental study

Figure 7.6 shows the diagram of three-span R2R control system for experimental study. In order to operate web, unwinder, infeeder unit, outfeeder unit and rewinder motors HC-KFS43 and Driver (MR-J2S-40A) with torque control mode (0~8 V) are used. The load cells are used to get the web tension and ultrasonic sensor MIC+25/IU/TC is used to determine the change of radii. System design with NI FPGA board (PXI 7813R reconfigurable I/O) shown in Figure 7.7 is integrated with input/output equipments. Depending on the inputs, the control program in Fig.

10 with proposed algorithm generates the torques to keep web velocity and tension at prescribed values

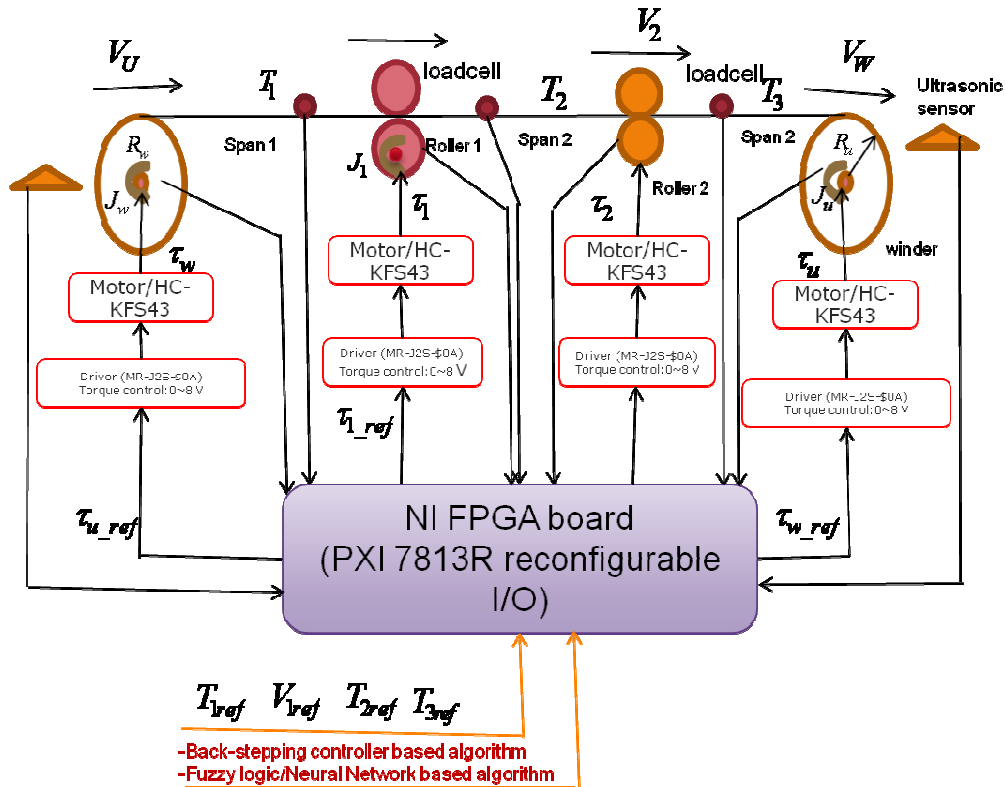


Figure 7.6: Diagram of three-span R2R web control system setup



Figure 7.7: The PXI 7813R reconfigurable I/O

By using the diagram in Figure 7.6, above mentioned mathematical model and Labview language, tension control program for R2R web system is given out as

shown Figure 7.8. In this program, the reference web velocity and tension can be changed arbitrarily by users. The control program displays the change of web tension and change of angular velocity of rewinder, infeed, outfeeder and unwinder as shown in Figure 7.8. The change of gains in backstepping is also available to help user understand and tune the gains to get the reference response of system in the presence of disturbance.

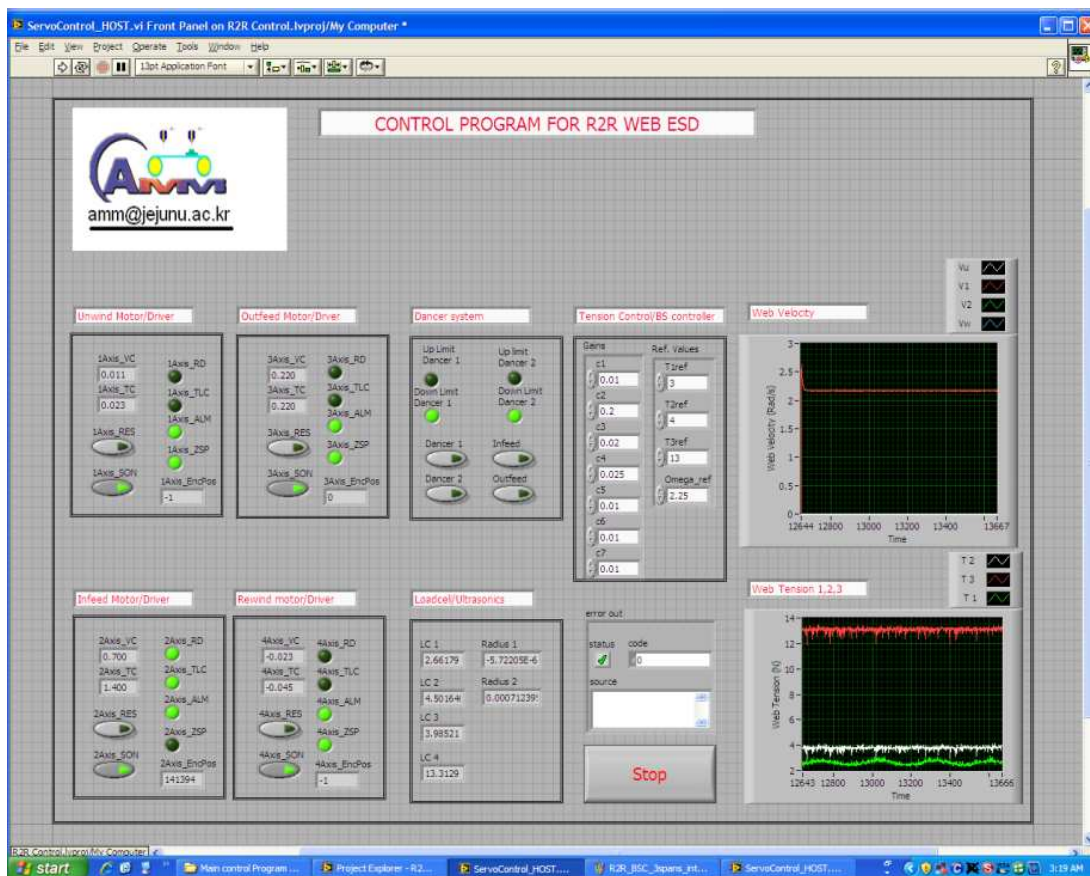


Figure 7.8: User interface of three-span R2R web control system

The desired web tension $T1_{ref} = 12$ (N), $T2_{ref} = 10$ (N), $T3_{ref} = 8$ (N) and the desired angular velocity change is 0.8 (rad/s). The experimental implementation is implemented in two cases. The first case is of zero initial condition and slow web velocity 4.6 m/min and the second case is done with nonzero initial condition and web velocity 12.5 m/min. This comes from the fact that the step and repeat process that is applied for printed electronics technology is always with reference web

tension at initial condition. The following is the experimental results to demonstrate the proposed algorithm:

Case 1: Zero initial condition and slow web velocity (4.6 m/min)

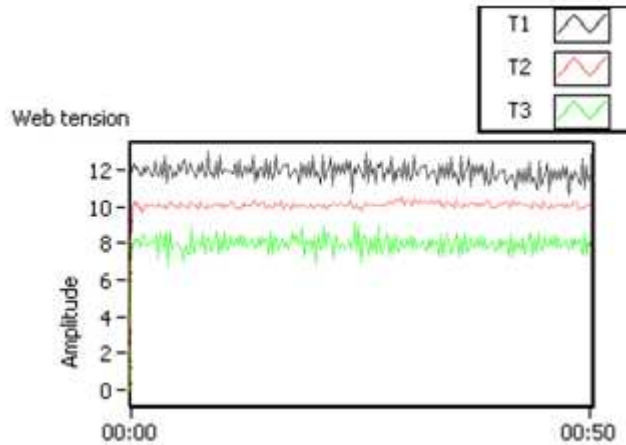


Figure 7.9: Web tension change of span 1, 2 and 3 in time

From the above results, the time response of web tension in three spans is of zero overshoot and fast response. By comparing to the simulation results in Figure 7.4, we conclude that the experimental results are coincided with the numerical simulation. The fact is that this web velocity is reasonable for printed electronic technology.

Case 2: Nonzero initial condition and web velocity (12.5 m/min)

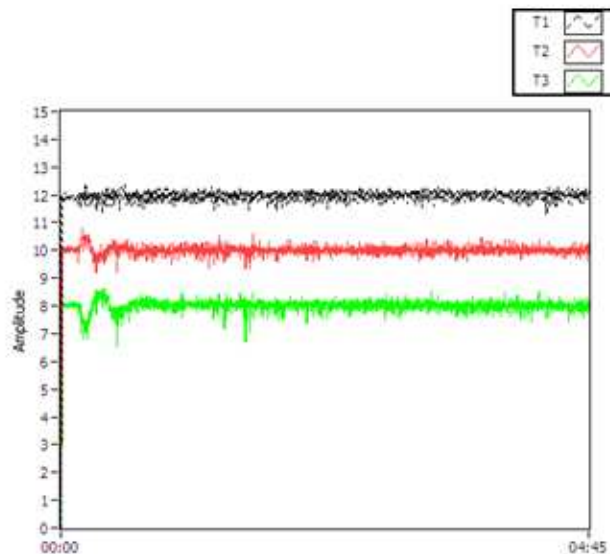


Figure 7.10: Web tension response with nonzero initial condition

Figure 7.9 shows the web tension change in span 1, span 2 and span 3 respectively with web velocity 12.5 m/min and initial condition $T_{10}=12$ (N), $T_{20}=10$ (N) and $T_{30}=8$ (N). The red and green lines shows the time response of web tension in span 2 and span 3 with overshoot about 6% and the black line shows the time response of the web tension in span 1 with zero overshoot. It is evident that the beginning of startup is with small overshoot due to the slack of web tension and high web velocity. The web tensions approach the reference values in short time.

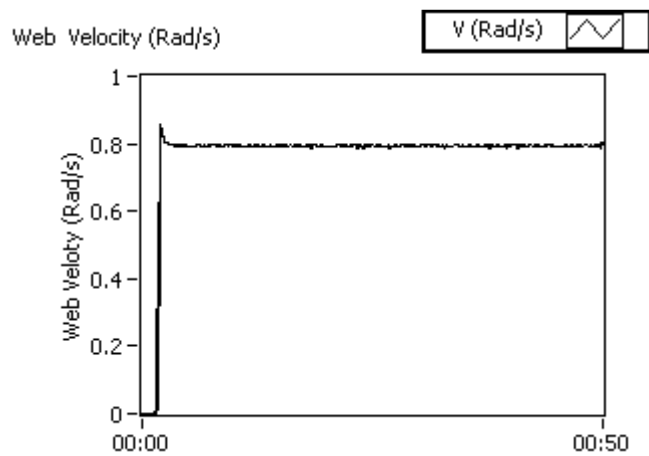


Figure 7.11: Angular velocity change in time of infeed

Figure 7.11 shows the change of angular velocity of the infeed. It can be observed that the system response with low velocity is with small overshoot. This result is acceptable as compared to the simulation results.

7.6 Analysis and Discussions

In this chapter, a mathematical model is developed for the three-span R2R web control system using the results in chapter 4. Based on the backstepping approach for the nonlinear dynamics systems, a procedure for obtaining the backstepping controller and a backstepping based web tension and velocity control algorithm are proposed using the theory developed in chapter 2 and chapter 3. The optimal gains of the BSC are determined by the MGA in chapter 3 and finally, the hardware and software scheme is discussed for experimental implementation.

In the proposed theory in the dissertation, we expected that the time response of web tension and velocity is with no overshoot and fast response. The simulation

results show that the proposed algorithm is reliable and able to meet the performance specifications, achieve an asymptotically global stability, and have a well-tracking command. Also, the experimental implementation is employed in two cases.

- The first case is of zero initial condition and slow web velocity 4.6 m/min. In this case, the time response of web tension in three spans is of zero overshoot and fast response. By comparing to the simulation results, we conclude that the experimental results are coincided with the numerical simulation in this case.
- The second case is done with nonzero initial condition and web velocity 12.5 m/min. In this case, the web tension response that implemented with web velocity 12.5 m/min and initial condition $T_{10}=12$ (N), $T_{20}=10$ (N) and $T_{30}=8$ (N) has overshoot about 6% in span 2 and zero overshoot in span 1. This is explained due to the length and weight of web in span 2 and 3.

Also, from the obtained results in Figure 7.9, it follows that the proposed algorithm using the BSC meets the desired performance specifications of the high stability in the presence of inertia change of the unwinder and rewinder and viscous friction. With the rapid development of sensors and electronic devices, the proposed control algorithm of BSC results in a control system with high precision and is useful for applications with high digital computational system.

8. Conclusions and Future Works

This chapter summarizes the main contributions, outcomes and applicability of the dissertation and then the results are analyzed briefly and some suggestions and directions are made for future works at the end of this chapter.

8.1. Conclusions

Nowadays, the rapid development of digital computer, sensor technology, and PC integrated devices leads many researchers and scientists to address design methods for nonlinear control systems. There are many methods to analyze and design for the nonlinear control systems. However, the exact feedback linearization and backstepping approaches are considered much in the literature. The state space exact linearization method for MIMO nonlinear control systems which utilizes the sequence of coordinate transformation and state feedback in order to transform the original system into a linear and controllable system is presented. However, such an approach often leads us to the complex expressions with MIMO nonlinear control systems and sometimes fails to obtain the final state feedback law. The question arises if coordinate transformations and state feedbacks are able to implement alternately for each subsystem. The idea of backstepping based design approach comes up to get over this obstacle. In this proposal, the whole system is divided into several subsystems. By applying consecutively the coordinate transformation and choosing feedback law via Control Lyapunov Function (CLF) to each subsystem from the lowest to highest order and rewrite the feedback law in the original coordinates, the resulted controllers called backstepping controller make original system a well-tracking command and asymptotically global stable. The main contributions of the dissertation are the following:

- An overall view of development, applications and potentials of R2R web control system for printed electronics are addressed and a mathematical model of multi-span R2R web control system is generated using the second Newton's law and the principle of mass conservation.
- A systematic procedure is for formulating the backstepping controller for a class of MIMO nonlinear control system and a backstepping controller based

algorithm for MIMO nonlinear control system is proposed to prove the zero overshoot response and short settling time with positive gains.

- A hardware and software design scheme for multi-span R2R web control system is drawn using the FPGA technology and FPGA Labview module.
- A modified genetic algorithm is proposed to determine optimally the design parameters of the BSC and an algorithm using the MGA is for updating online the gains is presented in the presence of changing radii and viscous friction.
- By applying the obtained theoretical model, backstepping based control algorithm of R2R web tension and velocity is applied successfully for a nonlinear single-span, two-span web control system. The numerical simulation and experimental implementation prove the reliability of the proposed algorithm.
- For three-span R2R web system, the proposed algorithm is working well with low velocity. This is reasonable for printed electronics technology.

8.2. Future works

In the development of mathematical model in this dissertation, it is assumed that the external disturbances such as printing pressure, friction between web and rollers, no slippage, and no effect of wrap angle are neglected. In reality, these factors and others are principal sources to reduce the precise of control system. The following are some suggestions for future works:

- The recent developed control algorithms have not counted into the external disturbances yet. Therefore, robust design problem of nonlinear R2R web control system should be considered in the presence of external disturbances and internal dynamics.
- For printed electronics technology with high accuracy, the small variation of web tension, longitudinal and lateral error leads to reduce the quality of the final product. Thus, the integrated algorithm of web tension and register control will play an important role for improving the quality of manufacturing processes.

- By the experimental implementations, the author realized that the alignment of rollers and wrap design or dynamics of rollers is also a factor to be addressed for web velocity control. Thus, the dynamic problem of moving web and rollers needs to be considered extensively.

References

- Alan F. Lynch, Scott A. Bortoff, and Klaus Robenack, "Nonlinear tension observer for web machine," *Automatica* 40, pp.1517-1524, 2004
- Andries P. Engelracht, "Computational Intelligence: An introduction" *Second Edition*, John Wiley & Sons, Ltd. 2002.
- Ahn, B. J., Choi, J. Y., Chang, Y. S., Lee, M. H., "Web guide process in cold rolling mill: modelling and PID controller," *KSME International Journal*, 7, 1074-1085 (2004).
- A. Isidori and A. J. Krener, "On feedback equivalence of nonlinear systems" in *System & Control Letters*, No. 2, Vol. 2, pp. 118-121.
- A. Isidori, "Nonlinear Control systems" in *The Third Edition*, Springer, 1995.
- A. J. Krener and A. Isidori, "Linearization by output injection and nonlinear observers" in *System & Control Letters*, No. 3, Vol. 2, pp. 47-52.
- Aravind Seshadri, Prabhakar R. P., "Design and development of a new edge sensor for web guiding," in *IEEE Sensors Journal*, 5, 698-706 (2007).
- Bong-Ju Lee, Sung-Hwan Kim, Chul-Goo Kang, "Analysis of a nonlinear web-tension control system of a high-speed gravure printing machine," *SICE-ICASE International Joint Conference 2006*, Oct. 18-21, 2006 in Bexco, Busan, Korea
- Bouazza S E, Abbassi H A (2007) Model based control system for hot steel strip rolling mill stands. *Asian Journal of information Technology*. 6:246-253.
- Brian Thomas Boulter, "Active disturbance rejection control for web tension regulation and control," in *IEEE conference on decision and control*, 2001.
- Chen C (1996) Back-stepping control design and its application to vehicle lateral

control in automated highway systems. *Doctor of Philosophy, University of California, Berkeley.*

Chen H C, Chang S H (2006) Genetic algorithm based optimization design of a PID controller for an active magnetic bearing. *IJCSNS*. 6:122-145

Chul-Goo Kang, Bong-Ju Lee, “Stability analysis for design parameters of a roll-to-roll printing machine,” *International Conference on Control, Automation and Systems 2007*, COEX, 2007, Seoul, Korea.

Chung D T, Shin K H (2004) Transient wrinkling analysis of steel web rolling. In *IEEE IAS 2004*: 886-890.

Cui Z, Xu B (2003) Generalized mathematical model for hot rolling process of plate. *J. mater. Sci. Technol.* 19:123-129.

D. Knittel, E. Laroche, H. Koc, “Tension control for winding systems with two degrees of freedom H_{∞} controller,” *IEEE Transactions on control systems technology*, Vol. 11, No 1, pp. 576-582, 2001.

Dean Frederick and Joe Chow, “feedback control problems using Matlab and the control system toolbox,” *BookWare Companion Series*, 2001.

Durovsky F, Ferkova Z (2008), “Computation of rolling stand parameters by genetic algorithm,” *Acta Polytechnica Hungarica*. 5:234-345.

Gaby Saad, “Multivariable Control of Web process” *A thesis for degree of Master of Applied Science, University of Toronto*, 2000.

Gray W. Steven, “Lecture notes on Nonlinear Control Systems,” *Spring 2012*.

Guan L, Lin J, Chen G, Chen M (2006), “Study for the offset printing quality

control expert system based on case reasoning,” *IEEE International conference*, 2006.

Hinge K C, Maniatty A M (1996), “The effect of skew angle on the axial pressure distribution between flexible rubber-covered rollers,” *Int. J. Mech. Sci.* 38:607-619.

Katsuhiko Ogata, “Modern Control Engineering,” *Second edition, Prentice Hall*, New Jersey 07632.

Kee-Hyun Shin, Jeung-In Jang, Hyun-Kyoo Kang, Seung-Ho Song, “Compensation method for tension disturbance due to an unknown roll shape in a web transport system,” *IEEE Transactions on Industry and Applications*, Vol. 39, No 5, 2003.

Kee-Hyun Shin, Soon-Oh Kwon, Sang-Hoon Kim, and Seung-Ho Song, “Feedforward control of the lateral position of a moving web using system identification,” *IEEE Transactions on Industry and Applications*, pp. 345-351, 2003.

Kyung-Hyun Choi, **Thanh T. Tran** and D. S. Kim, “A control system design of automatically tuning controller for roll to roll web system using the modified genetic algorithm,” *Proceedings of the 7th Asian Control Conference*, Hong Kong, China, August 27-29, 2009.

Kyung-Hyun Choi, **Thanh T. Tran**, Dong-Soo Kim, Jeong-Beom Ko, Su-Jin Kim, and Yang-Hoi Dohn “ A lateral control algorithm for roll-to-roll web system based on backstepping approach,” *Proceedings of the KSME 2008 Fall Annual Meeting*, pp. 1091-1097, Korea.

Kyung-Hyun Choi, **Thanh T. Tran**, and Dong-Soo Kim, “A precise control algorithm for single-span roll-to-roll web system using the backstepping

controller” *IEEE ISIE 2009*, Korea.

Kyung-Hyun Choi, **Thanh T. Tran**, and Dong-Soo Kim, “Backstepping Controller Based Web Tension Control for Roll-to-Roll Web Printed Electronics System,” *Journal of Advanced Mechanical Design, Systems, and Manufacturing*, Vol. 5, No. 1, pp. 7-21, 2011.

Kyung-Hyun Choi, **Thanh T. Tran**, and Dong-Soo Kim, “An new approach for intelligent control system design using the modified genetic algorithm” *Int. J. Intelligent Systems Technologies and Applications*, Vol. 9, Nos. 3/4, 2010.

Kyung-Hyun Choi, **Thanh T. Tran**, Bong-Su Yang and Dong-Soo Kim, “Printing Pressure Control Algorithm of Roll-to-Roll Web System for Printed Electronics” *Frontiers of Assembly and Manufacturing 2010*, pp. 187-226, Springer.

Kyung-Hyun Choi, **Thanh T. Tran**, P. Ganeshtangaraj, K. H. Lee, M. N. Nguyen, J. D. Jo and D. S. Kim “Web register control algorithm for roll-to-roll system based printed electronics” *6th annual IEEE Conference on Automation Science and Engineering*, Aug 21-24, 2010, pp. 867-872, Toronto, Canada

Ku Chin Lin, “Observer – based tension feedback control with friction and inertia compensation,” *IEEE Transactions on control systems technology*, Vol. 11, No 1, pp. 109-118, 2003.

Ku Chin Lin, Ming-Ching Tsai, Kung-Yi Chen, “Web tension control of a start-up process using observer techniques with friction and inertia compensation”, *The 27th annual conference of the IEEE industrial electronics society*, 2001.

Lee W H (2002), “Mathematical model for cold rolling and temper rolling process of thin steel strip,” in *KSME International Journal*. 16: 1296-1302.

Lee C W, Shin K H (2007), "A study on taper tension control considering telescoping in the winding system," in *IEEE*, 2007: 398-403.

Lisa Sievers, Mark J. B., and Andreas V. F., "Modelling of web conveyance systems for multivariable control," *IEEE Transactions on Automatic Control*, 6, 524-531 (1988).

Marcel, P. G. J., Camile H. L., Robert Babuska, "Modelling and identification of a strip guidance procs with internal feedback," in *IEEE Transactions on Control Systems Technology*, 1, 88-102 (1998).

Michael A. Randolph, "Commercial Assessment of Roll-to-Roll Manufacturing of Electronic Displays," in *Thesis of Master of Engineering, Massachusetts Institute of Technology*, 2006.

M. Krstic and I. Kanellakopoulos, and P. Kokotovi'c, "*Nonlinear and Adaptive Control Design*," New York: Wiley, 1995.

P. Kokotovic, "The Joy of feedback: Nonlinear and Adaptive" in *1991 Bode Prize Lecture, IEEE*, pp. 7-17, June 1992.

Prabhakar R. Pagilla, Nilesh B. Siraska, "Robust controllers for large-scale interconnected systems: applications to web processing machines," in *Book chapter*, Oklahoma State University, US.

Ramamurthy V. Dwivedula, Yongliang Zhu, Prabhakar R. Pagilla, "Characteristics of active and passive dancers: A comparative study," In *Control Engineering Practice* 14, 2006.

Renato A K, Joost P R (2001), "Design of optimal disturbance rejection PID controllers using genetic algorithms," in *IEEE Transactions on Evolutionary computation*. 5:78-82.

Richard, C. B., “Lateral dynamics of a moving web with geometrical imperfection,” in *Journal of Dynamic System, Measurement, and Control*, 124, 25-34 (2002).

Shankar Sastry and Marc Bodson, “Adaptive control: stability, convergence and robustness” Prentice Hall Advanced reference Series Engineering, 1989.

Petar V. Kokotović, “The joy of feedback: Nonlinear and adaptive,” in *IEEE*, 1992.

Seung rohk Oh, “The design of web tension control system using a nonlinear feedback controller,” *Trans. KIEE*, Vol. 55D, No 1, pp. 14-16, 2006.

Seung-Ho Song, Seung-Ki Sul, “A new tension controller for continuous strip processing line,” *IEEE Transactions on control systems technology*, Vol. 11, No 1, pp. 2225-2230, 1998.

Seyedkazaemi M, Akbarimajd A, Rahnamaei A, Baghbanpourasl A, “genetically tuned optimal PID controller,” in *Proceedings of the 6th WSEAS Int. Conf. on Artificial Intelligence*, Greece, 2010.

Shin, K. H., Kwon, S., O., “The effect of tension on the lateral dynamics and control of a moving web,” in *IEEE Transactions on Industry Applications*, 43, 403-411 (2007).

Sun H, George T. C. C (2002), “Motion synchronization for dual-cylinder electro-hydraulic lift systems,” in *IEEE Transactions on Mechatronics*. 7:171-181.

Takeshi Masui, Yoshiyuki Kaseda, and Kazumi Isaka, “Basic examination on strip wandering in processing plants,” in *ISIJ International*, 40, 1019-1023 (2000).

Tetsuzo Sakamoto, Yoshikazu Fujino, “Modeling and analysis of a web tension control system,” in *IEEE Catalog Number: 95TH8081*, pp. 358-362.

Thanh T. Tran, Kyung-Hyun Choi, Dong-Eui Chang and Dong-Soo Kim, “Web Tension and velocity Control of two-span Roll-to-Roll System for printed electronics ,” *Journal of Advanced Mechanical Design, Systems, and Manufacturing*, Vol. 5, No. 4, pp. 329-346, 2011.

Thanh T. Tran, P. Ganeshthangaraj, Muhammad Zubair, and Kyung-Hyun Choi “An evolution strategy based autonomous algorithm for roll-to-roll web control system” Accepted for publication on *Advances in Intelligent and Soft Computing of Springer, 2012*.

Thanh T. Tran and Kyung-Hyun Choi, “A backstepping based control algorithm for multi-span roll-to-roll web system” *International Journal of Advanced Manufacturing Technology*, revised for publication, 2012.

Wang H., Logghe D., and Miskin D., “Physical modelling and control of lateral web position for wallpaper making process,” *Control Engineering Practice*, 13, 401-412 (2005).

Yerashunas, J. B., De Abreu-Garcia, J. B., and Tom T. H., “Control of lateral motion in moving webs,” *IEEE Transactions on Control Systems Technology*, 5, 684-693 (2003).

Yoo, S. R., Choi, I. S., Nam, P. K., Kim, J. K., Kim, S. J., and Davene J., “Coating deviation control in transverse direction for a continuous galvanizing line,” *IEEE Transactions on Control Systems Technology*, 7, 129-135 (2007).

Zhunang M, Atherton D P, “Automatic tuning of optimum PID controllers,” in *IEE Proceeding-D*. 140:216-224, 1993.

Curriculum Vitae

THANH TRUNG TRAN, PhD

Department of Mechanical Engineering
Vietnam University of Mining and Geology
Dong Ngac – Tu Liem – Ha Noi – Viet Nam
Tel:+84-4-2183049 / Cell phone: +84-1668380479
Email: thanhtt@cheju.ac.kr
thanhvi@hotmail.com



Educational Background

- 08/1998 – 07/2002: Vietnam National University, Hanoi, Vietnam. Bachelor of Science's Degree in Mechanics (2nd rank in the batch)
- 10/2002 – 12/2005: Vietnam National University, Hanoi, Vietnam. Master of Science's Degree in Mechanics (GPA 8.0/10.0 or 3.5/4.0)
- 02/2008 – 06/2012: Jeju National University, Jeju, Republic of Korea. PhD Degree in Mechanical Engineering (GPA 4.33/4.50)

Academic Interests

- Dynamics and Control
- Manufacturing and Computer-Integrated Design
- Computational Intelligence and Intelligent Systems

Research/Work Experiences

- 10/2002–8/2004: Research Assistant for master degree, Vietnam University of Technology, Hanoi, Vietnam
Project: “*Numerical simulation and control of multi-body system*”
- 10/2004–10/2006: Lecturer at Department of Mechanical Engineering, Hanoi University of Mining and Geology, Hanoi, Vietnam
Lectures and researches in Mechanical Engineering
- 10/2006–02/2008: Deputy leader of Department of Mechanical Engineering, Hanoi University of Mining and Geology, Hanoi, Vietnam,
Lectures and researches in Mechanical Engineering
- 02/2008–06/2012: Research Assistant at AMM Laboratory, Department of Mechatronics Engineering, Jeju National University, Jeju, South Korea.
Project: “*Control algorithm development of web transport system: web tension control, lateral control, register control and integrated control algorithm development*”

Honors/Activities/Leadership/Special Skills

- September 2, 1998 – July 3, 2002: *Secretary of Youth Union*, Vietnam National University, Hanoi, Vietnam.
- May, 2001: *The third prize of Olympic of National Mechanics*, Ministry of Education and Training, Vietnam Mechanics Association, Vietnam Student Association, Vietnam.
- September, 2001: *The leader of Youth Union with excellent achievements in social activities*, Vietnam National University, Hanoi, Vietnam.
- July, 2001: *An exemplary figure of Vietnam National University*, Vietnam National University, Hanoi, Vietnam.
- Feb 16, 2008 – June 15, 2012: *PhD scholarship in Mechanical Engineering*, Jeju National University, South Korea.

Language Skills

- Vietnamese: Native
- English : Fluency

Software skills

- Programming C/C++, Matlab, Foxtran
- Application softwares: Inventer Autodesk, Ansys, Labview

Workshops

1. 2009 Joint workshop Jeju National University and RIKEN, Jeju, Korea, 2009.

Publications/ Journals

1. Kyung-Hyun Choi, **Thanh T. Tran**, and Dong-Soo Kim, “An new approach for intelligent control system design using the modified genetic algorithm” *Int. J. Intelligent Systems Technologies and Applications*, Vol. 9, Nos. 3/4, 2010.
2. Kyung-Hyun Choi, **Thanh T. Tran**, Bong-Su Yang and Dong-Soo Kim, “Printing Pressure Control Algorithm of Roll-to-Roll Web System for Printed Electronics” *Frontiers of Assembly and Manufacturing*, pp. 187-226, Springer, 2010.
3. Kyung-Hyun Choi, **Thanh T. Tran**, and Dong-Soo Kim, “BackStepping Controller Based Web Tension Control for Roll-to-Roll Web Printed Electronics System,” *Journal of Advanced Mechanical Design, Systems, and Manufacturing*, Vol. 5, No. 1, pp. 7-21, 2011.

4. **Thanh T. Tran**, Kyung-Hyun Choi, Dong-Eui Chang and Dong-Soo Kim, "Web Tension and velocity Control of two-span Roll-to-Roll System for printed electronics ," *Journal of Advanced Mechanical Design, Systems, and Manufacturing*, Vol. 5, No. 4, pp. 329-346, 2011.
5. **Thanh T. Tran** and Kyung-Hyun Choi, "A backstepping based control algorithm for multi-span roll-to-roll web system," revised for publication in *International Journal of Advanced Manufacturing Technology*, 2012
6. **Thanh T. Tran**, P. Ganeshtangaraj, Muhammad Zubair and Kyung-Hyun Choi "An evolution strategy based autonomous algorithm for roll-to-roll web control system" Accepted for publication on *Advances in Intelligent and Soft Computing of Springer*, 2012.

Publications/ Conferences

1. Nguyen Van Can, **Thanh T. Tran**, "The experimental study of blasting to determine the suitable element size of broken rock," *Proceeding of the 17th national conference on mining and geology 2007*, Hanoi, Vietnam.
2. Kyung-Hyun Choi, **Thanh T. Tran**, Dong-Soo Kim, Jeong-Beom Ko, Su-Jin Kim, and Yang-Hoi Dohn " A lateral control algorithm for roll-to-roll web system based on backstepping approach," *Proceedings of the KSME 2008 Fall Annual Meeting*, pp. 1091-1097, Korea.
3. Kyung-Hyun Choi, **Thanh T. Tran**, and Dong-Soo Kim, "A precise control algorithm for single-span roll-to-roll web system using the backstepping controller" *IEEE ISIE 2009*, Korea.
4. Kyung-Hyun Choi, **Thanh T. Tran** and D. S. Kim, "A control system design of automatically tuning controller for roll to roll web system using the modified genetic algorithm," *Proceedings of the 7th Asian Control Conference*, Hong Kong, China, August 27-29, 2009.
5. Kyung-Hyun Choi, **Thanh T. Tran**, Yang Bong-Su Dong-Soo Kim "A new approach for intelligent control system design using the modified genetic algorithm" *Proceedings of ICITA2009*, Hanoi, Vietnam.
6. Kyung-Hyun Choi, **Thanh T. Tran**, Yang Bong-Su and Dong-Soo Kim "On a new approach for gravure/offset printing pressure control algorithm development using the full state feedback controller" *IEEE ISAM2009*, Korea, 2009.
7. Kyung-Hyun Choi, **Thanh T. Tran**, P. Ganeshtangaraj, K. H. Lee, M. N. Nguyen, J. D. Jo and D. S. Kim "Web register control algorithm for roll-to-roll system based printed electronics" *6th annual IEEE Conference on Automation Science and Engineering*, Aug 21-24, 2010, pp. 867-872, Toronto, Canada, 2010.
8. **Thanh T. Tran**, P. Ganeshtangaraj, Muhammad Zubair, and Kyung-Hyun Choi "An Evolution Strategy Based Autonomous Algorithm for Roll-to-roll Web Control System" Accepted for Publication on *IAS-12*, Jeju, Korea, 2012.

Projects

1. “*The numerical simulation and control of the mechanical Systems*” Hanoi, Vietnam.
2. “*On a calculation of fixed foundation pile of offshore oil – ring on Vietnam’s territorial waters in accordance with computerization*” Hanoi, Vietnam.
3. “*Calculating the optimal displacement of pipe of executing on seabed*” Hanoi, Vietnam.
4. “*Control algorithm development of web transport system: web tension control, lateral control, register control and integrated control algorithm development*” Jeju, Korea.

References

- Prof. Dr. Kyung-Hyun Choi

Address: Department of Mechatronics, Jeju National University
Jeju, South Korea
Tel: 82-98983713
Email: khchoi@jejunu.ac.kr

- Prof. Dr. Sc. Dao Huy Bich

Address: Department of Mechanics, College of Science, Vietnam National University
334 – Nguyen trai Street, Hanoi, Vietnam
Tel: 84-4-7550438

- Prof. Dr. Tran Dinh Kien

Rector of Vietnam University of Mining and Geology
Address: Dong Ngac, Tu Liem, Hanoi, Vietnam
Tel: 84-4-8389633
Email: Trandinkien@hn.vnn.vn

- Prof. Dr. Sc. Do Sanh

Address: Department of Applied Mechanics, Hanoi University of Technology
1 Dai Co Viet Street, Hanoi City, Vietnam
Tel: 84-4-8693402
Email: dosanh@mail.hut.edu.vn